

**REPORT**  
**on the**  
**2021 EXPLORATION PROGRAM**  
**of the**  
**THANE PROPERTY**  
Omineca Mining District, British Columbia, Canada  
**for**  
**Interra Copper Corp.**  
**By**  
**CME Consultants Inc.**  
March 28, 2022  
Christopher O. Naas, *P. Geo.*

**Volume I of VI**

Latitude: 56°10'N  
*Longitude: 125°38'W*  
NTS 094C03/04/05

## TABLE OF CONTENTS

	<i>page</i>
1.0 SUMMARY .....	1
2.0 INTRODUCTION AND TERMS OF REFERENCE .....	2
3.0 PROPERTY DESCRIPTION AND LOCATION .....	2
3.1 TITLE.....	2
3.2 ACCESSIBILITY .....	6
3.3 CLIMATE.....	6
3.4 INFRASTRUCTURE .....	7
3.5 PHYSIOGRAPHY .....	7
4.0 HISTORY .....	7
4.1 EXPLORATION AND DEVELOPMENT BY PRIOR OWNERS.....	7
4.2 EXPLORATION AND DEVELOPMENT BY THANE MINERALS .....	14
5.0 GEOLOGICAL SETTING AND MINERALIZATION .....	16
5.1 REGIONAL GEOLOGY .....	16
5.2 REGIONAL MINERALIZATION.....	18
5.3 PROPERTY GEOLOGY .....	23
5.4 PROPERTY ALTERATION AND MINERALIZATION .....	32
5.5 PROPERTY STRUCTURE.....	33
6.0 CURRENT EXPLORATION .....	33
6.1 SOIL SAMPLING .....	34
6.1.1 Pinnacle Area .....	36
6.1.2 Gail Area .....	37
6.1.3 Mat Area.....	37
6.2 GEOPHYSICAL SURVEYING .....	41
6.2.1 Airborne Magnetics .....	41
6.2.2 Induced Polarization.....	41
6.3 GEOLOGICAL MAPPING .....	44
6.3.1 Pinnacle Geology .....	44
6.3.2 Pinnacle Alteration .....	46
6.3.3 Pinnacle Mineralization.....	47
6.3.4 Pinnacle Structure.....	49
6.3.5 Gail Geology .....	51
6.3.6 Gail Alteration.....	53
6.3.7 Gail Mineralization.....	54
6.3.8 Gail Structure .....	55
6.4 ROCK SAMPLING .....	57
6.5 DIAMOND DRILING .....	60
6.5.1 Cathedral Main.....	62
6.5.2 Cathedral Valley.....	80
6.5.3 Gully.....	82
6.5.4 Cathedral South .....	92
6.5.5 Pinnacle .....	96
6.5.6 Analytical Results.....	99
6.6 PETROGRAPHIC STUDIES .....	99
7.0 SAMPLE PREPARATION, ANALYSIS AND SECURITY .....	100
7.1 SAMPLE PREPARATION .....	100
7.2 SAMPLE ANALYSIS .....	100
7.3 QUALITY CONTROL .....	103
7.3.1 Control Samples .....	103

8.0 DISCUSSION .....	104
8.1 GAIL AREA .....	104
8.2 CATHEDRAL AREA.....	111
9.0 INTERPRETATIONS AND CONCLUSIONS .....	113
9.1 INTERPRETATIONS .....	113
9.1.1 Cathedral Area.....	114
9.1.2 Cathedral Valley.....	123
9.1.3 Pinnacle .....	124
9.2 CONCLUSIONS.....	126
9.2.1 Gail Area .....	126
9.2.2 Cathedral Area.....	126
10 RECOMMENDATIONS .....	128
10.1 NON DRILLING .....	128
10.2 DRILLING.....	129
10.3 BUDGET .....	131
11.0 REFERENCES.....	132
12.0 SIGNATURE PAGE AND CERTIFICATE .....	137

## LIST OF TABLES

	<i>page</i>
Table 1: List of mineral tenures, Thane property.....	5
Table 2: Summary of plutonic units, Hogen batholith.....	17
Table 3: Summary of grid and soil sampling.....	35
Table 4: Statistical analysis, 2020 and 2021 soil samples .....	36
Table 5: Statistical analysis, 2021 soil samples .....	36
Table 6: Pinnacle area vein structure .....	49
Table 7: Structural measurements from the Pinnacle area.....	50
Table 8: Vein structure – Gail Area .....	55
Table 9: Selected grab sample results >0.5% Cu, Pinnacle Area .....	57
Table 10: Selected grab sample results >0.3% Cu, Gail Area .....	58
Table 11: Chip samples, Mat Area.....	58
Table 12: Selected grab sample results >0.5% Cu, Gail Area .....	58
Table 13: Drill hole specifications .....	60
Table 14: Selected core sample results .....	99
Table 15: Certified reference material, rock samples .....	103
Table 16: Certified reference material, core samples.....	103
Table 17: Alkalic and calc alkalic porphyry deposit comparisons .....	112
Table 18: Alteration assemblages of an Alkalic Cu-Au porphyry system.....	113
Table 19: Recommended drill holes, Cathedral Area .....	130
Table 20: Proposed exploration budget.....	131

## LIST OF FIGURES

	<i>page</i>
Figure 1: Property location (1:3,000,000).....	3
Figure 2: Mineral tenures (1:150,000) .....	4
Figure 3: Regional geology and economic setting (1:1,500,000).....	19
Figure 4: Property geology (1:150,000).....	24
Figure 5: Geochemistry plan map, Arsenic (soil), Gold (rock), <i>Pinnacle Area</i> (1:10,000).....	38
Figure 6: Geochemistry plan map, Molybdenum, <i>Gail Area</i> (1:10,000).....	39
Figure 7: Geochemistry plan map, Arsenic (soil), Silver (rock), <i>Mat Area</i> (1:10,000).....	40
Figure 8: Geophysical Plan Map, <i>Pinnacle Area</i> (1:10,000).....	42
Figure 9: Geophysical Plan Map, <i>Gail Area</i> (1:10,000) .....	43
Figure 10: Geology and Rock Sampling Plan Map, <i>Pinnacle Area</i> (1:2,000).....	pocket
Figure 11: Geology and Rock Sampling Plan Map, <i>Gail Area</i> (1:2,000).....	pocket
Figure 12: Geochemistry plan map, Copper, <i>Aten (Central) Area</i> (1:10,000) .....	59
Figure 13: DDH Collar Location Map, <i>Cathedral Area</i> (1:10,000) .....	61
Figure 14: Drill hole trace with IP, TH21-1 and TH21-2 (schematic).....	67
Figure 15: Drill hole trace with IP, TH21-5 (schematic).....	75
Figure 16: Drill hole trace with IP, TH21-1 TH21-12 and TH21-6 (schematic).....	78
Figure 17: Drill hole trace with IP, TH21-7 and TH21-8 (schematic).....	86
Figure 18: Drill hole trace with IP, TH21-11 (schematic).....	91
Figure 19: Drill hole trace with IP, TH21-4 (schematic).....	96
Figure 20: Drill hole trace with IP, TH21-9 and TH21-10 (schematic).....	98
Figure 21: L2200N, Gail Grid, geological interpretation (schematic).....	104
Figure 22: L2400N, Gail Grid, interpretation (schematic) .....	106
Figure 23: L2500N, Gail Grid, interpretation (schematic) .....	107
Figure 24: Gail Area interpretation (schematic) .....	109

## LIST OF APPENDICES

- I. Abbreviations and Conversion Factors
- II. Sample Detail
  - a. Soil Samples
  - b. Rock Samples
- III. Certificates of Analyses
  - a. Soil
  - b. Rock
  - c. Drill Core
  - d. Age Dating
- IV. Geophysical Sections
  - a. Airborne Magnetic Survey
  - b. Pseudo Sections
  - c. Inversions
- V. Drill Logs
  - a. Geological Logs
  - b. Geotechnical Logs
  - c. Strip Logs
  - d. Cross Sections
- VI. Petrographic Study
  - a. Thin Section Report
  - b. Submitted Sample Descriptions
- VII. Sample Analyses
  - a. Analytical Methodology
  - b. CRM Specifications
  - c. CRM Performance

## 1.0 SUMMARY

The Thane property (the “Property”) is centred at latitude 56° 10’ N and longitude 125° 38’ W, approximately 180 kilometres northwest of Mackenzie and 185 kilometres north-northeast of Smithers, in the Omineca Mining Division of north-central British Columbia, Canada.

The Property is located in the highly prospective Quesnel Terrane, an accreted Mesozoic volcanic arc terrane that forms a 1,600 kilometre long, north-south trending linear belt of volcano-sedimentary rock sequences hosting coeval and post-accretionary Cretaceous intrusions, along the eastern margin of the Canadian Cordillera. On the Property the volcano-sedimentary units are represented by rocks of the Nicola Group (formerly described as the Takla Group), and intrusives represented by the Hogen Plutonic Suite. Numerous dykes, sills and small stocks are noted within both geological units. The Jurassic to Cretaceous age intrusions are commonly associated with significant alkalic porphyry copper deposits. Local examples include the Kemess South and Mt. Milligan mines, and the nearby Lorraine and Kwanika deposits.

A 22-person exploration camp was setup in late June 2021 to facilitate the summer helicopter-supported exploration program. On July 5, 2021, crews were mobilized to the Property to commence drill pad construction in preparation for a helicopter-supported diamond drill program. On July 19, 2021, Atlas Drilling Ltd. mobilized to the Property and commenced drilling on July 20, 2021. A total of 2,783.24 metres of NQ core was drilled in 12 holes from 9 drill pads with the last hole completed on August 21, 2021. Geological and soil sampling crews mobilized to the Property on July 5, 2021. Geological mapping and rock sampling was undertaken at the Pinnacle and Gail areas. Soil sampling was undertaken in preparation of the IP surveys at both Pinnacle and Gail, while soil sampling only was undertaken at the Mat showing. On September 3, 2021, Peter E. Walcott & Associates Ltd mobilized to the Property for seven days of induced polarization (IP) pole-dipole surveying at the Pinnacle and Gail showings. Approximately 5 line-km’s of grid was surveyed using an a-spacing of 25 metres. Earlier in the summer, a 8.3 km<sup>2</sup> helicopter airborne magnetic survey at the Cathedral Area with a line-spacing of 100 metres was undertaken by Walcott.

A tilted or off-set and possible hidden extension of a Cu-Au alkalic porphyry system dominated by potassic, propylitic and sodic altered diorite, quartz monzonite/quartz monzodiorite intrusive phases is interpreted for the Cathedral Area. Highly chargeable bodies of disseminated and fracture-controlled copper-gold mineralization appear proximal to and associated with an interpreted north-south trending moderate to steeply southeast dipping syenite, interpreted to be an intrusive phase of the Duckling Creek suite. Copper-gold mineralization is related to alkalic porphyry alteration and is structurally controlled by a series of moderate to strongly resistive late predominately south-southwest and south-southeast trending, chloritic fault/shear structures that crosscut the entire Hogen batholith suite of plutonic rocks.

Continued exploration work is recommended, which includes geological mapping and prospecting outside of the Cathedral Area to develop new drill targets, in addition to continued drilling at the Cathedral Area, at an estimated cost of \$2,280,000.

## 2.0 INTRODUCTION AND TERMS OF REFERENCE

This report has been prepared by CME Consultants Inc. (“CME”) at the request of Interra Copper Corp. (“Interra”). The report details the results of the work program conducted by CME on the Thane property and provides recommendations for future work. Fieldwork was carried out from July 5 to September 15, 2021 at the Cathedral (Cathedral Main, South, Valley, Gully and Pinnacle), Aten, Gail and Mat Areas. A road-supported base camp was setup to the southeast of the Property.

The objectives of the work program were to:

- follow up on historical results at the Aten and Mat areas;
- identify areas within the Pinnacle and Gail areas that warrant testing by diamond drilling; and
- test the depth potential of the prospective targets identified at the Cathedral Area, which includes the Cathedral Main, South & Valley, Pinnacle, and Gully areas:

To fulfill these objectives, the following work was completed:

- grid establishment and soil sampling;
- IP surveying
- petrographic studies;
- geological mapping;
- rock sampling;
- diamond drilling, and
- drill core analysis.

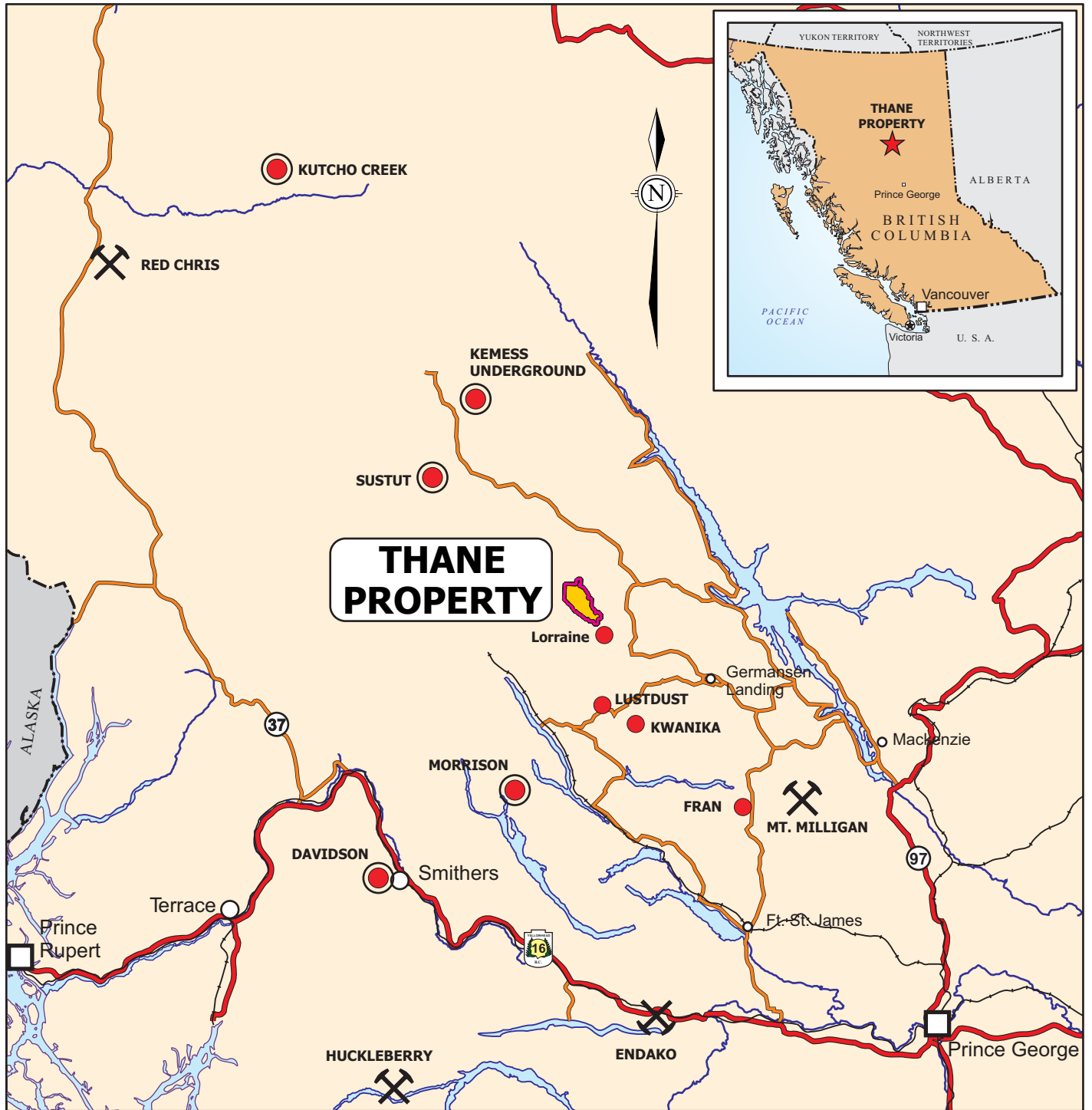
A list of definitions, abbreviations and conversion factors are presented in Appendix I. Structural orientations or Cartesian directions in this report are referenced with respect to true north.

## 3.0 PROPERTY DESCRIPTION AND LOCATION

The Thane property (the “Property”) is centred at latitude 56° 10’ N and longitude 125° 38’ W, approximately 180 kilometres northwest of Mackenzie and 185 kilometres north-northeast of Smithers (Figure 1). The Property is located in the Omineca Mining Division of north-central British Columbia, Canada.

### 3.1 TITLE

The 20,658.0347 hectare Property consists of 48 MTO cell tenures, which are 100% owned by Thane Minerals Inc., with a 1% NSR to the original claim owner. Mineral tenure details are presented in Table 1 and a plan map of the mineral tenures is presented in Figure 2.



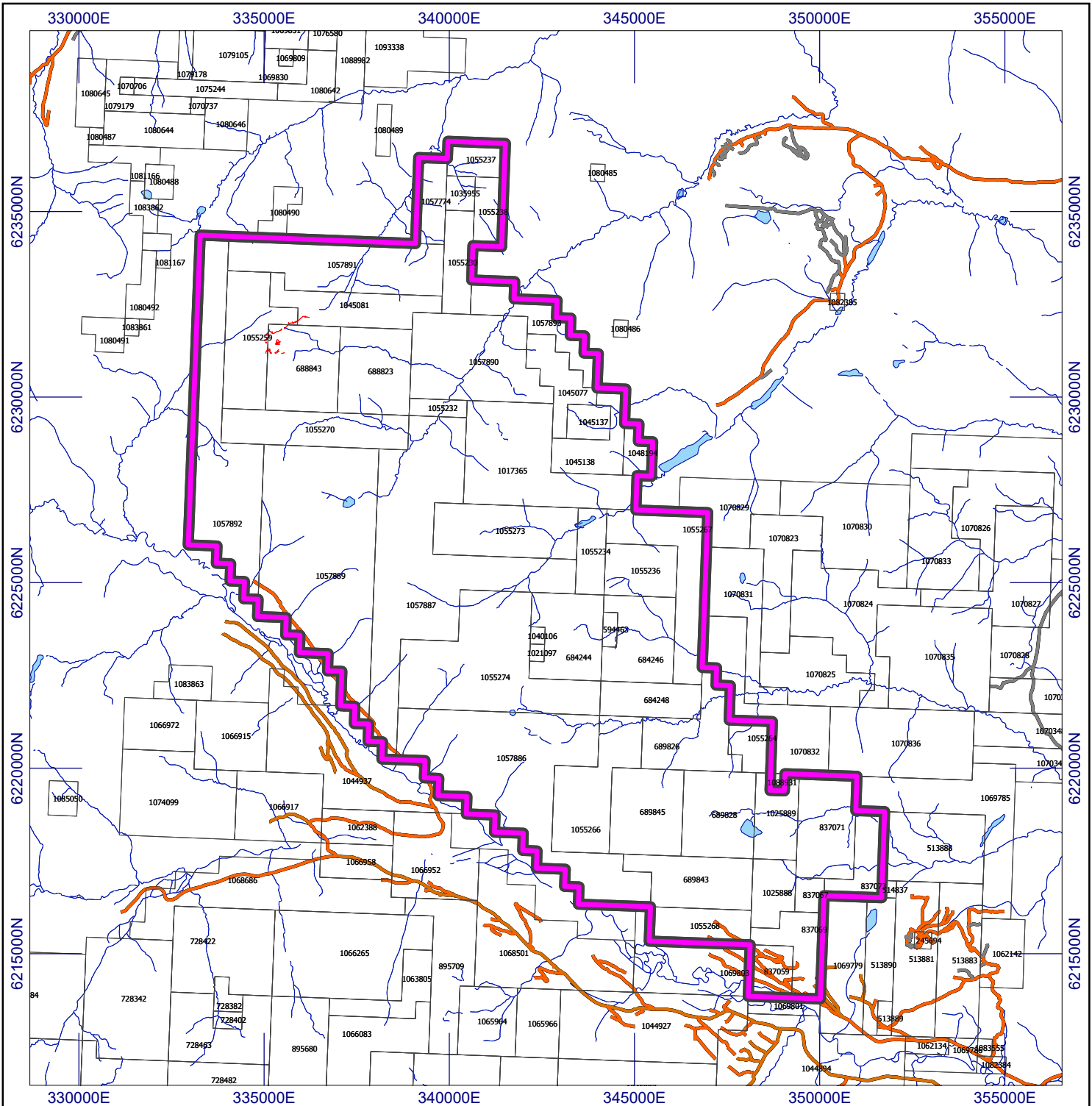
**LEGEND**

- Thane property
- Proposed mine or mine under construction
- Proposed mine development
- Major exploration project
- Highway
- Secondary routes
- Railway
- River
- Waterbody







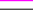
<b>INTERRA COPPER CORP.</b>	
<b>PROPERTY LOCATION MAP</b>	
Thane Property Omineca M.D., British Columbia, Canada	
Project No: P72	By: CN
Scale: 1:3,000,000	Drawn: TV, CN
Figure: 1	Date: March 2022





**LEGEND**

**TOPOGRAPHY**

-  Gravel road
-  Watercourse
-  Waterbody
-  Property outline
-  Mineral tenure boundary with tenure number (as of March 21, 202)



NAD83, UTM Zone 10 North  
94C/03, 04, 05, 06

**INTERRA COPPER CORP.**

**MINERAL TENURE MAP**

Thane Property  
Omineca M.D. British Columbia, Canada

Project No.: P72	By: CN
Scale: 1:150000	Drawn: CN
Figure: 2	Date: March 2022



Table 1: List of mineral tenures, Thane property

Tenure Number	Area (ha)	Owner	Tenure Type	Good To Date
594463	36.0654	Thane Minerals Inc.	MTO Cell	2023MAR/23
684244	414.7706	Thane Minerals Inc.	MTO Cell	2023MAR/23
684246	414.7606	Thane Minerals Inc.	MTO Cell	2023MAR/23
684248	252.555	Thane Minerals Inc.	MTO Cell	2023MAR/23
688823	450.1158	Thane Minerals Inc.	MTO Cell	2023MAR/23
688843	450.1199	Thane Minerals Inc.	MTO Cell	2023MAR/23
689826	433.0388	Thane Minerals Inc.	MTO Cell	2023MAR/23
689828	451.2893	Thane Minerals Inc.	MTO Cell	2023MAR/23
689843	415.3282	Thane Minerals Inc.	MTO Cell	2023MAR/23
689845	451.2932	Thane Minerals Inc.	MTO Cell	2023MAR/23
837059	162.6033	Thane Minerals Inc.	MTO Cell	2023MAR/23
837067	72.2301	Thane Minerals Inc.	MTO Cell	2023MAR/23
837069	252.8936	Thane Minerals Inc.	MTO Cell	2023MAR/23
837071	433.2248	Thane Minerals Inc.	MTO Cell	2023MAR/23
837073	216.6435	Thane Minerals Inc.	MTO Cell	2023MAR/23
1017365	864.7239	Thane Minerals Inc.	MTO Cell	2023MAR/23
1021097	18.0354	Thane Minerals Inc.	MTO Cell	2023MAR/23
1025888	198.6395	Thane Minerals Inc.	MTO Cell	2023MAR/23
1025889	252.7215	Thane Minerals Inc.	MTO Cell	2023MAR/23
1035955	71.9387	Thane Minerals Inc.	MTO Cell	2023MAR/23
1040106	18.0336	Thane Minerals Inc.	MTO Cell	2023MAR/23
1045077	234.071	Thane Minerals Inc.	MTO Cell	2023MAR/23
1045081	377.9497	Thane Minerals Inc.	MTO Cell	2023MAR/23
1045137	108.0609	Thane Minerals Inc.	MTO Cell	2023MAR/23
1045138	252.1758	Thane Minerals Inc.	MTO Cell	2023MAR/23
1048194	90.0613	Thane Minerals Inc.	MTO Cell	2023MAR/23
1055230	215.9103	Thane Minerals Inc.	MTO Cell	2023MAR/23
1055232	72.0359	Thane Minerals Inc.	MTO Cell	2023MAR/23
1055234	180.2442	Thane Minerals Inc.	MTO Cell	2023MAR/23
1055236	270.3817	Thane Minerals Inc.	MTO Cell	2023MAR/23
1055237	143.8463	Thane Minerals Inc.	MTO Cell	2023MAR/23
1055238	143.8938	Thane Minerals Inc.	MTO Cell	2023MAR/23
1055259	468.037	Thane Minerals Inc.	MTO Cell	2023MAR/23
1055264	144.352	Thane Minerals Inc.	MTO Cell	2023MAR/23
1055266	523.4329	Thane Minerals Inc.	MTO Cell	2023MAR/23
1055267	540.7679	Thane Minerals Inc.	MTO Cell	2023MAR/23
1055268	252.8778	Thane Minerals Inc.	MTO Cell	2023MAR/23
1055270	468.2975	Thane Minerals Inc.	MTO Cell	2023MAR/23
1055273	540.6773	Thane Minerals Inc.	MTO Cell	2023MAR/23
1055274	1100.2454	Thane Minerals Inc.	MTO Cell	2023MAR/23
1057774	179.8537	Thane Minerals Inc.	MTO Cell	2023MAR/23
1057886	1588.3245	Thane Minerals Inc.	MTO Cell	2023MAR/23
1057887	1748.4763	Thane Minerals Inc.	MTO Cell	2023MAR/23
1057889	1784.4579	Thane Minerals Inc.	MTO Cell	2023MAR/23
1057890	774.1504	Thane Minerals Inc.	MTO Cell	2023MAR/23

Table 1: List of mineral tenures, Thane Property (*cont'd*)

Tenure Number	Area (ha)	Owner	Tenure Type	Good To Date
1057891	737.7081	Thane Minerals Inc.	MTO Cell	2023MAR/23
1057892	1080.7358	Thane Minerals Inc.	MTO Cell	2023MAR/23
1057893	305.9846	Thane Minerals Inc.	MTO Cell	2023MAR/23

### 3.2 ACCESSIBILITY

Road access to the Property from Prince George is gained by taking Highway 97 north to Highway 39 (Mackenzie turnoff). At 16.2 kilometres along Highway 39, a 300 metre all-weather road exits to the west and connects to the Finlay FSR at the 8.2 km marker. At this junction, northbound travel heads to Mackenzie while southbound travel heads to Williston Lake via the Causeway and on to the Phillips Connection at the 18.6 km marker. At the Phillips Connection, the Mt. Milligan mine site and Fort St. James are accessed via the FSR that exits to the west, while access to the Thane property is north via the Finlay FSR. Continuing northward on the Finlay FSR, at the 173 km marker is the junction with the Finlay-Osilinka FSR. The Finlay FSR heads north to several small settlements such as Fort Ware, while the Finlay-Osilinka FSR heads west for 46.5 kilometres to the junction of the Osilinka FSR (46.5 km marker eastbound, 46 km marker westbound). At this junction, road signage designates the Finlay-Osilinka FSR as the Tenakihi Mainline. An abandoned logging camp is located to the northwest of the junction. The Tenakihi Mainline continues approximately 168 kilometres northwest from the junction to the closed Kemess South mine site.

From the Tenakihi Mainline/Osilinka FSR junction, access is limited to the southern and eastern fringes of the Property. Access to the southern part of the Property is by the Thane Mountain FSR (63 km marker) and the Upper Osilinka Mainline (64 km marker), which is gained via the Osilinka FSR. Access to the eastern part of the Property is by the Tenakihi FSR (14.5 km marker), which is gained via the Tenakihi Mainline. Access to the northern part of the Property is unknown, as an unnamed logging road exits to the west of the Tenakihi Mainline at the 23.8 km marker, but topographic maps show this road as being washed out.

Alternatively, helicopter charters can be obtained from Smithers, Fort St. James and Mackenzie. An airstrip is located 3.2 kilometres north of the Tenakihi Mainline/Osilinka FSR junction along the Tenakihi Mainline (west side). The condition and capabilities of this airstrip for fixed wing aircraft is unknown.

### 3.3 CLIMATE

The climate of this region of British Columbia is typically cool and moderate with warm, moist summers and cold winters. The lower elevations are typically snow-free from the end of April until the beginning of November. Snow at the higher elevations may be present well

into summer months and begins falling in September. Total snowfall ranges from 3 to 5 metres.

### **3.4 INFRASTRUCTURE**

Forest roads afford limited access to the peripheries of the property. A 240 kV transmission line follows the Finlay FSR, Finlay-Osilinka FSR and Tenakihi Mainline that serviced the past-producing Kemess South mine. The transmission line right-of-way is located approximately 8 kilometres east of the Property at its closest approach.

### **3.5 PHYSIOGRAPHY**

The property is located in Osilinka Ranges of the Omineca Mountains. The property is characterized by steep mountainous terrain. Elevations range from 960 metres in the Osilinka River valley along the southwestern boundary of the property to 2,360 metres above sea level at the mountain peaks. Numerous small tarns are found in the many cirques. Drainage is dendritic with a general flow to the southeast.

The Property is located on the eastern side of the Continental Divide and all drainage flows into Williston Lake, a man-made reservoir formed behind the W.A.C. Bennett dam and hydroelectric generating station. Drainage continues on to the Arctic Ocean.

## **4.0 HISTORY**

### **4.1 EXPLORATION AND DEVELOPMENT BY PRIOR OWNERS**

The Property has been subject to a number of preliminary regional exploration projects with only localized detailed exploration and sampling in specific areas.

Exploration of the Hogem batholith and surrounding area was initiated in the late 1800's with placer gold being discovered in the district in 1868. During the 1930's Consolidated Mining and Smelting Ltd. explored the margins of the Hogem batholith and conducted underground exploration on several properties for gold, silver, lead and mercury. Kennco Explorations Ltd. explored and staked portions of the Hogem batholith near Duckling Creek in the 1940's. In the early 1970's, mineralization on the Lorraine property discovered by Kennco and subsequently held by Granby Mining Company represented the only significant mineralization found to that date. At the time it was estimated that the Lorraine deposit contained a maximum of 10 million tons grading 0.70% copper.

In the late 1960's and early 1970's the Belgian company, Union Miniere Exploration and Mining Corp. Ltd (UMEX) of Montreal conducted extensive regional exploration in north-central British Columbia, over the Property and surrounding areas. Regional work, carried out by Dolmage Campbell & Associates Ltd., included aeromagnetic surveying and silt sampling (Kahlert, 2006). The aeromagnetic survey outlined three anomalies along the

northeast flank of the Hogem batholith. The silt sampling revealed anomalous copper values at the headwaters of Matetlo Creek. Further investigation found low-grade copper mineralization in fractures and disseminated in both the volcanic and intrusive rocks. In 1970, a soil sample grid was established over what was known as the western half of the Mate 2 claim. An open-ended east-west trending copper anomaly (>100 ppm) measuring 1500 by 750 meters was outlined. Anomalous copper values were found in silts in the headwaters of the south fork of Matetlo Creek.

Stevenson (1991) reports that during the summer of 1971, Amoco Canada conducted a reconnaissance stream sediment sampling-mapping program over the Hogem batholith in search of porphyry copper-molybdenum deposits. A total of 7,376 silts, water, rock and soil samples were collected from an area of approximately 2,400 square kilometers and analyzed for copper and molybdenum. Amoco did not assay for gold in any of these samples. Numerous areas with anomalous copper and/or molybdenum in stream sediments were detected. Four areas were staked and worked by Amoco during 1972 and 1974. These areas were known as the Tyger, Needle, Oy and Hawk properties. Property work consisted of reconnaissance and detailed soil sampling and geological mapping. The latter three properties were restaked by Cyprus in 1990 and named the Steele, Ten and Hawk properties, respectively. It is unclear how much overlap is between the Oy property and the subsequent Ten property. The former, based on limited information appears to have been located east of the Ten area, in and around the current OY occurrence (Minfile 094C 071). Geology and Exploration and Mining (1973) describes this as an area of monzodiorite and diorite, invaded by numerous dykes and apophyses of fine-grained quartz monzonite and monzonite which are in contact with Takla Group rocks. Chalcopyrite occurs as fracture coatings, coarse grains in quartz veins, and minor disseminations over the whole property. Mineralization includes chalcopyrite and specular hematite. No reports of the results of work undertaken are known.

In 1971, Fortune Island Mines Ltd. located several copper occurrences proximal to the earlier UMEX showings. Chip samples from disseminated and fracture-controlled mineralization in propylitized intrusive assayed up to 0.23% and 0.38% copper over 50 and 30 feet respectively. A chip sample across the core of a six foot wide quartz-vein assayed 2.18% copper over 3.5 feet (1.07 m). A six inch (15 cm) chip sample from a four foot (1.22 m) wide quartz-vein returned 3.52% copper and 0.02 oz/ton gold and represents the only gold assay reported. Four aeromagnetic positive anomalies were identified on and adjacent to the Mate property.

In 1972, Noranda Exploration Company, Limited staked the Gail Group claims encompassing a copper-molybdenum prospect located in a small north-facing cirque at the headwaters of Tenakihi Creek. Work on the Gail Group in 1973, included line cutting, soil sampling (40), rock geochemistry (30 talus chips representing a 200 foot section of the contour sampling traverse line), prospecting and mapping at a scale of 1"=400'. Soil and talus samples were analyzed for copper, molybdenum and zinc in Noranda's company laboratory in Vancouver, British Columbia. It was noted that in soils, zinc values were erratic and didn't correlate well with either copper or molybdenum, both of which were considered to be anomalous over the entire grid. The talus chips were noted as having values consistent with observed copper

mineralization in the cirque walls to the south and southeast and its noted absence on the walls to the west.

Major General Resources Ltd. (now Commander Resources Ltd.) acquired the extensive UMEX database when UMEX closed its Canadian operations in the early 1980's. With the discovery of the Mt. Milligan deposit and favorable metal prices, interest in copper-gold porphyry deposits resurged in the late 1980's.

In 1990, Cyprus Gold (Canada) Ltd. investigated several properties in the Thane Creek area. These included the Ten claims encompassing the Gail Area as well as the ET, OS, Hawk and Steele claim groups located south of the Property. All prospects were explored for potential gold mineralization.

Work done on the Ten and the ET claims included reconnaissance style geological mapping, soil sampling, rock sampling and proton magnetometer surveying. All soil and rock samples were analyzed for gold and copper.

On the Ten property there were no significant gold values returned from the analyses and as such, no further work was recommended for gold exploration. It was noted that the property did host several broad, moderate to strong copper anomalies associated with strongly potassic-altered syenites. Some of these anomalies were traced for greater than 1,400 metres along strike and up to 400 metres in width, with copper values ranging from 300 ppm to 600 ppm copper and a high noted at 1,200 ppm copper. From these significantly anomalous copper results, it was recommended that the property should be investigated further for its porphyry copper potential.

Soil and rock geochemistry results from the ET property yielded low gold values with a single high gold-in-soil value of 25 ppb and the highest gold value in rocks being 315 ppb. In terms of copper, several rock samples yielded results of >5000 ppm with the highest value being 1.9% copper found in float and 1.1% copper returned from an outcrop. Soil samples generally outline broad anomalous copper zones associated with the anomalous rock sample values. The largest anomalous zone measures 600 metres by 300 metres and has soil values ranging from 300 ppm to 500 ppm copper. Further exploration for gold on the ET property was dissuaded, however, as the property hosts several significant copper soil anomalies, further exploration of the property's porphyry copper potential was recommended.

The TK 1 and TK 2 mineral claims were staked by Electrum Resource Corporation in June of 1990 and subsequently worked on in the 1991 and 1992 field seasons. In 1992, preliminary mapping was done at a scale of 1:15,000 and 19 rock chip samples and 1 heavy mineral stream sediment sample were collected and analyzed. The highest copper value to come out of the 1992 work was 2,907 ppm copper from a piece of intensely calcified Takla volcanic float. The setting indicated that the float is locally derived and that further work was needed in order to define where the sample originated.

In 1991, Major General utilized the UMEX data to select specific porphyry targets within the Hogem batholith. Major General staked and subsequently explored number of properties, including the Mate property encompassed by the current Property.

Also in 1990 and 1991, a program of prospecting and sampling was performed around the Link claims which included rock, silt and soil samples. Disseminated chalcopyrite, magnetite and pyrite were noted in rock samples. Soil samples returned anomalous copper up to 261 ppm copper and a rock sample returned 1,547 ppm copper (Ethier, 1991, BC Minfile 094C 123).

Regional mapping in 1991 by BC Geological Survey crews resulted in the defining of several new occurrences on and around the Mate property, which have been added to the provincial mineral occurrence database (MINFILE). These include 094C 113 (Yak), 114 (Koala), 115 (Intrepid), 116 (Bill), 117 (Yeti) and 118 (Dragon).

During the 1991 and 1992 field season, Major General's Mate property was explored under an option agreement with Swannell Minerals Corporation. Prospecting, silt sampling and geological mapping, followed by grid-controlled soil sampling over the previously identified soil anomaly, were carried out. Mapping noted that Takla volcanics on the property were intruded by a monzonite stock in the central portion of the then current Mate property and by the Hogem batholith in the south. Narrow granodioritic dykes cut Takla volcanics proximal to the monzonite stock. Mineralization occurred as disseminated magnetite and pyrite in monzonite and volcanics; fracture-controlled malachite, azurite with or without minor chalcopyrite, and, magnetite and pyrite in monzonite; magnetite veins up to 15 cm wide with rare chalcopyrite and quartz veins with azurite, malachite and rare bornite. While extensive propylitic or potassic alteration was not found, two areas of significant copper mineralization were identified. Of particular note was malachite-azurite in quartz monzonite traced in talus for 200 metres along the base of a slope.

Lithogeochemical response from the work on the Mate claims include 7 samples of greater than 1,000 ppm copper with a maximum 3.08% copper and 0.039 oz/ton gold. Gold response was generally <15 ppb with the exception of one other sample that ran 175 ppb gold and 2135 ppm copper and two with 107 and 500 ppb gold, both with copper <65 ppm. A total of 228 soil samples were collected. Copper ranged from 14 to 468 ppm. Gold ranged from 1 to 152 ppb. Material sampled was primarily talus fines and stream sediment. Additional work including detailed mapping and sampling was recommended on the Mate property. However, interest in porphyry targets waned and shortly thereafter a major decline occurred in the provincial mineral sector leading to the inability to raise exploration funds to pursue the targets and the property was allowed to lapse.

Swannell Minerals Corporation was also working on an area designated as the Aten group of claims, partially encompassed by the current northeastern portion of the Property, and enclosing three Minfile showings: Gail, Ten and Tenakihi Creek. In 1991, Swannell contracted Reliance Geological Services Inc. to explore the Aten group of claims for its alkalic porphyry copper-gold potential. During October 1991, a program of rock sampling (11 samples), stream sediment sampling (31 samples) and reconnaissance geological mapping at a scale of

1:10,000 was carried out. Two rock samples returned copper values of 2.82% and 2.83%. Based these values and on anomalous results from stream drainages, three target areas were identified. From there, further work was recommended consisting of grid establishment, detailed geological mapping, soil sampling, and talus fines sampling.

In 1993, Swanell Minerals Corporation worked on the Aten property encompassing the Tenakihi Creek Minfile occurrence. Fieldwork was designed to follow-up the anomalous rock and soil geochemistry identified in earlier exploration. Fieldwork consisted of a surveyed grid laid out over the north-central area of the property, geological mapping on the gridded area at a scale of 1:10,000, collection of 23 rock samples and 88 soil samples both analyzed for copper and gold. Litho-geochemistry results includes 9 samples of >1,000 ppm copper with a maximum of 3.20% copper. Gold response was lower and erratic, with 4 samples greater than 100 ppb gold and a maximum of 205 ppb gold and 3,599 ppm copper. Gold response from the 88 soil samples collected was noted as being below the 5 ppb detection limit, the only exceptions being two high values of 28 and 32 ppb gold. Further work was recommended targeting three specific areas on the property.

During 1994, a regional geochemical survey was carried out by the BCGS sampling drainages throughout the 1:250,000 scale NTS map area, 94C (Mesilinka River). A total of 1068 sites were visited. Anomalous samples collected from the Property area included 302 ppm copper from a creek draining the ET area, 246, 258 and 270 ppm copper from creeks draining the Mate/Mat areas, and 216 ppm, 220 ppm and 246 ppm copper draining areas in the Ten/Gail area. Several strong gold-in-silt anomalies were also noted particularly in the north of the property (154 ppb gold) from a creek draining into Matetlo Creek. In the Ten area a sample yielded 86 ppb gold and associated with copper values greater than 200 ppm.

Phelps Dodge Corporation staked claims in the area in late 1999 after completing a regional silt sampling and prospecting program consisting of collecting 16 rock samples and 8 silt samples.

The following year, Phelps Dodge Corporation conducted preliminary soil, bedrock and silt sampling and geological mapping in the Tenakihi Creek area, located near the eastern part of the property. A total of 83 bedrock and float samples, 15 chip samples and 25 silt samples were collected from the claim area and an additional 36 rock, 8 soil and 29 silt samples collected outside the claim area. Of the grab samples collected, 23 returned greater than 0.5% copper, and 8 samples returned greater than 2% copper (Kulla, 2001). This preliminary evaluation of the Tenakihi claims identified widespread disseminated chalcopyrite, chalcopyrite-bornite-malachite-magnetite veins and chalcopyrite-bearing quartz-carbonate veins. Numerous anomalous copper zones appear to be hosted in monzonitic intrusions of the Hogem batholith and are locally associated with prominent but discontinuous east-west trending faults and shear zones within the intrusions. Results from the work of Phelps Dodge were deemed favourable, warranting a follow-up program of detailed mapping, soil sampling and trenching as well as additional prospecting outside the claim boundaries.

In 2005, renewed interest in porphyry copper-molybdenum occurrences, inspired by increased metal prices, prompted Commander Resources to review their in-house data and former



projects of the entire area. The Mate property, the Aten property, and four other prospective areas were acquired. In August 2005, a short prospecting program was completed on the Mate with 31 soil samples and 2 rock samples taken. From this cursory program further recommendations were made. These were that a detailed soil and induced polarization survey be completed, that all showings were to be re-sampled and assayed for gold and that drilling be done on any IP chargeability highs outlined in the follow-up.

On the Aten property, Commander Resources conducted a limited soil surveying and prospecting in August 2005. A total of 11 soil samples and 17 rock samples were collected while prospecting the property. This short program was successful in discovering a new high-grade copper prospect called the CJL Area, located in the southern part of the property. The CJL Area is hosted in highly altered, foliated syenite, not previously noted on the Aten property. Float samples were noted with values ranging as high as 12.4% copper. A program of detailed geological mapping, prospecting, gridding and magnetics surveying was recommended for follow-up, as well as diamond drilling on the CJL Area should it warrant further work.

Also during 2005, Geoscience BC sponsored a program of increasing the ASTER imagery dataset for the BC Ministry of Mines, Energy and Petroleum Resources. Four alteration images for each scene were prepared using combinations of the standard ASTER bands. The images are designed to map the relative abundances of siliceous rocks, iron oxides, sericite and illite, and alunite and/or kaolinite (Kilby and Kilby, 2006). This work includes coverage over the current Property.

In 2006, Geoinformatics Exploration Canada Ltd (Geoinformatics) acquired a large tract of land totaling 126,664 hectares in the Mesilinka area of the Hogen batholith through staking and option agreements with Commander Resources and Norwest Enterprises. Commander conducted a regional exploration and data compilation on the ground, focusing on porphyry copper and copper-gold skarn potential within central to northern Quesnel Terrane. The fieldwork followed an extensive phase of digital data capture, integration and interpretation, and subsequent regional target generation. The data captured and compiled included 3,168 stream sediment samples, 4,491 rock samples (and rock chip samples), and 1,455 soil samples. Of the stream samples, 226 of the were collected over the southern portion of their project area during the 2006 field season due to insufficient data available in the public domain on that particular area. In addition to the stream sediment sample collection, a two hole diamond drill campaign totaling 751.5 metres on the previously drilled Kliyul copper-gold skarn located north of the Property, aimed to further evaluate the skarn potential.

From the work done on the Mesilinka project in the 2006 season, the regional stream sediment sample program identified a number of strongly anomalous catchments to focus the 2007 field program and validate copper-gold targets identified through the data compilation process. This both confirmed the significance of known copper-gold prospects and Minfile occurrences, and identified new target areas.

Follow-up work in 2007 by Geoinformatics involved geological mapping and diamond drilling on several prospects derived from the data gathered in the previous year's work.

Within the greater area of their project, four main areas were investigated through detailed geological mapping and subsequent diamond drilling. These prospects were Norwest, Abe, Aten and Pal prospects with the Aten and Pal prospects closest to the current Property area. Two (2) diamond drill holes totaling 885.4 metres were drilled on Aten and three (3) diamond drill holes totaling 510.9 metres were drilled on Pal. Results at the Aten and Pal prospects were deemed insignificant and no further work was recommended.

Also during 2007, Geoscience BC commissioned airborne geophysical surveys including magnetics and gravity surveys as part of the QUEST Project. The surveys covered ground of the Quesnel Terrane from Williams Lake to Mackenzie, BC. The Property lies at the extreme northwestern edge of the survey coverage. Processed gravity data is available as images that cover the entire Property. Magnetic surveying did not completely cover the Property area so complete gridded coverage is not available.

During 2010, CME Consultants Inc. carried out a comprehensive compilation program of the Property and the surrounding area using data from assessment reports as well as public domain sources of geochemical, geophysical and geological data. This compilation led to identify four areas of interest. Three of the four areas of interest were visited over four days in August and September 2010. Exploration consisted of prospecting, rock sampling (69 samples) and stream sediment sampling (10 samples). In Area 1, rock sampling identified numerous anomalous samples (>0.1%) with copper and/or gold mineralization of up to 13.9% copper, and 23.6 g/t gold (also 27.6 g/t Ag). Other highlights included 1.23% copper and 0.65% copper. In Area 2, rock sampling also identified numerous samples of anomalous copper and/or gold mineralization including 2.85% copper and 265 ppb gold and 1.08% copper and 435 ppb gold. Significant results in Area 3 included 0.84% copper and 195 ppb gold and 0.54% copper and 45 ppb gold (Naas, 2011).

Follow-up exploration by CME during 2011 focused on the Cathedral Area and the Link Area in the southern portion of the Property. The Cathedral Zone has been previously referred to as Area 1 (Naas, 2011). The Link Area is in the area of the BC Minfile showing 094C 123 (Link). Geochemical sampling consisted of rock, silt and soil sampling. Numerous high-grade rock samples of over 1% copper and 1 g/t gold were collected from a variety of locations in the explored area. Sampling at the Cathedral Area in the vicinity of a high-grade copper-gold sample collected the previous year (13.9% copper, 23.6 g/t gold) returned another high-grade rock samples grading 3.29% copper and 20.1 g/t gold. Silt samples yielded strongly anomalous copper values of up to 419 ppm copper in the northwest portion of the Cathedral Area, an area which remains relatively unexplored. Silt samples from a creek draining the eastern portion of the Cathedral Area yielded anomalous gold values of up to 80 ppb gold. Soil sample analysis by a hand-held XRF unit returned anomalous copper values in the area of the Link Showing and suggest several parallel to sub-parallel zones of greater than 100 ppm copper striking in a north-north west direction with lengths of up to 500 metres and widths of up to 150 metres.

## 4.2 EXPLORATION AND DEVELOPMENT BY THANE MINERALS

In 2012, Thane Minerals (TMI) acquired the Property from CME and undertook geological mapping, rock sampling, and soil sampling within the Cathedral, Gail, Cirque and Lake Areas. Detailed silt sampling was undertaken in the Lake Area. Results returned up to 13.9% Cu from the Cathedral Showing, up to 13.0 g/t Au from the Pinnacle Showing and 4.56% Cu from the Lake Area. Silt samples from the drainage of the Lake Area returned up to 627 ppm Cu (Naas 2013).

In 2013, TMI undertook a prospecting program at the Pinnacle Showing and at the Lake Area (Naas, 2014). A total of 54 rock samples were collected at the Pinnacle Showing, while 23 rock samples were collected at the Lake Area. Additionally, a 2.275 line-km survey grid was established at the Lake Area from which 96 soil samples were collected.

At the Pinnacle Showing, series of narrow fault structures over a width of 60 metres was mapped, which contained a minimum of seven faults striking 150° to 170° and dipping 50° to 60° W. Sampling from the two westernmost and two easternmost faults of the fault returned the most significant gold results (up to 3.60 g/t Au and 7.78 g/t Au respectively), though anomalous gold is also present within the central structures of the 60 metre wide zone. Significant gold samples were found to have anomalous arsenic values, although the converse did not necessarily hold.

Of the 54 rock samples collected from the Pinnacle Showing (and its strike extensions), 16 returned greater than 0.1 g/t Au and 7 returned greater than 1.0 g/t. Additionally 8 samples returned greater than 0.1% Cu with a maximum of 2.91% Cu.

In 2015, an airborne geophysical survey was undertaken on all mineral tenures of the Thane Property and four days of prospecting at the Mat and Pinnacle Showings and the ET and Lake Areas (Naas, 2016a). The work program consisted of:

- 974 line-km of helicopter-borne magnetic and radiometric surveying;
- 22 rock samples and 7 sediment samples for geochemical analysis.

The results from the prospecting program confirmed the presence of historically reported copper mineralization at the ET Showing and silver at the Mat Showing. Stream sediment sampling at the ET Showing failed to duplicate historical tin values.

Copper mineralization was discovered in a new area within the Lake Area, north of current known mineralization.

In 2016, prospecting was undertaken on select areas of the Property (Naas, 2016b). A total of 56 rock samples and 79 soil samples were collected at the newly acquired CJL Showing. A total of 6 stream sediment samples, 49 soil samples and 24 rock samples were collected to test a historical sediment sample of anomalous gold values from the northern portion of the property, west of the Mat Showing (RS Creek). At the OY Showing, a total of 22 stream sediment samples and were collected.

At the CJL Showing, a total of 31 of the 56 samples returned greater than 0.10% Cu, with 10 samples returning greater than 1.0% Cu. The style of mineralization at the CJL Showing was observed to be a copper-rich magnetite/specular hematite breccia

At RS Creek, although the anomalous historical gold-in-silt sample was confirmed with a sample that returned 0.582 ppm Au, this sample was considered to be the result by glacial till contamination and not from bedrock sources.

At the OY Showing, the historical gold-in-silt sample was confirmed, but no other anomalous samples were returned from the creek.

In 2017, a structural and alteration study was undertaken at the Cathedral Area. Mineralization was considered to be the result of a structurally controlled alkalic porphyry system. Due to the moderate dip of the mineralization, the system was speculated to be tilted post-emplacement about a north-south to northwest-southeast axis of approximately 45 degrees, similar to Mount Milligan (Gordon *et al.*, 2018).

In 2019, 27 rock samples collected during the structural and alteration study of 2017 were submitted for petrographic study. To complement this study, samples were also submitted for multi-element and gold analysis. The petrographic study confirmed the field mapping of syenite rock at the Cathedral Showings and supports the interpretation from 2017 that mineralization at the Cathedral Area is related to an alkali porphyry system (Naas, 2019).

Sulphide mineralization consisted of pyrite and lesser chalcopyrite. The strongest copper values were found to be structurally controlled. A 2 cm quartz vein, contained within a north-south fracture system hosted in quartz monzonite, returned the highest copper grade of 1.33% Cu.

In August of 2019, 8.4 km of Induced Polarization surveying was undertaken at the Cathedral Area as a test to determine the effectiveness of this type of geophysical study. A total of 5 survey lines were established at an orientation of 080-260 Az. with stations established at 100 metre intervals. The pole-dipole survey utilized a 100 metre dipole array. Results returned three geophysical anomalous zones, with each zone returning both narrow near-surface and broad at-depth features.

In May 2020, the new ownership of TMI undertook a study to determine the quality of the results from samples previously collected by TMI that were only analyzed by pXRF. The study involved the submission for geochemical analysis of 452 rock samples pulps originally collected in 2012 from through-out the Property, and 223 contour soil samples, originally collected in 2012 from the Cathedral Area. The analytical results for both rock and soil samples returned similar values to the values returned from the pXRF. In addition to confirming the copper values, all rock samples previously collected by TMI now have multi-element results.

The first field work conducted by the new ownership of TMI undertook a two month exploration program, which commenced in early July. The program consisted of 18.05 km of

grid establishment from which 610 soil samples were collected and 12.5 km of IP surveying was completed. Geological mapping, the collection of 203 rock and three silt samples was undertaken on several areas of the property. At the end of the program 41 samples were submitted for petrographic analysis. The results from this study identified a new area which hosts gold mineralization (Ootes Showing) in addition to providing sufficient support to recommend diamond drilling at the Cathedral Area.

## **5.0 GEOLOGICAL SETTING AND MINERALIZATION**

### **5.1 REGIONAL GEOLOGY**

The Property is situated within the Quesnel Terrane, on the eastern flank of the northern end of the Hogem batholith (Figure 3). The Quesnel Terrane is an accreted Mesozoic volcanic arc terrane that forms a north-south trending linear belt of rocks approximately 1,600 kilometre long along the eastern margin of the Canadian Cordillera. The terrane is dominantly Upper Triassic to Lower Jurassic volcano-sedimentary sequences that include the Takla, Nicola and Stuhini groups. Coeval and post-accretionary Cretaceous intrusions are scattered throughout this terrane. The Jurassic to Cretaceous Hogem multi-phase batholith is the largest of these intrusions, forming the spine of this island arc allochthonous, intermontane superterrane. The northwest trending elongate Hogem batholith extends for approximately 120 kilometres from Chuchi Lake at the southernmost limits, to the Mesilinka River at the northern limit. It is bound on the west by the Pinchi Fault and on the east by the Upper Triassic to Lower Jurassic Takla volcanics.

Ootes (2019) organized the intrusive phases of the Hogem batholith into four suites, modified after Woodsworth (1976) and Woodsworth et al (1991), all of which are deformed. These suites include the Thane Creek, Duckling Creek, Mesilinka and Osilinka. Recent geochronological data complemented by bedrock mapping and geochemical studies indicate a punctual emplacement of the four distinct intrusive suites during a protracted (ca. 80Ma) interval from 207 to 128 Ma within the northern area of the batholith (Jones et al 2021). As a result, an adjustment to the suite order and several rock types within the suites has been completed within the Hogem batholith (Table 2). Ootes adopted the term Nicola Group rocks, as these rocks matched similar rocks in the southern part of the Quesnel Terrane.

Table 2: Summary of plutonic units, Hogem batholith

Suite	Rock Type	Age Range	Relative Magnetism	Other Features	Mineralogy of Note
Mesilinka	K-feldspar porphyritic granite	135-128 Ma	low	Undivided equigranular, abundant aplite, latite and pegmatite dykes, local contact parallel magmatic foliation	local garnet and muscovite, allanite common
	granodiorite to qtz. monzonite		moderate to high	contains quartz, variable amounts of biotite, weakly altered	pristine igneous mineralogy, magnetite, allanite and titanite common
	tonalite		low	typically grey and lacks K-feldspar	plagioclase and quartz.
Osilinka	equigranular granite	<160 Ma	low to moderate	Low mafic mineral content	typically <5% biotite noted, local muscovite
Duckling Creek	syenite to monzonite	182-175 Ma	moderate to high	Magmatic layering and foliated range from massive, equigranular to porphyritic, zoned K-feldspar and	K-feldspar rich and quartz. deficient, porphyritic varieties of monzonite contain orthoclase phenos frequently >5cm
	pyroxenite		high to highest	magmatic layering and foliated	high biotite content, typically contains copper mineralization and malachite
Thane Creek	diorite to qtz. monzodiorite monzodiorite and minor gabbro	207 to 194 Ma	low to high	equigranular; foliated to locally mylonitic, local moderate to extensive alteration;	pyroxene-hornblende-plagioclase bearing, coincide with K-feldspar-bearing, magnetite common
	hornblendite		high to highest	foliated, black coarse-grained to pegmatitic; locally mingled with diorite	coarse amphibole is overgrown by secondary amphibole and biotite, titanite, magnetite, and chalcopyrite common

(adapted from Ootes, 2019 and Jones et al 2021.

The Hogem batholith is transected by numerous north and north-west trending dextral transcurrent faults that span the Cretaceous to Tertiary. The Thane property is located at a dextral transfer from the Ingenika fault that lies to the west to the Pinchi fault to the East.

These dextral transfer zones commonly result in positive flower or pop-up structures as well as reverse and thrust faults within the transfer zone (Nelson and Bellefontaine, 1996).

## 5.2 REGIONAL MINERALIZATION

The Property lies in a north-northwest trend of Early to Middle Jurassic aged alkalic-type porphyry deposits that include the now operational Mount Milligan mine, the Lorraine deposit to the south and the historic Kemess mine to the north. In general, porphyry mineralization along this trend is characterized by high gold values, low-silica hydrothermal systems, alkaline progenitor intrusions and a lack of molybdenum as well as the absence of phyllic and argillic alteration assemblages (Logan and Mihalynuk, 2014).

Several of the key deposits of this area are discussed below. Locations of these and other notable occurrences are shown on Figure 3.

### Lorraine

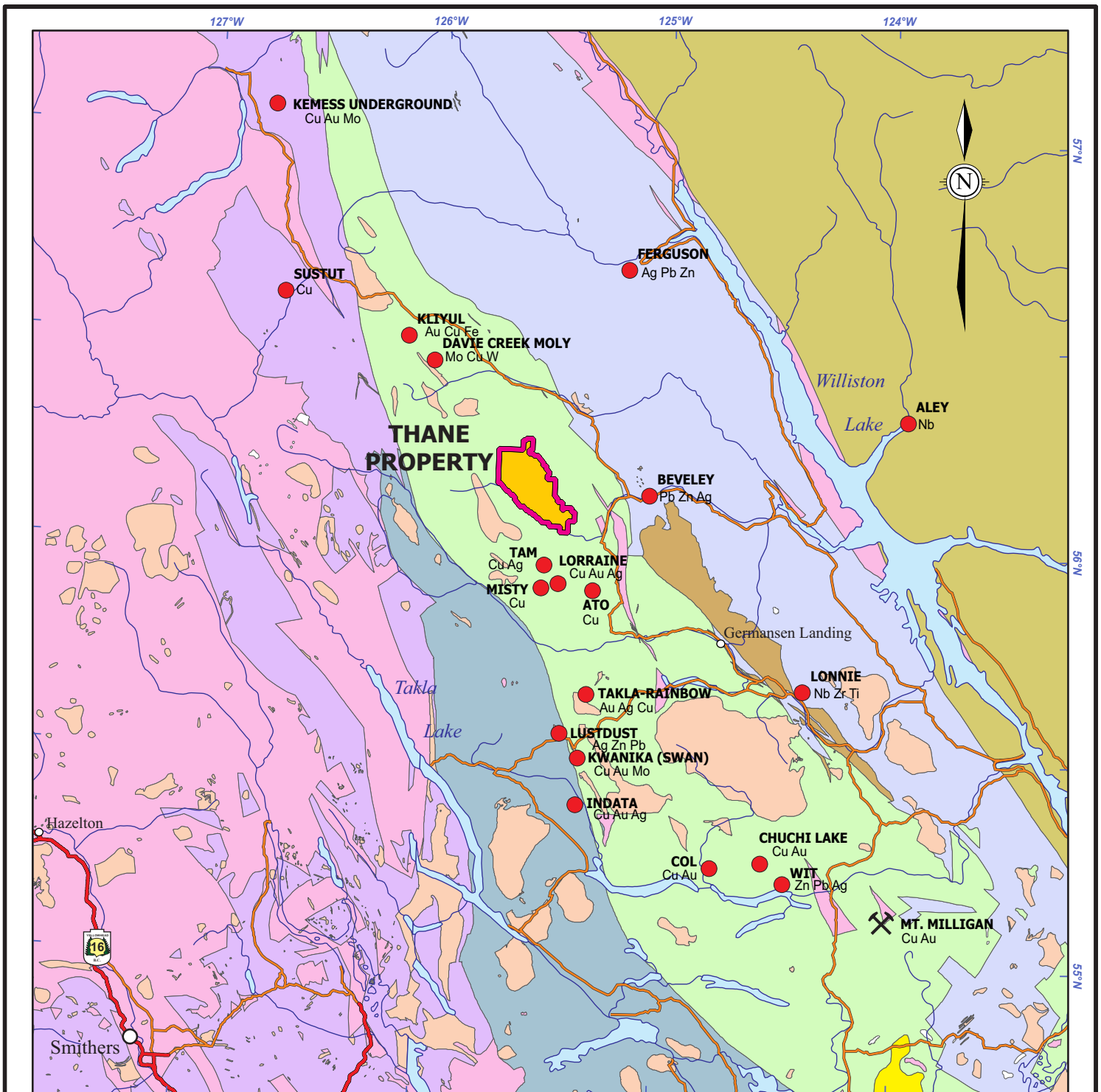
The Lorraine deposit is located approximately 16 kilometres south of the southern boundary of the Property. The deposit is hosted within rocks assigned to the Middle Jurassic Duckling Creek Syenite Complex, although rocks representing all three intrusive phases are present in the area. The complex forms a northwesterly trending, roughly elliptical body approximately 5 kilometres wide and 32 kilometres long. Rocks in the complex vary considerably in texture, mafic content and specific mineralogy, but have been subdivided into two main divisions:

- 1) pink holofelsic syenite, varying in texture from aplitic to pegmatitic; and,
- 2) pink, fine to medium-grained syenite migmatite.

Copper mineralization (with or without gold), consisting of predominantly disseminated chalcopyrite and bornite, occurs within the mafic-rich portions of foliated syenite migmatite adjacent to the northeast contact of the complex with the Phase I monzonite.

The Lorraine deposit consists of two fault-bound mineralized zones (greater than 0.25% Cu), referred to as the Upper Main and Lower Main zones. The Upper Main zone is well exposed and deeply weathered, whereas the Lower Main zone is concealed and relatively unweathered. The Upper Main zone consists of one continuous mineralized body; the Lower Main zone comprises several smaller bodies. Both zones occur in distinctly orange-coloured, foliated syenite migmatite that contains metasomatized relicts of pyroxenite, diorite, monzonite and finely banded, possibly metavolcanic basement rocks. Aplitic to pegmatitic leucocratic syenite and syenite feldspar porphyry form dikes and sills that are younger than the syenite migmatite. Aplitic to pegmatitic leucocratic granite dikes occur throughout the Upper Main zone. The dykes parallel well-developed, northeasterly trending, nearly vertical fractures and were emplaced after the period of sulphide enrichment (Minfile 093N 002).

Many other zones and areas of interest occur around the Lorraine deposit including the South Main, Copper Peak and Bishop Zones.



**LEGEND**

**GEOLOGY**

- Younger volcanics
- Post Accretionary
- Cache Creek Terrane
- Cariboo/Cassiar Terrane
- Quesnel Terrane
- Slide Mountain Terrane
- Stikine Terrane
- Overlap Assemblage
- North America

**SYMBOLS**

- Thane property
- Producing mine or mine under construction
- Major exploration project
- Highway
- Secondary routes
- Railway
- Watercourse
- Waterbody

0 50km

**INTERRA COPPER CORP.**

**REGIONAL GEOLOGY  
& ECONOMIC SETTING**

Thane Property  
Omineca M.D., British Columbia, Canada

Project No: P71	By: CN
Scale: 1:1,150,000	Drawn: TV, CN
Figure: 3	Date: March 2022





The most recent resource estimate was presented in a 2012 NI43-101 report, which included the Upper Main, Lower Main and Bishop zones. The resource estimated 6.419 Mt grading 0.61% Cu and 0.23 g/t Au of measured and indicated and 28.823 Mt grading 0.45% Cu and 0.19 g/t Au of inferred (Giroux and Lindinger, 2012).

### **Kemess**

Aurico Gold Inc.'s (Aurico) Kemess property is located in the southern part of the Toodoggone mining district in north-central British Columbia. The Toodoggone district lies within the eastern margin of the Intermontane Belt and is underlain by a northwesterly trending belt of Paleozoic to Tertiary sediments, volcanics and intrusions covering an area of 90 by 25 kilometres. The basement rocks are Proterozoic metasedimentary equivalents of the Hadrynian Ingenika Group. These rocks are unconformably overlain by volcanic and sedimentary units of the Permian Asitka Group which are in turn overlain by Upper Triassic basaltic to andesitic flows, volcanoclastics and minor limestone of the Takla Group. Volcanoclastic rocks of the Lower Jurassic Hazelton Group and rhyolitic to dacitic flows, intrusions and volcanoclastics of the Lower Jurassic Toodoggone Formation (Hazelton Group) overlie the Takla Group. Further to the west, non-marine sediments of the Cretaceous Sustut Group overlie the volcanic strata and form the western margin of the district.

The Early Jurassic Black Lake Suite of quartz monzonitic to granodioritic composition has intruded the older strata in the central and eastern parts of the region, and formed the eastern margin of the Toodoggone district. Within the district, syeno-monzonitic and quartz feldspar porphyritic dikes may be feeders to the Toodoggone Formation.

Bedrock is poorly exposed on the Kemess Property. Drilling and mapping show the geology to consist of Takla Group volcanics and sediments that have been intruded by Lower to Middle Jurassic quartz monzonite. Other intrusive compositions include granodiorite, quartz diorite and some syenite. Most of the volcanic rocks intersected in drilling are presumed to have been flows, with compositions in the basalt to andesite range. Their fine grain size and a strong alteration overprint obscure their primary mineralogy. A few crystal tuff units and lapilli-stones exist. They are not volumetrically significant and in most instances are associated with sedimentary units. Sedimentary rocks intersected in drill holes include chert, cherty tuff, argillite and graphitic argillite. The sediments are interlayered with the volcanic flows (Minfile 094E 094).

Aurico's Kemess Property hosts the past-producing Kemess South mine. This was a large alkalic gold-copper porphyry deposit. The deposit contained three principal types of ore:

- 1) a primary-sulphide hypogene ore;
- 2) a copper-enriched secondary sulphide ore; and,
- 3) an oxidized, leached cap ore.

The ore body measured 1,700 metres long by 650 metres wide and ranged from 100 metres to over 290 metres thick. A blanket of copper-enriched supergene mineralization, containing native copper, overlies hypogene ore and comprised 20 per cent of the deposit (Minfile 094E 094). The deposit itself is hosted in part in the rhyolite and mineralization consists of pyrite,

magnetite, chalcopyrite and bornite with minor amounts of molybdenite and traces of gold. They occur on fractures and in veins and interstitial to feldspars. The most important alteration is sericite which may form up to 25 per cent of the rock. A less abundant alteration is a pink potash feldspar alteration which forms selvages on quartz and/or sulphide veins and stockworks. Below this type of alteration is found, near the lower edge of the pluton, a hematite, clay, carbonate, and silica rich zone. The supergene zone, on the other hand, is above these alteration zones and it is increasingly developed as small pinprick flakes of native copper that become leaf like and eventually coalesce to form sheets of native copper at the top of the zone, in red oxidized clay rich rock. At the top is the "leach cap" which is enriched in gold and contains very little copper (Minfile 094E 094; EM Fieldwork 1998)

An initial resource estimate on Kemess South was 221 Mt grading 0.224% Cu and 0.563 g/t Au. This was a pre-feasibility resource done in 1993 by Kilborn Engineering Pacific Ltd. for El Condor and St. Phillips (Royal Oak Mines Inc., 1997). Reserves as of the end of 2009 were reported to be 22.7 Mt grading 0.14% Cu and 0.28 g/t Au. Measured resources include another 1.73 Mt grading 0.14% Cu and 0.17 g/t Au ([www.northgateminerals.com](http://www.northgateminerals.com)). The Kemess South mine ceased production in March 2011.

In an October 26, 2011 news release, AuRico Gold Inc. announced its completed acquisition of Northgate Minerals Corporation. Northgate's assets included the Kemess Underground Project located 5.5 km north of the past producing Kemess South mine.

In 2011, a Preliminary Economic Assessment for the Kemess Underground Project was completed by AMC Mining Consultants (Canada) Ltd. for Northgate Minerals Corporation, which outlined the development of an underground block/panel cave operation. Highlights of the Study include:

- indicated resource of 136.5 Mt grading 0.56 g/t Au, 0.29% Cu and 2.10 g/t Ag;
- inferred resource of 6.0 Mt grading 0.42 g/t Au, 0.22% Cu and 1.65 g/t Ag; and,
- approximate 12-year mine-life.

The Kemess Underground Project is a porphyry copper-gold occurrence hosted in the Toodoggone formation. The copper-gold mineralization forms an inclined tabular zone centered on the East Cirque porphyritic monzodiorite. Alteration and mineralization are associated with, and zoned both vertically and laterally from, the quartz diorite/quartz monzonite intrusive intersected at depth beneath the East Cirque. The highest grade gold-copper zones occur at or near the quartz monzonite-Takla volcanic contact. This zone occurs mostly within the quartz monzonite stock and to a lesser extent within the andesite adjacent to the intrusive stock. The protolith is commonly completely replaced. The quartz monzonite/quartz diorite stock and associated quartz-magnetite zone is interpreted as the heat source driving the porphyry copper-gold system ([www.auricogold.com](http://www.auricogold.com)).

### **Mt. Milligan**

Mt Milligan is located approximately 150 km south-southeast of the Property. Also located in the Quesnel Terrane, the Mt. Milligan area rocks consist of Triassic to Lower Jurassic volcanic and sedimentary rocks of the Takla Group. The Takla Group rocks are informally

subdivided into a lower, predominantly sedimentary, Inzana Lake Succession and an upper, predominantly volcanoclastic, Witch Lake Succession. The latter hosts the deposit and is characterized by augite-phyric volcanoclastic and coherent basaltic andesites with subordinate epiclastic beds and it intruded by coeval Takla Group and post-Takla Group intrusions. The coeval intrusions comprise most of the Mt. Milligan intrusive complex and consist mainly of monzonitic rocks with minor dioritic/monzodioritic and gabbroic/monzogabbroic rocks. The mineralization is hosted in monzonitic rocks (Wardrop, 2007).

Widespread disseminated mineralization accompanied by lesser veinlet and fracture-filling mineralization occurs. Mineralization consists mostly of chalcopyrite, lesser magnetite and minor bornite in areas of potassic alteration, and pyrite in areas of propylitic alteration (Minfile 093N 191).

Sporadic supergene enrichment also occurs in the Southern Star deposit. Secondary copper minerals identified in these areas consist of the sulphides, covellite, chalcocite and djurleite; the oxides, cuprite and tenorite; the carbonates, malachite and azurite and; native copper. The sulphides occur as rims around chalcopyrite; and the oxides, in particular cuprite, occur as surface coatings on native copper. Secondary copper minerals commonly occur with goethite, magnetite, hematite and siderite. Limonite, which includes goethite, commonly replaces sulphide minerals or occurs as coatings on fracture surfaces and hairline cracks.

Proven and probable reserves currently stand at 191 Mt grading 0.23% Cu and 0.39 g/t Au ([www.centerragold.com/operations/mount-milligan/production-and-reserves](http://www.centerragold.com/operations/mount-milligan/production-and-reserves)).

### **Kwanika (Swan)**

The Kwanika (Swan) deposit is situated in the northern reaches of the Quesnel Terrane. The area is structurally complex with the Pinchi fault zone being the most prominent feature. Its proximity to Kwanika Creek has resulted in strong to intense fracturing, faulting and brecciation. Fracturing within any single outcrop usually shows several orientations and these display complex crosscutting relationships. Northeast-striking faults appear to be the best developed in the area. Pyrite (with or without chalcopyrite) stringers, quartz veinlets, calcite, potassium feldspar, hematite, chlorite and epidote commonly occur within fractures.

The most common mineral present is pyrite which occurs as disseminated grains, blebby masses up to 10 centimetres across in shears and as fracture fillings in the hybrid quartz-bearing monzonite and quartz monzonite to granite phases. Pyrite as large blebs, 2 to 3-millimetre wide stringers and disseminations forming up to 20 per cent of the outcrop also occurs in rusty gossanous zones associated with intense shearing. Chalcopyrite is most often associated with pervasive chlorite alteration in the hybrid quartz-bearing monzonite phase. Here, it occurs as disseminated fine grains with pyrite and local bornite. Chalcopyrite also occurs in the quartz monzonite to granite phase as blebs up to 5 millimetres in size (with malachite and rarely azurite), as halos and on fracture surfaces. Molybdenite is rare in the hybrid quartz-bearing monzonite and quartz monzonite to granite phases. It has, however, been observed in the hybrid quartz-bearing monzonite as blebs in quartz veins. In the quartz monzonite to granite phase, it is associated with chalcopyrite and argillic alteration, occurring as disseminated grains. A gold assay value of 1.081 grams per tonne was obtained from a

sample of silicified, limonitic hybrid quartz-bearing monzonite hosting 5 per cent pyrite/chalcopyrite (Minfile 093N 073; Morton, 1989 AR 19373).

The deposit consists of two mineralized areas known as the Central Zone and the South Zone. Resources at the Central Zone are 182.6 Mt of indicated resources grading 0.29% Cu and 0.28 g/t Au and 28.5 Mt of inferred resources grading 0.18% Cu, 0.2 g/t Au. At the South Zone resources include 129.1 Mt of inferred resources grading 0.30% Cu, 0.09 g/t Au gold, 1.76 g/t silver, and 0.010% Mo. Resource grades are based upon a 0.25% Cu cutoff. Resource estimates and classifications were completed as per guidelines and definitions recommended by NI43-101 ([www.serengetiresources.com /s/Kwanika.asp](http://www.serengetiresources.com/s/Kwanika.asp)).

### **5.3 PROPERTY GEOLOGY**

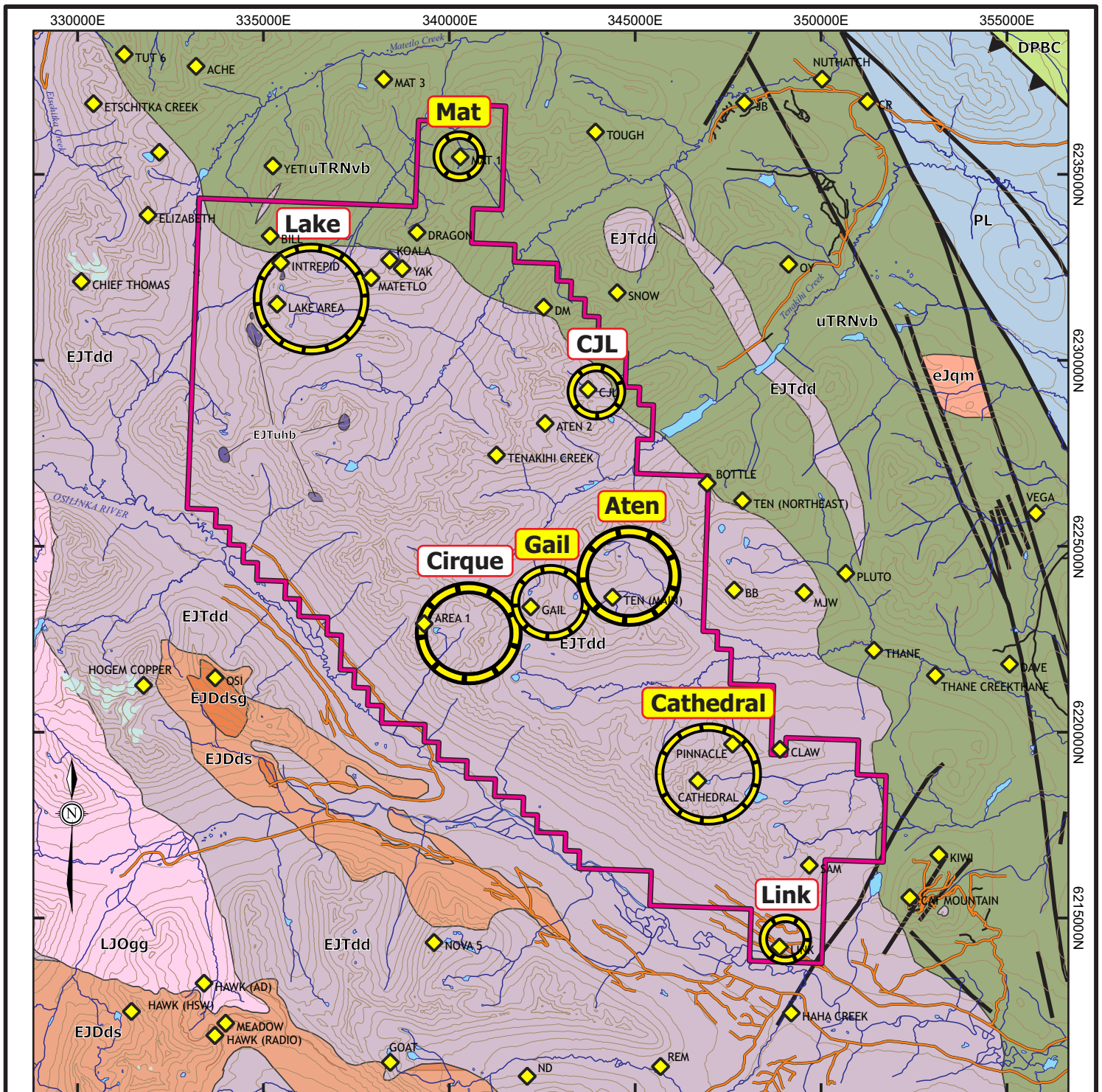
The Property is predominantly underlain by intrusive rocks of the Hogem Plutonic Suite. Undivided mafic volcanic and lesser sedimentary rocks of the Upper Triassic Nicola Group, Plughat Mountain succession are in contact with the Hogem batholith at the northeastern portion of the Property (Figure 4).

#### **Hogem Plutonic**

##### ***Hornblendite***

Predominately, within the northern areas of the Thane property, several alkali rich gabbroic whole rock classified bodies ranging from peridotgabbro (olivine bearing) to alkalic gabbro are currently interpreted to represent hornblendite classified rock types within the Thane Creek Suite. Recently provided updates to the more mafic bodies observed in these areas however have separated the more mafic-ultramafic bodies into the Abraham and Dortatelle Creek intrusive complexes. They differ from the hornblendite bodies typically found in the Lake prospect area by containing olivine and clinopyroxene rich minerals. The age of these complexes currently remains unknown, but they are considered to be Late Triassic to Early Jurassic in age (Ootes et. al, 2020b). The hornblendites observed within the Lake area occur as <10m dyke swarms in addition to small tens of centimeters to several ten's of meter sized pods and xenoliths scattered within the diorite phases. The hornblendites appear to be entirely within the diorite, display both sharp and diffuse contact margins, the latter indicating magma co-mingling and have been interpreted to be comagmatic with the diorite plutons (Ootes et., al., 2019a,b). Recent geochronological studies on a hornblendite sample yielded a CA-TIMS  $^{206}\text{Pb}/^{238}\text{U}$  zircon age of  $197.6\pm 0.1$  Ma and has been interpreted as an accurate and best estimate of crystallization age (Jones et al., 2021).

A single dark grey to black, fine-to medium grained clinopyroxenite sample collected within a xenolith hosted within monzodiorite compositionally contained 55% weakly actinolite altered clinopyroxene, 20% hornblende, 10-15% moderate to strongly K-spar and sericite altered plagioclase, 5-7% magnetite, 1-2% quartz and 1-2% apatite. The xenolith is interpreted to represent an ultramafic from either the Abraham Creek or Donatelle Creek intrusive complex



Geology after Ootes et al (BC Open File 2020-02) and BC Geofile 2005-1  
 Topographic data © Department of Natural Resources. All rights reserved



**LEGEND**

**GEOLOGY**

- Hogem batholith**
- Osilinka suite*
- LJOgg: Equigranular unfoliated granite
- Duckling Creek suite*
- EJDds: Granodiorite to Quartz diorite/monzodiorite
- EJDdsg: Biotite pyroxenite
- Thane Creek suite*
- EJTdd: Diorite to monzodiorite
- EJTuhb: Hornblende
- Nicola Group**
- uTrNvb: Undifferentiated volcanic rocks
- La Range Assemblage**
- PL: volcaniclastic rocks
- Big Creek Group**
- DPBC: mudstone, siltstone, shale

**SYMBOLS**

- ▲ Fault, thrust
- ┌ Thane property
- Secondary routes
- Contour (100 metre interval)
- Watercourse
- Waterbody
- Icefield
- ◆ ND Minfile location with name
- ⊙ Gail Prospect location with name
- ⊙ Mat 2021 Study area

**INTERRA COPPER CORP.**

**PROPERTY GEOLOGY**

Thane Property  
 Omineca M.D., British Columbia, Canada

Project No: P72	By: CN
Scale: 1:150,000	Drawn: TV, CN
Figure: 4	Date: March 2022



The hornblendite is black to dark green and weathers a dark grey. It is medium- to coarse grained and frequently pegmatitic with a 60-70% mafic component. Compositionally, it contains 50-60% black to dark green amphibole crystals, with rare corroded pyroxene and rarely talc/serpentine olivine cores, 10-30% fine to coarse grained plagioclase and where present, is interstitial between amphibole and 0-20% generally medium grained biotite. Magnetite abundance within the hornblendite varies from 1-5%, and as a result these rocks have a moderate to strong magnetic signature. Accessory minerals include subhedral titanite and euhedral to subhedral crystals of apatite are also common. Subtle epidote secondary alteration is noted within the hornblendite.

Trace amounts of disseminated to blebby pyrite and chalcopyrite occur and locally copper mineralization comprises a few percent of these rocks in areas where fractures and veinlets are noted with malachite or iron rust staining on weathered surfaces.

The magnetic susceptibility of the pyroxenite sampled in the Lake prospect area is high with a single reading of  $108.37 \times 10^{-3}$  SI units. In comparison, the hornblendite, also considered relatively high has an average of  $35.03 \times 10^{-3}$  SI units on the Property.

#### ***Diorite to Quartz Diorite***

The diorite bodies encountered appear analogous to those classified rock types within the Thane Creek Suite and with monzodiorite intrusive phases form the bulk of the mountainous areas mapped within the Property. Recent geochronological analyses on a single quartz diorite sample yield a weighted mean  $^{206}\text{Pb}/^{238}\text{U}$  date of  $206.6 \pm 0.9$  Ma (Jones et al., 2021). This weighted mean is interpreted as the best estimate for the crystallization age of quartz diorite. A single sample of diorite reports a  $196.6 \pm 0.9$  Ma zircon crystallization age, determined by CATIMS Ootes et al. (2020b, c).

They weather dark grey-green, are equigranular and medium- to coarse grained. Proximal to areas of alteration and locally mineralization they typically contain moderate to intense patchy to pervasive texturally destructive alteration with variable values of magnetic susceptibility. Where albite alteration predominates, the diorite is pale green to buff white grey in color and in areas of moderate to intense patchy to pervasive K-feldspar alteration they are orange pink in color. Quartz diorite bodies are locally noted however they frequently occur in the flanking areas of later more siliceous intrusive phases and or localized silicification. In northern and eastern areas of the property they are noted to contain a moderate to strongly developed foliation observed predominately by the alignment of mafic minerals and locally as elongated ultra mafic to mafic xenoliths of hornblendite and or volcanics.

Contacts with later intrusive phases are observed as sharp, frequently faulted and in areas with increased alteration and local mineralization, difficult to discern as they are frequently diffuse and as a result frequently inferred.

Magnetic susceptibility values of the diorite are a function of proximity to type and intensity of alteration in addition to abundance of mafic xenolithic component. Overall, the diorite has a moderate to high magnetic susceptibility with an average of  $30.61 \times 10^{-3}$  SI units on the Property.

### ***Monzodiorite to Quartz Monzodiorite***

The monzodiorite to quartz monzodiorite bodies encountered appear analogous to those classified rock types within the Thane Creek Suite. Recent geochronological analyses on a single monzodiorite sample yield a weighted mean  $^{206}\text{Pb}/^{238}\text{U}$  date of  $194.0 \pm 1.1$  Ma (Jones et al., 021). This weighted mean is interpreted as the best estimate for the crystallization age of monzodiorite.

Similarly, to the diorite phases, they weather dark grey-green, and are frequently equigranular and medium- to coarse grained with a pinkish to light green hue as a result of increased primary K-feldspar and often patchy epidote alteration of plagioclase and primary mafics. Monzodiorite phases are noted as transitional phases with the diorite and occur to some extent within all prospect areas on the Property. Monzodiorite samples collected within the Property do not contain a developed foliation at this stage; however as with the diorite have been noted to contain mafic to ultra mafic xenoliths of hornblendite, Nicola volcanics and clinopyroxenite specifically within the Lake Area. Quartz monzodiorite bodies are locally noted within the Property at the southern area of the Cirque and within the Gail Areas.

Contacts have frequently been noted within faulted areas and often appear diffuse resulting in inferred contacts.

The monzodiorite has a high magnetic signature with susceptibility values that average  $45.52 \times 10^{-3}$  SI units whereas the quartz monzodiorite bodies at Cirque contain a much lower magnetic signature with an average susceptibility of  $15.58 \times 10^{-3}$  SI units, and likely results as a function of a reduced ultra mafic to mafic xenolith component.

### ***Quartz Monzonite***

The quartz monzonite in addition to the granodiorite and tonalite are now analogous to the Mesilinka intrusive suite of S-type granites. Recently provided geochronological updates from a granodiorite phase yielded an  $^{40}\text{Ar}/^{39}\text{Ar}$  age for hornblende of Ca. 139Ma (Ootes et al., 2020b).

The quartz monzonite is fine-to medium grained, equigranular and typically weathers light grey to pinkish white depending on type and intensity of alteration. Significant outcrops of the quartz monzonite are noted within the Cathedral Area seemingly trending somewhat north south on both the East and West side of the Gully fault. At this time, they are noticeably absent or significantly reduced at the Cirque and Gail Areas where granodiorite intrusive phases predominate. Ootes has suggested these rocks to be younger than the diorite phase due to a noted lack of hornblendite phases, strong deformation and potassic alteration and older than the Duckling Creek suite as they are cut by younger K-feldspar pegmatites. Within this study these relationships have also been noted except for notable potassic alteration, specifically within the Cathedral Area, where variable moderate to strong potassic alteration dominated by K-feldspar and lesser biotite has been observed.

Comparable to the findings with Ootes, intrusive contacts are difficult to observe as virtually all are masked by either strong to intense alteration, and or within areas of strong to intense

deformation proximal to major faults and shears. As a result, most contacts are diffuse and frequently fault bounded.

Similar to the diorite phases, the quartz monzonite recorded magnetic susceptibility values are a function of proximity to type and intensity of alteration and within this study typically have a low to moderate magnetic signature with susceptibility values averaging  $22.70 \times 10^{-3}$  SI units.

### ***Granodiorite***

The granodiorite appears analogous to part of the Thane Creek Suite containing granodiorite to quartz monzonite lithologies (Ootes et al., 2019). Recently provided geochronological updates from a granodiorite phase yielded an  $^{40}\text{Ar}/^{39}\text{Ar}$  age for hornblende of ca. 139Ma (Ootes et al., 2020b) and with the quartz monzonite within this suite have now classified both units to be within the Mesilinka intrusive suite of S-type granites.

The granodiorite is fine-to medium grained, equigranular and typically weathers a light grey to greenish white. It is wholly noted to occur within the Cirque and potentially within the Gail Areas with a single potential albite altered outcropping in the higher elevations of the Cathedral area. Locally, increased silicification and patchy potassic alteration dominated by K-feldspar is observed proximal to alkali-granite (aplite) and quartz syenite pegmatitic dykes. Within the Cirque Area, a large body of the phase separates the Cirque and the Cirque East areas and dykes of the granodiorite are noted to trend northwest and dip moderate to steeply north-northeast.

Ootes has suggested these rocks to be younger than the diorite phase due to a noted lack of hornblendite phases, strong deformation and potassic alteration and older than the Duckling Creek suite as they are cut by younger K-feldspar pegmatites. Within this study these relationships related to the granodiorite are agreeable to those within his report with the exception of the cross-cutting relationship with the K-feldspathic pegmatitic bodies as they have been noted to cross-cut and locally significantly K-spar alter the granodiorite.

Intrusive contacts are typically observed as sharp and locally contain stoned diorite xenoliths proximal to contact margins. Silicification of the diorite proximal to granodiorite bodies is common and often an increase in secondary booky biotite within the diorite is noted potentially indicating hornfels of the host. At this stage, the granodiorite has only been noted to cross-cut the diorite phase within the Thane property.

The granodiorite has a low magnetic signature with susceptibility values averaging  $13.68 \times 10^{-3}$  SI units.

### ***Monzonite***

The Monzonite is analogous to part of the Duckling Creek Suite containing syenite to monzonite lithologies. Rocks within this suite are K-feldspar rich, quartz poor and texturally heterogenous ranging from equigranular to porphyritic to pegmatitic (Ootes et al., 2019). At the Lorraine Cu-Au deposit, K-feldspar rich monzonite lithologies are considered Stage 2 timing within the Duckling Creek suite constrained by U-Pb zircon ages ca 178.8 to 178.4 Ma. (Devine et al., 2014).



The monzonite weathers a mottled grey-pink to grey-green-in color, is fine- to medium grained and equigranular. Within the Cathedral Area, the monzonite frequently contains pervasive and texturally destructive strong to intense potassic and propylitic alteration. Intrusive contacts within the Cathedral Area are virtually never preserved and or exposed other than a single contact trending northeast-southwest within a brittle structure. At the Lake Area, it is observed as fine- to medium grained, rarely coarse grained, sub-trachytic, dykes (<100m in width), north-south trending moderately fractured bodies that cross-cut and biotite hornfels diorite and monzodiorite phases proximal to faulted contacts.

The monzonite contains a moderate magnetic signature with an average magnetic susceptibility of  $20.53 \times 10^{-3}$  SI units.

### ***K-Feldspar Megacrystic Monzonite Porphyry***

The K-Feldspar megacrystic monzonite porphyry is classified as part of the Duckling Creek Suite containing syenite to monzonite lithologies (Ootes et al., 2019). At the Lorraine Cu-Au deposit, the K-feldspar megacrystic monzonite porphyry along with massive syenite (below) are considered Stage 3 timing within the Duckling Creek suite constrained by U-Pb zircon ages ca 177 to 175 Ma (Devine et al., 2014).

The megacrystic monzonite porphyry is wholly observed within the Cathedral Area as localized north-south trending and rare east-west trending, frequently moderately to strongly fractured, calcium carbonate altered and faulted dykes (<3m wide). They typically weather a pale grey to pink color and are easily identifiable due to the presence of frequent megacrystic K-feldspar phenocrysts <10cm in size that are often trachytic and define a flow texture within an aphyric groundmass.

Intrusive contacts are locally sharp, chilled with a trachytic texture and predominately noted cross-cutting the diorite phase proximal to major north-south trending structures.

The K-feldspar megacrystic monzonite porphyry contains a low magnetic signature with an average magnetic susceptibility of  $9.65 \times 10^{-3}$  SI units.

### ***Syenite***

The syenite is classified as part of the Duckling Creek Suite that are K-feldspar rich and quartz deficient intrusive bodies (Ootes et al., 2019). The syenite, at the Lorraine Cu-Au deposit is considered within both stage 2 and stage 3 timing of the Duckling Creek suite. The stage 2 syenite is interpreted as porphyritic, occurs spatially with the K-feldspar megacrystic monzonite and has been historically constrained by U-Pb zircon ages ca 178.8 to 178.4 Ma (Devine et al., 2014). The stage 3 syenite is massive, occurs spatially with K-feldspar pegmatites and has been historically constrained by U-Pb zircon ages ca 177 to 175 Ma (Devine et al., 2014). Recent geochronological timing using hornblende separated from a porphyritic syenite sample yielded an integrated  $^{40}\text{Ar}/^{39}\text{Ar}$  age of ca. 177.6 Ma (Ootes et al., 2020b) and overlaps with uncertainty with a previously reported  $^{40}\text{Ar}/^{39}\text{Ar}$  biotite age of  $177.1 \pm 0.9$  for a similar syenite (Devine et al., 2014).

A massive and porphyritic variety of syenite were originally considered as a north-south trending body through the Gully and Cathedral areas. Defining and constraining their lithological boundaries relative to each other had proved difficult due to abundant alteration and structural complexity within the area. As such, they had been classified together as a single intrusive body. In comparison to the Lorraine deposit, the syenite was interpreted to be the progenitor to the alkalic porphyry system within the Cathedral Area due to both spatial proximity and temporal overlap between emplacement and copper mineralization.

Surface samples collected over the past several seasons indicate the syenite to occur as localized outcrops in a north-south trend within a gully on the western flank (hang wall) of the Gully thrust fault. Compositionally, the syenite intrusive phase contains a high K-feldspathic component and is observed to lack appreciable mineralization. As a result, it is considered a highly resistive body with a low chargeability. As most of the syenite is subsurface, current interpretations based on field surface studies combined with the use of the modelled 2D IP Pole-Dipole resistivity high and chargeability low appear to confirm the interpreted location and trend of the syenite body and its close proximity to the Gully Thrust. The highly resistive and low chargeable syenite is traceable through all east west trending IP lines and appears to dip moderately to the southeast below the Gully area.

In outcrop they weather pink to greyish orange, typically appear as massive, rarely porphyritic, and are fine- to medium grained. Post syenite emplacement veinlets of epidote +/- quartz locally with K-feldspar alteration selvages are noted to post date syenite emplacement. Syenite intrusive bodies appear to strike south-southwest and have moderate southeasterly dips. They range from unmappable cm-scale dyke swarms up to mappable bodies more than 100 meters in width, frequently with very sharp contacts that cut most observed units. Proximal to dyke contacts, the host contains predominately K-feldspar alteration with localized actinolite, chlorite and epidote alteration with localized pyrite and chalcopyrite mineralization.

Magnetic susceptibility readings for the syenite are moderate to predominately low with an average of  $17.20 \times 10^{-3}$  SI units.

### ***Quartz Syenite***

The quartz syenite may be analogous to the either the Osilinka suite or potentially an earlier phase of the Mesilinka Suite, both of which contain K-feldspar and quartz rich intrusive bodies. Preliminary studies conducted by the BCGS thought the Osilinka suite of granites was the youngest mappable suite within the batholith (Ootes et al., 2019), however recent interpretations now have this suite to be older than the Mesilinka suite (Ootes et al., 2020). Findings within this study indicate this intrusive phase is generally; poor in primary mafic's that are generally noted as biotite and are cross-cut by the alkali-granite of the Mesilinka suite. As a result, this study finds the quartz syenite is best relegated to and agree with the recent older age interpretation of the Osilinka suite relative to the Mesilinka suite.

Within the Property, the quartz syenite is at this stage wholly noted within the Cathedral Area as small intrusive dykes frequently however not exclusively proximal to or on contacts with the north-south trending (quartz) monzonite. At this stage, they appear to have a structural

preference to north-south to northwest-southeast trending and southwest dipping structures within the area of the Gully structure. They commonly contain a significant increase in both K-feldspar and silica alteration proximal to contact margins.

The quartz syenite is typically ranges from a fine- to medium grained and equigranular unit to a coarse grained to pegmatitic unit that weathers light pinkish white to orange. Thin section analysis for the fine-medium grained quartz syenite specify felsic minerals consist of 60-65%, <2mm., randomly oriented, subhedral, interlocking K-feldspar; 13-25%, <2mm., subhedral to interstitial quartz; and 10-15%, <2mm., sub-euhedral, tabular to lathe weakly sericite altered plagioclase. Mafic minerals are typically <10%, relict moderate to strongly chlorite altered, <1mm., biotite and 1-2%, <1mm., variable hematite altered magnetite. Coarse grained to pegmatitic varieties consist of 55-66%, <6mm., randomly oriented, subhedral, tabby to lathe-like microperthitic K-feldspar poikilolitically enclosing albite; 10-15%, <5mm., ragged subhedral to interstitial quartz; and 15-20%, <5mm., sub-euhedral, tabular to lathe-like weakly sericite altered plagioclase. Mafic minerals are typically <7%, <7mm., moderate actinolite±epidote altered clinopyroxene, <1mm., 1-3% <3mm chlorite altered biotite and 1-3%, <1mm., variable hematite altered magnetite. Trace sulphides of bornite, chalcocite and chalcopyrite are also noted associated with quartz+epidote fractures suggesting mineralization potentially post dates Osilinka suite host rocks.

Dyke contacts with earlier intrusive phases are noted as sharp with a <1 meter K-feldspar and silica alteration halo.

Magnetic susceptibility readings for the quartz syenite are low with an average of  $7.80 \times 10^{-3}$  SI units.

#### ***Alkali-Granite (Aplite to Pegmatite)***

The alkali-granite (aplite) appear analogous to the Mesilinka Suite that contain K-feldspar and quartz rich intrusive bodies. Within the Property this phase of intrusive is observed predominately as thin (<2m) aplitic to pegmatitic dykes, dyklets and pencil veins that cross-cut and alter both the Thane Creek and Duckling Creek suites of rocks. They are also noted to cut the quartz syenite (see above) and localized observations indicate the pegmatitic phase cuts the aplitic phase.

Within the Cathedral Area, the aplite occur as late crosscutting north-south to northeast-southwest trending sub-vertical to moderately west dipping fine grained dykes and local <1 meter gradational swarms. Within the Lake and Gail Areas they occur as more east west trending and sub-vertical. The pegmatitic varieties are observed frequently as thin dyklets <1 meter in size and often proximal to its aplitic counterpart and major structures. Where they cross-cut earlier intrusive phases, up to 1 meter K feldspar and silica alteration halos exist.

Thin section analysis for the alkali-granite/aplite specify felsic minerals consist of 55-60%, <1mm., randomly oriented, sub-anhedral K-feldspar; 15-20%, <1mm., randomly oriented, interstitial, sub-euhedral quartz and 10-15%, <3mm., randomly oriented, tabular, sub-euhedral, variably sericite and calcium carbonate altered plagioclase. Mafics are comprised of

7-10%, <1mm., variably chloritized, ragged, subhedral biotite and actinolite. Accessory variably hematite altered magnetite 1-2% and pyrite <1% are noted.

No thin section analysis has yet to be completed on the pegmatitic variety. From hand sample descriptions it is composed of ~60-65%, <15mm., coarse grained to pegmatitic, sub-euhedral, salmon-pink K-feldspar; 10-15%, <10mm sub-euhedral translucent grey quartz; 5-7%, <7mm sub-euhedral, variably sericite altered plagioclase and 5-7%, <10mm., sub-euhedral moderately chlorite altered hornblende.

Both the aplitic and pegmatitic phase are noted to crosscut all lithologies. Dyke contacts with earlier intrusive phases are noted as sharp with a <1 meter K-feldspar and silica alteration halo. Locally, late post emplacement quartz, epidote and lesser pyrite+/-chalcopyrite veining is observed within both.

Magnetic susceptibility readings for this suite are low with an average of  $7.59 \times 10^{-3}$  SI units.

### ***Porphyry Sheets (Latite Porphyry)***

Feldspar and Quartz-feldspar porphyry dykes frequently containing contact parallel magmatic foliation (trachytic texture) have been noted within virtually all study areas of the Property and were originally considered to be the latest intrusive phase analogous to the porphyry sheets and dykes suite mapped by Ootes et., al., 2019.. At Cathedral they are noted to cut both the Thane and Duckling Creek suites and locally contain magnetite veining, K-feldspar alteration and low grade copper mineralization. Often however, they are relatively fresh with a low relative magnetism and commonly contain chilled and sheared margins (Ootes et. al., 2019). Two compositionally different subtypes are noted and range in mafic composition from biotite to amphibole bearing, the latter noted to contain a trachytic texture with minor quartz and coincides with the two types observed by Ootes. Recent geochronological studies however consider these as Osilinka sheets or a felsic porphyry observed cutting rocks within the Osilinka suite. A  $^{206}\text{Pb}/^{238}\text{U}$  date of  $162.2 \pm 2.6$  Ma from a zircon has been identified, however it is unclear if this is a magmatic or inherited zircon and therefore the  $^{206}\text{Pb}/^{238}\text{U}$  date is interpreted as the maximum crystallization age (Jones et al., 2021)

In outcrop they weather a dark grey-green to brown in color, and frequently contain variable calcium carbonate, Fe-oxide and locally increased silicification and alteration. They are predominately fine-to medium grained with an obvious porphyritic texture defined by variable sericite and epidote altered fine-medium grained plagioclase, fine grained biotite or amphibole phenocrysts within an aphyric greyish brown- to green groundmass. Within the Cathedral prospect area particularly proximal to major structures they are deformed and highly chloritized. The latite porphyry occur as late crosscutting predominately north-south to northeast-southwest trending sub-vertical to moderately west to southwest dipping dykes <5meters in width.

Thin section analysis for the latite porphyry specify felsic minerals consist of 20-40% sub- to euhedral, variably clay, sericite and epidote altered tabular to latite-like plagioclase phenocrysts <5mm long, 10-15% slender, euhedral, acicular and variable tremolite/actinolite and chlorite altered amphibole phenocrysts <2 mm (rarely up to 4mm) long and 15-20%

rectangular, euhedral weakly carbonate, chlorite and epidote altered biotite phenocrysts <2mm in size. Primary quartz is not discernable in hand sample and is noted only within the trachytic textured amphibole bearing varieties as weakly strained and scattered within the groundmass in an abundance of <2%. Accessory minerals include very fine-grained magnetite 2-3% trace apatite and sphene. The aphanitic groundmass is grey-green consisting of predominately K-feldspar ranging from 25-50% in addition to plagioclase, amphibole, biotite and magnetite. Veinlets of epidote and prehnite appear to be associated with increased clay-sericite-epidote alteration of the phenocrysts.

Contacts with earlier intrusive phases range from sharp to diffuse, locally potassic to propylitic altered and frequently faulted.

The Latite porphyry is moderately magnetic with an average magnetic susceptibility of  $22.66 \times 10^{-3}$  SI units.

#### **5.4 PROPERTY ALTERATION AND MINERALIZATION**

Alteration and mineralization observed throughout the Thane Property ranges from Alkalic Cu-Au Porphyry related (Cathedral) to potential Calc-alkaline porphyry and vein hosted mineralization (Cirque, Gail, Lake and Mat Areas).

The principal areas of copper mineralization on the Property are the Cathedral (Cathedral Main, Cathedral South, Pinnacle and Gully Showings), Cirque, Gail, CJL, Mat and Lake Areas.

Copper mineralization consists predominantly of chalcopyrite with rare occurrences of bornite and chalcocite. In the Cathedral Area, areas of massive mineralization have been identified including pyrite, chalcopyrite, specularite and magnetite. Throughout the Property malachite±azurite staining is common on exposed rock faces. Molybdenite, galena and sphalerite occur as occasional accessory disseminated sulphides to more typical localized fractures and veins. Arsenopyrite, often containing significant gold mineralization is noted at the Pinnacle and Gully Showings at Cathedral commonly within or proximal to quartz+carbonate veins and southeast trending structures.

At the CJL, chalcopyrite is associated with magnetite +- specular hematite breccias. At the Mat showing, argentite and galena occurs within milky white quartz veins up to 0.4 metre in thickness.

Controls on mineralization are not yet well-defined. General observations thus far indicated that mineralization in the southern portion of the Property (i.e. Cathedral Area, Pinnacle Showing) is principally structurally controlled by south-southeast trending west to southwesterly dipping chloritic shears and brittle reactivation along easterly trending southerly dipping structures. The northern portions (i.e. Cirque and Gail Area) show a more north-south trending sub-vertical quartz-sulphide vein style of mineralization whereas the

Lake Area hosts fine grained disseminated mineralization typically within massive hornblendite.

Field relations and petrographic work indicate that the sulphide mineralization is related to the lithologically complex Hogem batholith. A rare earth element (REE) geochemistry study done on several samples taken from the Property indicates that most of the intrusive phases have a common parent magma (Naas, 2011).

Mineralization observed at the Property is similar to other well-studied alkalic porphyry copper systems in BC. Similarities include the variability and chemistry of the host intrusive complex and the style and grade of mineralization. Look-alike deposits include the deposits of the Iron Mask camp (Afton, Rainbow, DM), Galore Creek and Lorraine (Naas, 2011).

## **5.5 PROPERTY STRUCTURE**

Historical studies on the structural setting within the Cathedral prospect area in 2017 found the structural features of the Property are interpreted to be a local expression of province-scale, dextral strike-slip faulting in the Eocene. The property lies within a step-over domain from the north-northwest striking Ingenika fault to the Pinchi fault (Figure 3). The anticipated structure within such a setting would be northwest-verging reverse faults in the northern extent of the domain and southeast-verging in the southern domain. The moderate west-dipping dextral-reverse faults of the Thane property are considered to be a second order structure that is oblique and synthetic to the first order Pinchi fault. As the geometry of these faults coincides with the geometry of the speculated sinistral-normal Jurassic faults, many may reflect Eocene reactivations (Gordon *et al.*, 2018).

## **6.0 CURRENT EXPLORATION**

Fieldwork was carried out from July 5 to September 15, 2021 and consisted of:

- setup and operation of a 22 person tent camp;
- 7.5 line-km grid established at 25 metre stations (312 stations);
- 8 km<sup>2</sup> helicopter airborne magnetic surveying;
- 182 soil samples (multi-element and gold analysis);
- 5.05 line-km IP surveying
- 1.08 km<sup>2</sup> geological mapping at 1:2,000 scale; and
- 69 rock samples (multi-element and gold analysis);
- 4 rock saw discharge sludge samples (multi-element and gold analysis);
- 2,783.24 m of NQ diamond drilling from 12 holes and 9 pads;
- 2,389 core samples (multi-element and gold analysis);
- 151 standards, including 148 for core samples and 3 for rock samples.

A road-supported tent camp was established southwest of the Property at UTM10N 354315E 6212205N. An Astar B2 helicopter and pilot were supplied by Canadian Helicopters out of Smithers BC and was based full time at the Property.

Grid establishment and soil sampling was undertaken at the Pinnacle, Gail and Mat Areas. Geological mapping and rock sampling was undertaken at the Pinnacle, Aten and Gail Areas. IP surveying was undertaken at the Pinnacle and Gail areas, while drilling was undertaken at the Cathedral Area.

Details of the work undertaken at each area included the following:

- Cathedral
  - 8 km<sup>2</sup> helicopter airborne magnetic surveying;
  - 2 rock samples;
  - 2,783.24 metres of NQ diamond drilling in 12 holes from 9 pads;
  - 2,398 core samples;
- Pinnacle
  - 2.825 line-km grid established with 25 m stations (116 stations);
  - 76 soil samples;
  - 2.825 line-km IP surveying (25 m a-spacing);
  - 0.33 km<sup>2</sup> geological mapping at 1:2,000 scale;
  - 18 rock samples;
- Gail
  - 3.15 line-km grid established with 25 m stations (130 stations);
  - 53 soil samples;
  - 2.225 line-km IP surveying (25 m a-spacing);
  - 0.15 km<sup>2</sup> geological mapping at 1:2,000 scale;
  - 17 rock samples;
- Aten
  - 27 rock samples;
- Mat
  - 1.525 line-km grid established with 25 m stations (66 stations);
  - 53 soil samples;
  - 5 rock samples;

## 6.1 SOIL SAMPLING

A total of 17.5 line-km of grid was established during the work program, which included 2.825 line-km in 3 lines at the Pinnacle Area, 3.15 line-km in 3 lines at the Gail Area and the extension of two existing lines totaling 1.525 line-km at the Mat Area.

At Pinnacle, lines were oriented at 030° Az with stations established at 25 metres intervals. At Gail, lines were established at 055° Az with stations established every 25 metres. At the Mat Area, both existing lines were extended, with orientations of 060° Az with stations set at 25

metres. Due to extreme topographic relieve, one line was set to 025° Az, which allowed the line to follow the crest of the ridge.

GPS readings were collected at each station using a GLONASS equipped Garmin C66 handheld GPS receiver. Soil sampling was carried out at every station where appropriate soil material was available. Soil samples were collected from the B horizon, where possible, at depths ranging from 5 to 40 cm with an average depth of 12.0 centimetres. Soil material was placed into labeled kraft sample bags at site. Grid and sample logistics are presented in Table 3.

A total of 182 samples were delivered to ALS Minerals of Kamloops, BC for sample preparation and analysis. Analysis consisted of multi-element ICP-MS with aqua regia digestion and gold by fire assay. Methodology for sample preparation and analysis is presented in sections 7.1 and 7.2, respectively.

Table 3: Summary of grid and soil sampling

Study Area	Line	Station Start	Station End	Distance (m)	Station Spacing (m)	Station Quantity	Sample Quantity
Pinnacle	4900N	2525N	3475N	975	25	40	32
Pinnacle	5000N	2500N	3500N	1000	25	41	31
Pinnacle	5100N	2550N	3400E	850	25	35	13
Gail	2200N	4675E	5000E	325	25	14	9
Gail	2300N	3950E	4875E	925	25	38	11
Gail	2400N	3900E	4900E	1000	25	41	18
Gail	2500N	4025E	4900E	900	25	37	15
Mat	23900N	4200E	4475E	225	25	12	12
Mat	23900N	5275E	6300E	1025	25	42	12
Mat	24000N	6025E	6300E	275	25	12	11

## **Results**

Sample details, including location coordinates and selected analytical results, are presented in Appendix IIa. Certificates of analysis are presented in Appendix IIIa

Table 4 presents the results of a simple statistical analysis for arsenic, copper, gold and molybdenum using all soil samples collected by Interra from the Property since 2020. The sample population consists of 610 samples collected during the 2020 field program and 182 samples collected in 2021. For comparison, statistical analysis using a population of only samples collected during the current work program is presented in Table 5.

Historical rock samples have noted a correlation between gold and arsenic mineralization at the Cathedral Area, so arsenic is treated as a pathfinder element.



Table 4: Statistical analysis, 2020 and 2021 soil samples

Element	Sample Pass*	No. Samples	Minimum	Maximum	Mean	Standard Deviation
Arsenic (ppm)	Pass 1	792	0.8	1115.0	17.510	45.257
	Pass 2	783	0.8	107.5	14.450	15.425
Copper (ppm)	Pass 1	792	12.1	2230.0	223.640	240.176
	Pass 2	764	12.1	663.0	187.590	129.241
Gold (ppm)	Pass 1	792	0.0005	5.9900	0.0363	0.2250
	Pass 2	786	0.0005	0.4300	0.0237	0.0354
Molybdenum (ppm)	Pass 1	792	0.11	66.80	48.470	6.962
	Pass 2	754	0.11	18.30	3.620	3.120

\* Pass 2 is a calculated by using the mean + 2 standard deviation from Pass 1 as the maximum allowable value.

Table 5: Statistical analysis, 2021 soil samples

Element	Sample Pass*	No. Samples	Minimum	Maximum	Mean	Standard Deviation
Arsenic (ppm)	Pass 1	182	2.3	1115.0	30.355	87.345
	Pass 2	180	2.3	171.5	23.109	28.630
Copper (ppm)	Pass 1	182	40.0	1730.0	281.728	268.354
	Pass 2	173	40.0	663.0	230.905	139.651
Gold (ppm)	Pass 1	182	0.0005	0.1660	0.0188	0.0212
	Pass 2	173	0.0005	0.0610	0.0153	0.0128
Molybdenum (ppm)	Pass 1	182	0.48	66.80	103.160	10.157
	Pass 2	173	0.48	26.30	4.662	5.105

\* Pass 2 is a calculated by using the mean + 2 standard deviation from Pass 1 as the maximum allowable value.

### 6.1.1 Pinnacle Area

Significant mineralization at the Pinnacle Area occurs within auriferous, structurally controlled narrow quartz-arsenic breccia veins. Since arsenic is closely related to gold mineralization, Figure 5 presents arsenic values from soil samples along with gold mineralization for rock samples. Only rock samples collected within the current work program are shown on Figure 5, while soils collected in 2021 and 2020 are shown.

Anomalous arsenic levels were returned from three areas that are oriented in a northerly direction. These anomalies occur within the two most westerly lines, as the most easterly line did not return a single anomalous sample. The lack of anomalous samples in this easterly line (L5100E) is assumed to be due to the lack of a soil horizon, since the line is located at the base of the westerly facing cliff face. Of the 35 stations along L5100E, soil samples were only obtained from 13 stations.

The most northerly of the three arsenic anomalies returned the highest arsenic grades of 1115 ppm As (L5000E 3125N) and 250 ppm As (L5000N 3100). This anomaly is expressed over

125 metres from L5000N (3100E-3225E) and 100 metres on L4900N (3225N to 3325E) with the Pinnacle Showing occurring within this anomaly.

A second north-south trending arsenic anomaly occurs over 100 metres on L5000N (2750N-2850N) and 50 metres on L4900E (3025E-3075E). This anomaly returned the third highest arsenic value of 128.5 ppm As.

Approximately 750 metres to the south of the Pinnacle Grid, anomalous levels of arsenic were returned from stations located on lines L5400N and L5500N of the Cathedral Grid. The location of these samples is approximately along strike of the mapped quartz-arsenopyrite breccia veins of the Pinnacle Showing (150° Az).

### **6.1.2 Gail Area**

At the Gail Area, significant molybdenum mineralization has been returned from historical rock and soil sampling. As a result, Figure 6 presents molybdenum for both soil and rock samples collected during the current work program at a 1:10,000 scale.

The highest molybdenum value of 66 ppm Mo was returned from L2300N 4200E. This sample also returned the highest copper value of 1730 ppm Cu, which is in the centre of a 100 metre long soil anomaly on L2300N from station 4175E to 4275E. This group of samples is located approximately 80 metres down slope (northwest) of the Gail Showing. Further downslope and to the northwest, this molybdenum anomaly can be traced to L2400N (4150E-4300N) and to L2500N (4200N-4250N).

Additional molybdenum anomalies occur to the east of the above referenced soil anomaly. This anomaly covers all survey lines from L2200N (4775E – 4875E) to L2500N (4575E-4625E) with the highest molybdenum of 52 ppm Mo returned from L2300N 4800E.

Further discussion on the soil sample results is presented in Section 8.1.

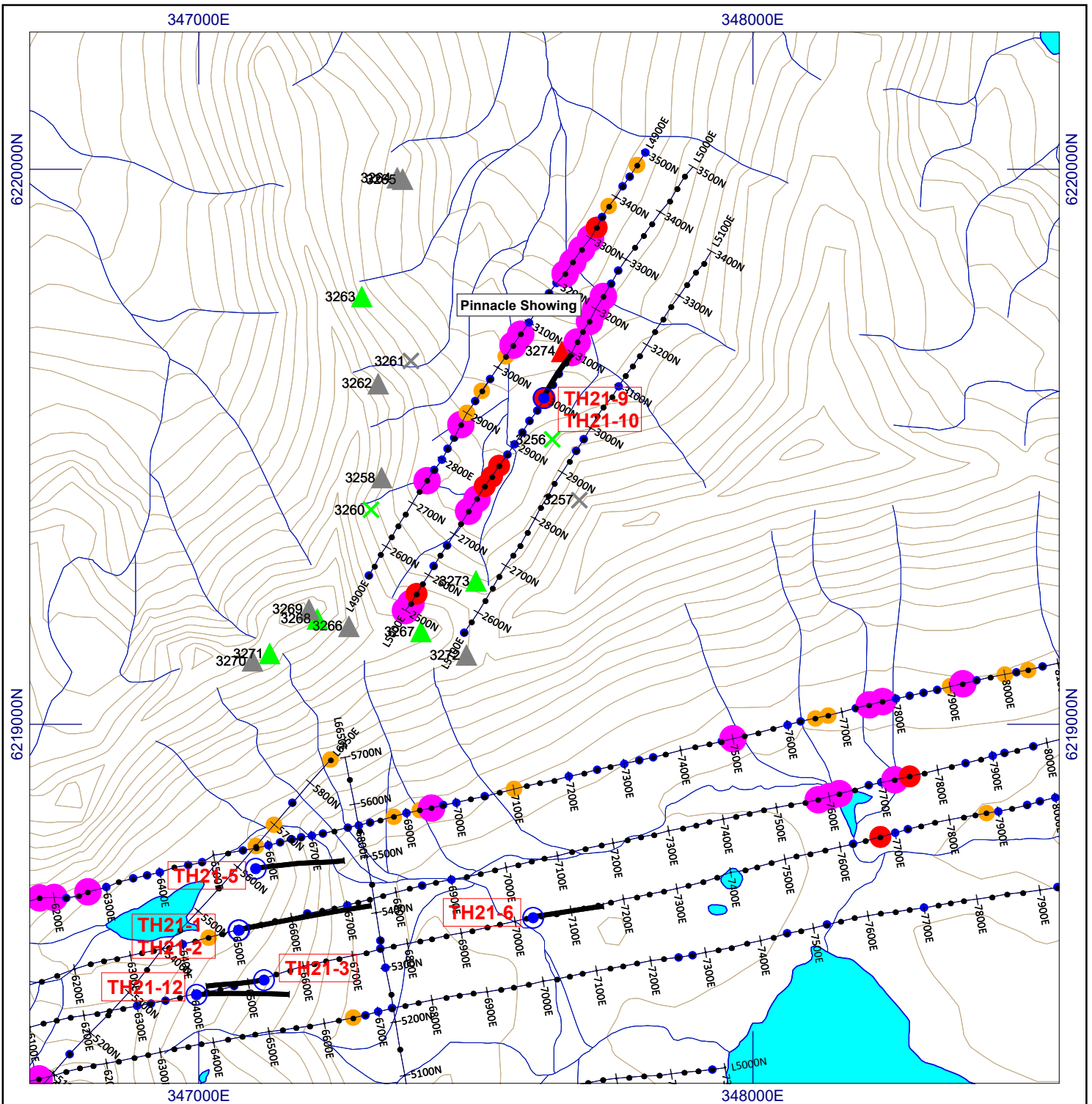
### **6.1.3 Mat Area**

Soil samples illustrating arsenic concentrations at the Mat Area at 1:10,000 scale is presented in Figure 7. Arsenic mineralization was the only element that returned anomalous levels that were traceable between lines.

Work consisted of extending the two 2020 grid lines to the west and to the east.

The extension of the grid lines refined the boundary of the arsenic anomaly discovered in 2020. This anomaly extends from 5975E to 6075E on L2400N, with a high of 63.1 ppm As. This 125 metre long anomaly is traceable for 100 metres to the southeast to L23900N from 6000E to 6125E.

A spot anomaly of 97.6 ppm As occurs at the most westerly sample collected from L23900N at 4200E, which is also the highest arsenic value from the Mat Area.



**LEGEND**

**TOPOGRAPHY**

- Contour (20m interval)
- Watercourse
- Waterbody

**SAMPLING**

- Soil
- Soil (100m station mark)
- Soil: no sample
- Rock: outcrop - grab
- Rock: outcrop - chip (m)
- Rock: float

**GEOCHEMISTRY**

**SOIL - As (ppm)**

- < 14
- 14 to 30
- 30 to 45
- 45 to 61
- > 61

**ROCK - Au (ppm)**

- < 0.1
- 0.1 to 0.5
- 0.5 to 1.0
- > 1.0

**DRILLING**

- Diamond drill hole collar location and trace with number



0 250m

NAD83, UTM Zone 10 North  
94C/03, 04, 05, 06

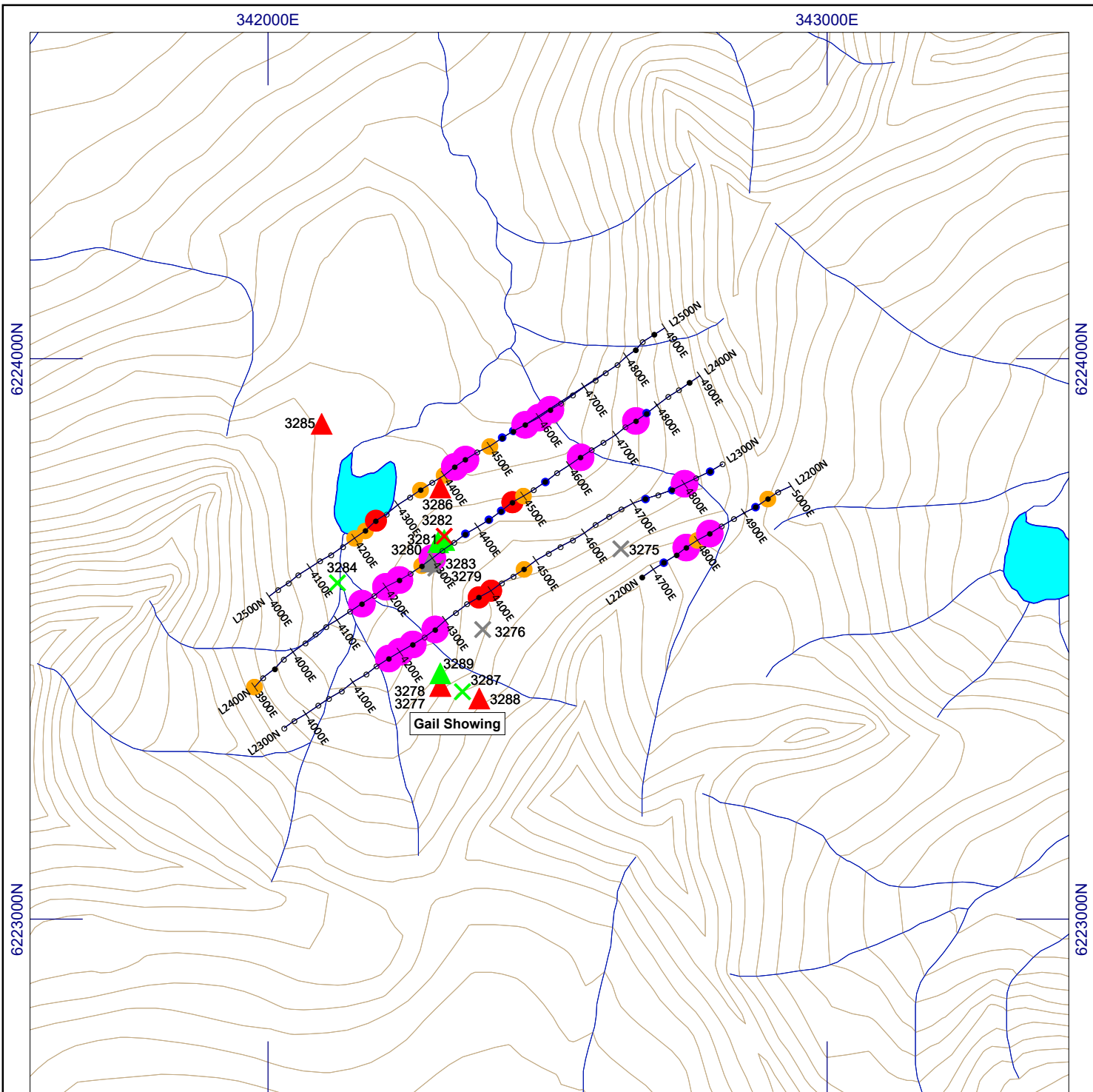
**INTERRA COPPER CORP.**

**GEOCHEMISTRY PLAN MAP  
PINNACLE AREA  
Arsenic (As) SOIL, Gold (Au) ROCK**

Thane Property  
Omineca M.D. British Columbia, Canada

Project No.:	P72	By:	CN
Scale:	1:10000	Drawn:	CN
Figure:	5	Date:	March 2022





**LEGEND**

**TOPOGRAPHY**

- Contour (20m interval)
- Watercourse
- Waterbody

**SAMPLING**

- Soil
- Soil (100m station mark)
- Soil: no sample
- Rock: outcrop - grab
- Rock: outcrop - chip (m)
- Rock: float

**GEOCHEMISTRY**

**SOIL - Mo (ppm)**

- < 4
- 4 to 7
- 7 to 10
- 10 to 13
- > 13

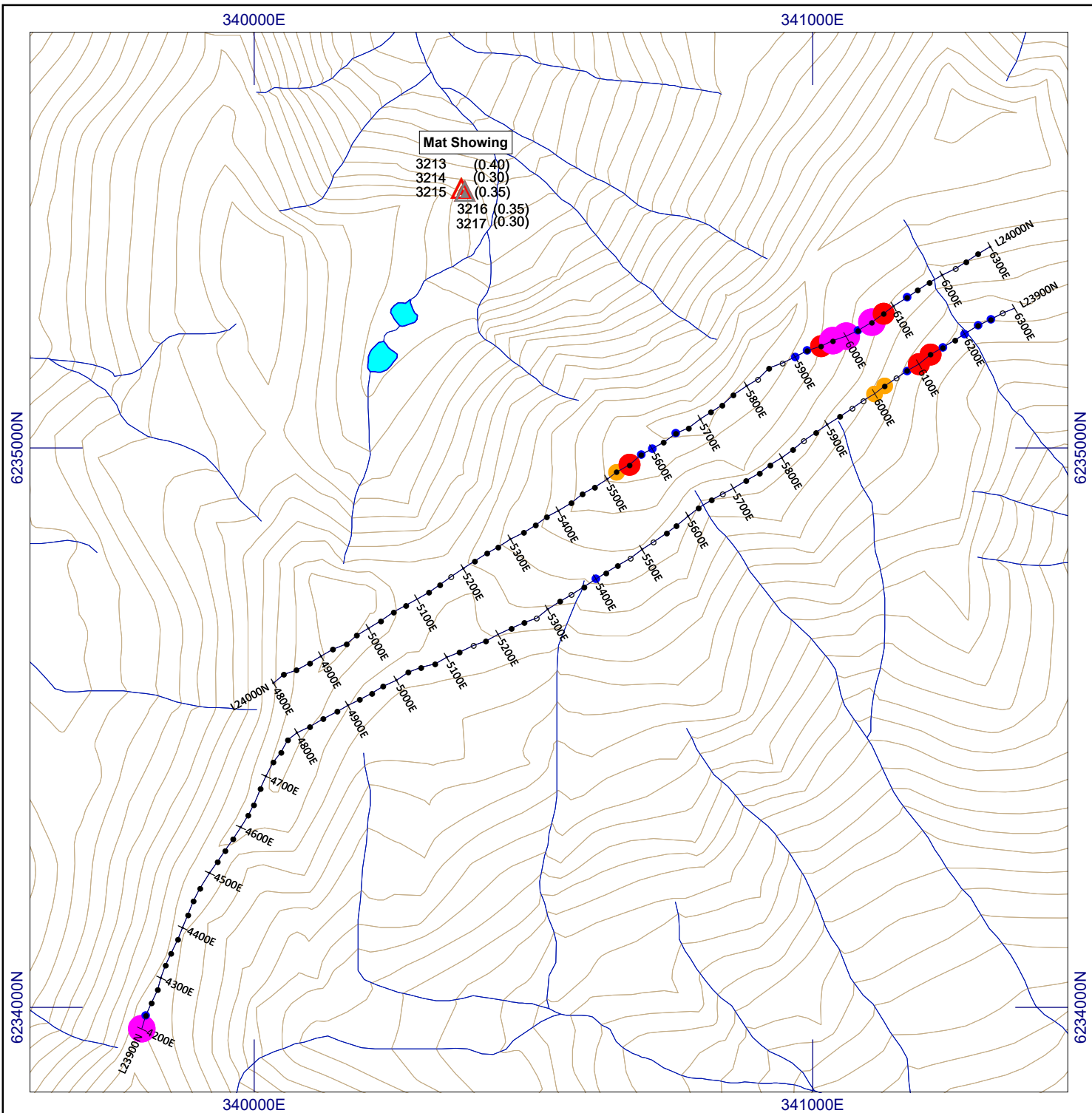
**ROCK - Mo (ppm)**

- < 10
- 10 to 50
- 50 to 100
- > 100



NAD83, UTM Zone 10 North  
94C/03, 04, 05, 06

<b>INTERRA COPPER CORP.</b>	
<b>GEOCHEMISTRY PLAN MAP</b>	
<b>GAIL AREA</b>	
<b>Molybdenum (Mo)</b>	
Thane Property Omineca M.D. British Columbia, Canada	
Project No.: P72	By: CN
Scale: 1:10000	Drawn: CN
Figure: 6	Date: March 2022



Mat Showing	
3213	(0.40)
3214	(0.30)
3215	(0.35)
3216	(0.35)
3217	(0.30)

**LEGEND**

**TOPOGRAPHY**

- Contour (20m interval)
- Watercourse
- Waterbody

**SAMPLING**

- Soil
- Soil (100m station mark)
- Soil: no sample
- Rock: outcrop - grab
- Rock: outcrop - chip (m)
- Rock: float

**GEOCHEMISTRY**

**SOIL - As (ppm)**

- < 14
- 14 to 30
- 30 to 45
- 45 to 61
- > 61

**ROCK - Ag (g/t)**

- < 10
- 10 to 50
- 50 to 100
- > 100



NAD83, UTM Zone 10 North  
94C/03, 04, 05, 06

<b>INTERRA COPPER CORP.</b>	
<b>GEOCHEMISTRY PLAN MAP</b>	
<b>MAT AREA</b>	
<b>Asenic (As) SOIL, Silver (Ag) ROCK</b>	
Thane Property Omineca M.D. British Columbia, Canada	
Project No.: P72	By: CN
Scale: 1:10000	Drawn: CN
Figure: 7	Date: March 2022

## **6.2 GEOPHYSICAL SURVEYING**

All geophysical work was undertaken by Peter E. Walcott & Assoc. Ltd (“Walcott”) of Coquitlam, BC. Although the airborne survey was not part of the original work program for 2021, Walcott was undertaking a helicopter-airborne magnetic survey in the area of the Property. Historical airborne surveys of the area had line spacing of 400 metres, so Walcott was contracted to cover 8 km<sup>2</sup> of the Cathedral Area at 100 metre line spacing. The survey was undertaken during the first week of July. On September 3, Walcott returned to undertake 5.05 line-km of Induced Polarization (IP) surveying at the Pinnacle and Gail areas.

### **6.2.1 Airborne Magnetics**

As of the date of this report, a report detailing the work undertaken and results has not been received. A Total Magnetic Intensity (TMI) plan map of the survey that was supplied by Walcott is presented in Appendix IVa.

### **6.2.2 Induced Polarization**

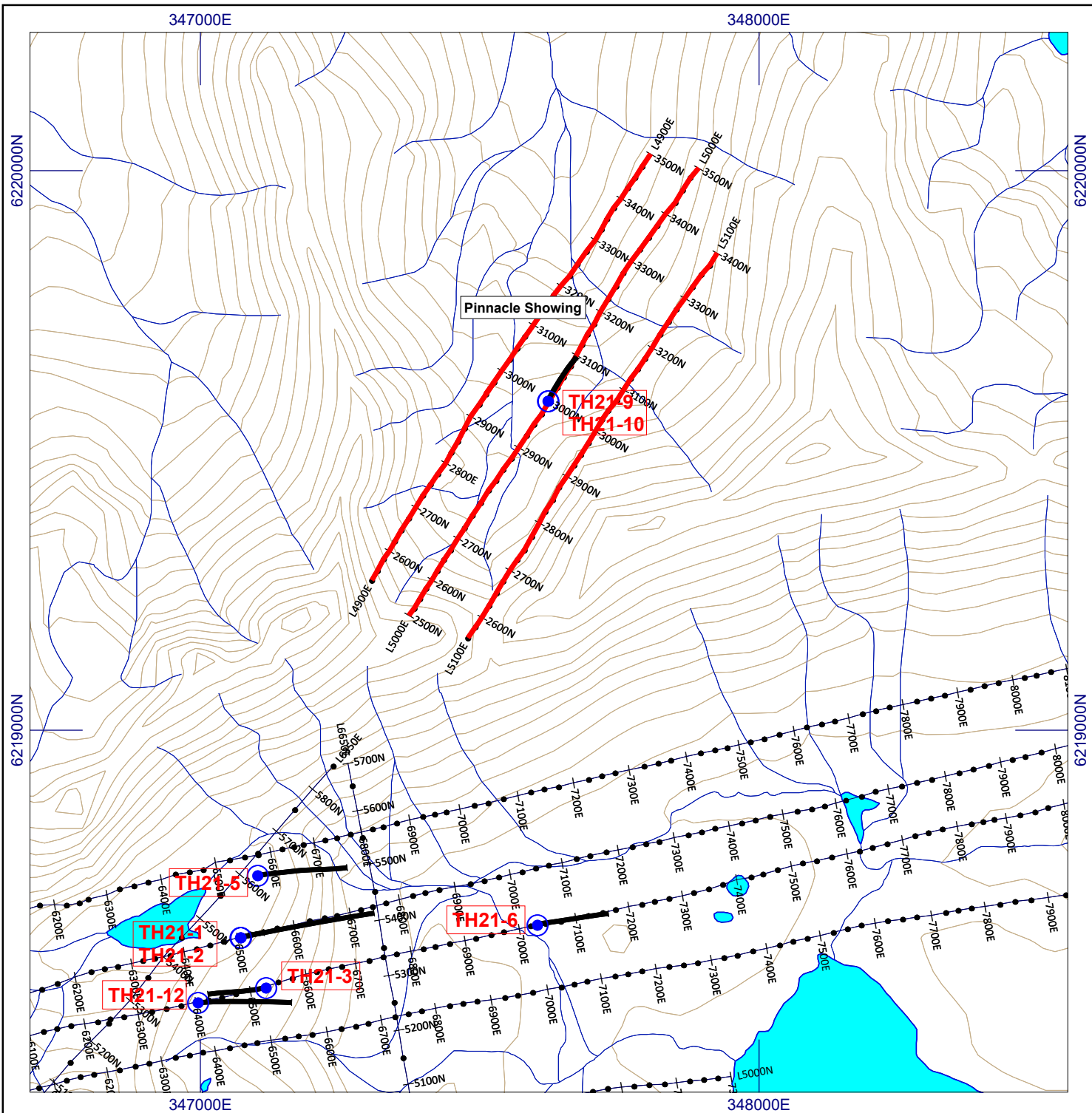
As of the date of this report, a report detailing the work undertaken has not been received. The description of the survey in this section utilized the description provided by Walcott for the IP survey undertaken at the Thane Property in 2020, since the same equipment was utilized during the current work program.

Figures supplied by Walcott are presented in Appendix IVb and c. Individual pseudo section plots of apparent resistivity and apparent chargeability at a scale of 1:2000, and 1:10,000 respectively generated using Geosoft Oasis Montaj is presented in Appendix IVb. In addition, data was subjected to 2D inversion and presented as model sections.

A total of 5.05 km of induced polarization (IP) surveying was undertaken on the Property, which consisted of 2.825 km at the Pinnacle grid (Figure 8) and 2.225 km at the Gail grid (Figure 9).

The induced polarization (IP) survey was conducted using a pulse type system, the principal components of which were manufactured by Walcer Geophysics Ltd. of Enniskillen, Ontario, and by Instrumentation GDD of St. Foy, Quebec.

The system consists basically of three units, a receiver (GDD), transmitter (Walcer) and a motor generator (Honda). The transmitter, which provides a maximum of 9.0 kw dc to the ground, obtains its power from a 20 kw 60 cps alternator driven by a Honda 24 hp gasoline engine. The cycling rate of the transmitter is 2 seconds “current-on” and 2 seconds “current-off” with the pulses reversing continuously in polarity. The data recorded in the field consists of careful measurements of the current (I) in amperes flowing through the current electrodes C1 and C2, the primary voltages (V) appearing between any two potential electrodes, P1 through P7, during the “current-on” part of the cycle, and the apparent chargeability, (Ma) presented as a direct readout in millivolts per volt using a 200 millisecond delay and a 1000



**LEGEND**

**TOPOGRAPHY**

- Contour (20m interval)
- Watercourse
- Waterbody

**GRID**

- Soil
- Soil (100m station mark)
- Soil: no sample
- IP survey coverage

**DRILLING**

- Diamond drill hole collar location and trace with number



0 250m

NAD83, UTM Zone 10 North  
94C/03, 04, 05, 06

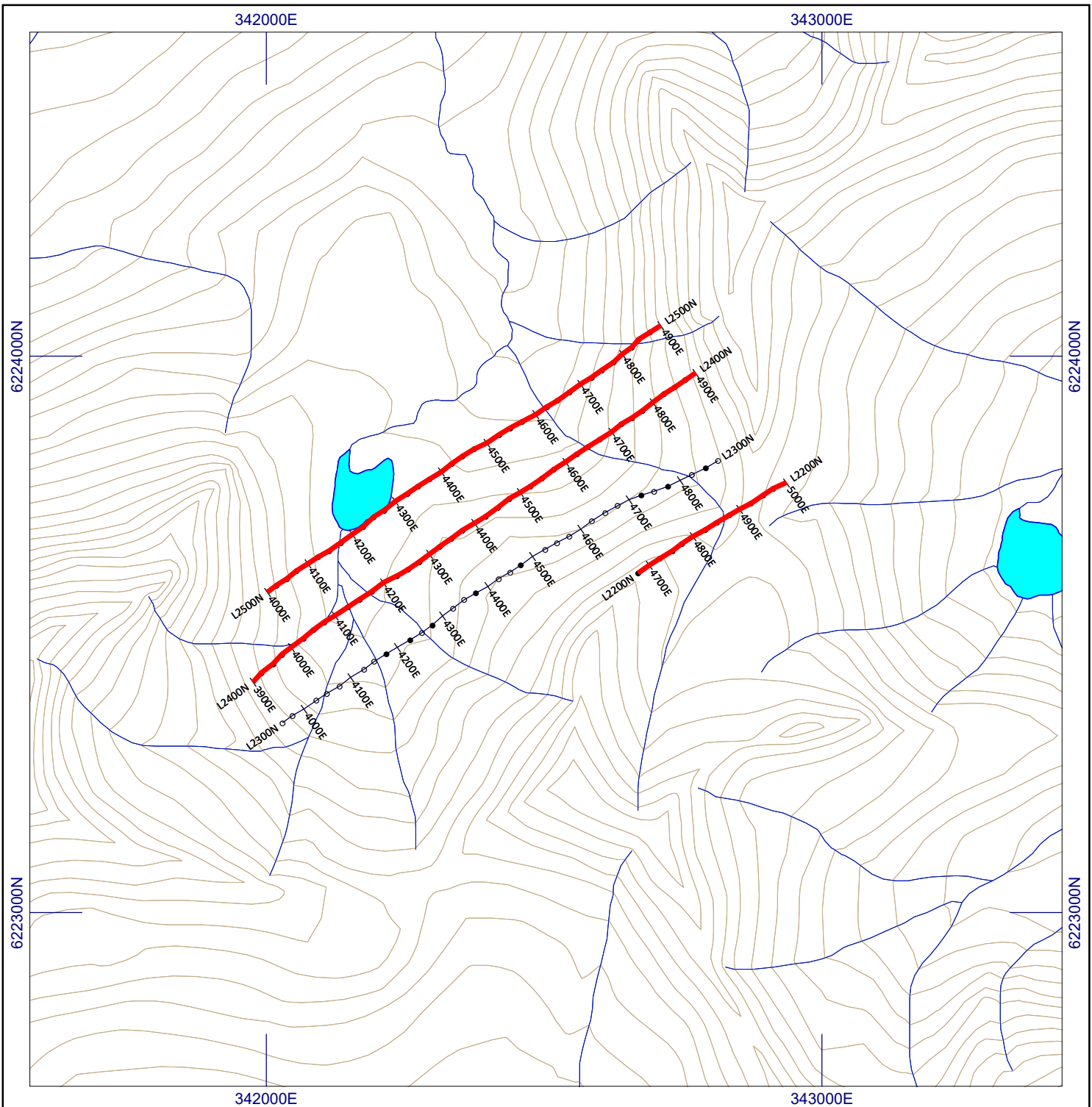
**INTERRA COPPER CORP.**

**GEOPHYSICAL PLAN MAP  
PINNACLE AREA  
IP Survey Coverage**

Thane Property  
Omineca M.D. British Columbia, Canada




Project No.:	P72	By:	CN
Scale:	1:10000	Drawn:	CN
Figure:	8	Date:	March 2022









**LEGEND**

**TOPOGRAPHY**

-  Contour (20m interval)
-  Watercourse
-  Waterbody

**GRID**

-  Soil
-  Soil (100m station mark)
-  Soil: no sample
-  IP survey coverage (2021)



NAD83, UTM Zone 10 North  
94C/03, 04, 05, 06

**INTERRA COPPER CORP.**

**GEOPHYSICAL PLAN MAP  
GAIL AREA**

**IP Survey Coverage**

Thane Property  
Omineca M.D. British Columbia, Canada

Project No.:	P72	By:	CN
Scale:	1:10000	Drawn:	CN
Figure:	9	Date:	March 2022





millisecond sample window by the receiver, a digital receiver controlled by a micro-processor – the sample window is actually the total of twenty individual windows of 50 millisecond widths.

The apparent resistivity ( $\rho_a$ ) in ohm metres is proportional to the ratio of the primary voltage and the measured current, the proportionality factor depending on the geometry of the array used. The chargeability and resistivity are called apparent as they are values which that portion of the earth sampled would have if it were homogeneous. As the earth sampled is usually inhomogeneous the calculated apparent chargeability and resistivity are functions of the actual chargeability and resistivity of the rocks.

The survey was carried out using the “pole-dipole” method of surveying. In this method the current electrode, C1, and the potential electrodes, P1 through Pn+1, are moved in unison along the survey lines at a spacing of “a” (the dipole) apart, while the second current electrode, C2, is kept constant at “infinity”. The distance, “na” between C1 and the nearest potential electrode generally controls the depth to be explored by the particular separation, “n”, traverse.

A 25 metre dipole was employed and first to sixth separations readings were obtained for both study areas.

## **6.3 GEOLOGICAL MAPPING**

Geological mapping was undertaken at the Pinnacle and Gail Areas at a scale of 1:2,000. Geology plan map for Pinnacle is presented in Figure 10 and for Gail in Figure 11.

### **6.3.1 Pinnacle Geology**

#### **Diorite**

As seen in other mapping areas, the diorite forms part of the Thane Creek suite within the Hogen batholith (Ootes et al., 2021) as discussed within the Regional Geology. At the Pinnacle Area, the diorite is fine to medium grained, equigranular and rarely observed foliated, xenolithic bearing, and unaltered. It weathers dark grey-green in color, is the dominate rock type throughout the area and typically occurs as a weak to moderately propylitic altered host.

Propylitic alteration is commonly pervasive throughout and is dominated by fracture fill, veins and pods of epidote, interstitial and fracture fill calcite and chlorite altered mafics. Chlorite is also common along joint-slip planes and hairline fractures within and proximal to localized shears frequently with secondary quartz. Increased patchy to pervasive K-feldspar dominate potassic alteration occurs contiguous to (quartz) monzonite as contact related K-feldspar alteration. Secondary K-feldspar alteration is also observed as vein selvage alteration proximal to localized magnetite veining and quartz+epidote veining whereby the latter often includes increased silicification. Both are noted to overprint pervasive propylitic alteration.

Contacts with later intrusive phases range from sharp to diffuse and are frequently inferred due to broad areas of talus cover and faulting that obscure or obliterate surface exposure. Sharp contact boundaries are generally associated with late dykes of megacrystic monzonite and latite porphyries that crosscut the diorite. Contacts of (quartz) monzonite intrusives tend to have diffuse contact margins due to increased K-feldspar alteration often associated with magnetite veining as well as chlorite sheared and localized brittle brecciation and overprinting carbonate (calcite) alteration and infill.

### **(Quartz) Monzonite**

The (quartz) monzonite forms part of the Duckling Creek suite within the Hogem batholith (Ootes et al., 2020). Rocks within this suite are K-feldspar rich, quartz poor and texturally heterogeneous ranging from equigranular to porphyritic to pegmatitic (Ootes et al., 2019). At Pinnacle, the (quartz) monzonite is a relatively large north-south trending intrusive body that cuts through the diorite along the base of the western north-south trending ridgeline. The unit weathers a mottled grey-pink to grey-green in outcrop and is easily differentiated from the diorite away from contacts by its fine to medium equigranular grain size. Sharp contacts between the (quartz) monzonite and diorite are rarely observed typically due to strong secondary K-feldspar related to magnetite±pyrite veins and fractures. Pyrite is generally disseminated in trace amounts within the (quartz) monzonite however, proximal to or within magnetite veins and localized chloritic shears can be highly concentrated in amounts  $\leq 35\%$  alteration. A single clear contact was noted trending southwest and dipping moderately westward.

### **K-Feldspar Megacrystic Monzonite Porphyry**

A single K-feldspar megacrystic monzonite porphyry dyke comparable to intrusions considered as Stage 2 timing within the Duckling Creek suite at the Lorraine Cu-Au deposit (Devine et al., 2014) and Phase 3 within the Cathedral area (Naas *et al* 2020) is observed along the southernmost ridgeline within the Pinnacle area. It occurs as a  $\leq 4\text{m}$  wide southeast trending moderately southwest dipping dyke that cuts the diorite.

In outcrop, it is observed highly fractured and locally faulted and weathers a pale grey to pinkish orange in color. It is easily identifiable by the presence of large K-feldspar phenocrysts ( $\leq 10\text{cm}$ ) within a greenish pink-brown aphyric groundmass (Plate 1). Smaller phenocrysts of plagioclase ( $\leq 5\text{mm}$ ) are often moderate to strongly replaced by fine sericite and calcite. Small weak to moderately chlorite altered hornblende phenocrysts ( $\leq 5\text{mm}$ ) are also noted. The groundmass contains moderate to strong sericite-chlorite-carbonate alteration.

No sulphides were observed within or along the contacts at this location. At this stage, the megacrystic monzonite porphyry is considered to represent one of the latest intrusive emplacements at the Cathedral Area and appears to post-date porphyry related alteration and mineralization.



Plate1: K-Feldspar megacrystic monzonite porphyry within the Pinnacle Area.

### **Porphyry Sheets (Latite Porphyry)**

A single occurrence of a  $\leq 7$ m wide southeast trending moderately southwest dipping latite porphyry dyke was observed cutting the diorite along a steep section of the southernmost ridgeline within the eastern area. In outcrop it weathers dark grey-green in color and is easily identified due to its porphyritic and trachytic texture. The dark green aphyric groundmass hosts moderate to strong carbonate-chlorite alteration. Plagioclase phenocrysts ( $\leq 4$  mm) are often weak to moderately replaced by sericite and lesser epidote. Mafic phenocrysts of hornblende ( $\leq 4$  mm) contain moderate chlorite and carbonate (calcite) alteration.

### **6.3.2 Pinnacle Alteration**

#### **Main Stage Propylitic**

Throughout most of the mapped area the diorite and (quartz) monzonite display what is considered to be variable main stage outer propylitic alteration defined by chlorite, epidote, quartz and calcite as described previously. Pyrite is ubiquitous throughout, occurring concentrated within veins and shears, or frequently disseminated in trace amounts within most intrusive hosts.

Increased chlorite alteration at Pinnacle is most intense along shear zones that cut or typically within or proximal to diorite-monzonite contacts. Several chloritic shear structures have been identified throughout the area, at the Pinnacle Showing and within drill holes TH21-9 and TH21-10. The shears range in width from a couple centimeters to almost a meter and are centralized around a band of foliated chlorite where the host rock has been completely

obliterated. The surrounding rock is strongly chlorite altered, with weak to moderate sericite, silica and carbonate (calcite) alteration the latter frequently occurs interstitially proximal to late calcite veins and fractures. Locally, magnetite as veinlets appear to crosscut and infill shears as blebby masses surrounded by chlorite and where increased quartz+calcite noted magnetite is often altered to hematite. Pyrite is frequently observed disseminated within shear zones and or within veins with concentrations up to 50% replacing magnetite (Plate 2). Quartz or quartz-carbonate veins and breccias (Plate 2) may or may not be present along the same plane as the shear. If quartz is present, K-feldspar flooding of the host rock usually occurs, indicating potassic fluids are also utilizing the same structures.

### **Main Stage Chlorite-Sericite**

Given the strong presence of chlorite and the frequent increase in sericite alteration of plagioclase to sericite at the Pinnacle Showing, there is a possibility the showing and areas 700 meters to the southwest and 400 meters to the west fall within the chlorite-sericite alteration zone. Within the zone, diorite tends to exhibit a characteristic pale green color and scratches easily indicative of increased sericite. Other minerals that are relatively abundant in the zone and support the existence of chlorite-sericite alteration are hematite, pyrite, and an increase in clay.

### **6.3.3 Pinnacle Mineralization**

#### **Late Stage Veins**

At least four unique vein systems are recognized within at Pinnacle. The most common veins bearing significant mineralization mapped at surface are vuggy and or crustiform quartz-carbonate±arsenopyrite±pyrite±chalcopyrite veins. These are most common along chloritic shear planes and are best established at the Pinnacle Showing. Given the banded nature of these veins and their dual mineralogical composition, they likely represent cycles of hydrofracturing and resealing of the shears from multiple generations of hydrothermal fluid pulses, which has caused an enrichment in remobilized sulphides. A single silica breccia vein with minor carbonate and trace pyrite±chalcopyrite (Plate 3) was also mapped along an east-west trending fault zone within the northern part of the study area. Milky quartz ± epidote ± calcite veins with K-feldspar selvages are observed within both the diorite and (quartz) monzonite. These veins locally contain pyrite within the K-feldspar alteration selvage replacing chlorite altered primary mafics. Magnetite + pyrite ± chalcopyrite veins occur frequently proximal to the diorite-(quartz) monzonite contact areas.



Plate 2: Sample #3261 (left) is a float sample taken below a chloritic shear zone containing semi-massive pyrite replacing magnetite. Sample #3264 (right) is a 7cm quartz-calcite breccia within an east-west trending fault zone containing trace disseminated pyrite±chalcopyrite.

### **Chlorite-Shear Hosted Mineralization**

The Pinnacle Showing is the most mineralized area within the study area. Arsenopyrite+pyrite+chalcopyrite±molybdenite mineralization occurs within a chloritic shear zone within the contact area between diorite and (quartz) monzonite (Plate 3).



Plate 3: Mineralized chloritic shear zone at the Pinnacle Showing. The dashed yellow lines delineates 10cm southeast trending moderate southwest dipping quartz-calcite vein. The dashed red lines delineates arsenopyrite+pyrite within sinistral chlorite shear parallel to sulphide veins.

Mineralized chlorite shears are not restricted to the Showing, however significant arsenopyrite mineralization is restricted to the Showing. Chloritic shears have been located virtually everywhere at Pinnacle with the exception of directly north of the Showing where dense

vegetation conceals outcrop. Along the far eastern extent of Pinnacle (beyond line 34800 E) the shears are significantly less altered and contain trace to nil sulphide mineralization, indicating an eastern boundary for mineralization. To the south and west shears within the diorite range from intensely chlorite altered bearing semi-massive pyrite ~ 400 meters south and ~ 300 meters west of the showing, to progressively less chlorite altered with only a few percent pyrite beyond those distances. This trend correlates with the boundaries of the chlorite-sericite alteration zone discussed in the alteration section above.

### **Disseminated Porphyry-Type Mineralization**

Outside of diorite-(quartz) monzonite contacts, localized shear zones and areas of increased quartz-carbonate vein breccias, disseminated pyrite±chalcopyrite is noted within the diorite, (quartz) monzonite, and latite porphyry typically in trace amounts. The only rock noted to be unmineralized is the K-feldspar megacrystic monzonite porphyry. In general, an increase in chlorite alteration relative to shears and shear related fractures as well as K-feldspar relative to magnetite and quartz±epidote usually correlates to higher concentrations of disseminated sulphides.

### **6.3.4 Pinnacle Structure**

#### **Hydrothermal Vein Geometry**

A total of 16 hydrothermal veins (Table 6) were mapped at Pinnacle. Overall, there appears to be two major structural patterns: The first are northwest-southeast trending and west dipping (note: five occur within 100 meters at the Pinnacle Showing) and the second are northeast-southwest trending and west dipping. A rare quartz-carbonate (calcite) breccia vein is east-west trending and sub-vertical.

Table 6: Pinnacle area vein structure

<b>Vein Type</b>	<b>Strike</b>	<b>Dip</b>	<b>Width (cm)</b>	<b>Easting</b>	<b>Northing</b>
Quartz	178	62	3	347271	6219177
Qtz-Carb	155	90	not measured	347925	6219393
Qtz-Carb	156	42	3	347324	6219614
Qtz-Carb	156	62	not measured	347636	6219671
Quartz	147	48	not measured	347648	6219674
Quartz	165	70	7	347655	6219672
Quartz	147	42	not measured	347668	6219688
Qtz-Carb	145	42	10	347675	6219684
Magnetite	172	78	not measured	347331	6219754
Quartz	206	88	5	347500	6219258
Magnetite	186	52	< 1	347311	6219420
Quartz	220	54	2	347330	6219444
Qtz-Carb	198	78	not measured	347627	6219666
Quartz	222	85	2-4	347294	6219771
Quartz	204	69	1	347368	6219982
Si Breccia	100	90	7	347358	6219985

### **Geological Contacts**

The (quartz) monzonite is the largest intrusive body noted to cut the diorite within at Pinnacle. Contact interpretation suggests the (quartz) monzonite is a north-south trending body, at minimum 60 meters wide traceable for approximately 800 meters along the base of the western north-south trending ridgeline.

The K-feldspar megacrystic monzonite porphyry dyke can be traced along strike for 130 meters cutting the diorite. Two sharp contact measurements taken 40 meters apart indicate the dyke trends southeast and dips moderately southwest. As a result of significant faulting, the contacts were noted to be highly fractured and may be offset.

The latite porphyry appears to follow the same structural plane as the K-feldspar megacrystic monzonite porphyry dyke. It was also observed cutting the diorite on a sharp contact trending southeasterly and dipping moderately southwest. At Pinnacle, it appears both dykes may utilize late east-southeast trending south-southwest dipping structures. Similar trending structures, typically containing increased quartz-carbonate (calcite) are also noted locally within the Cathedral Main and Cathedral South areas. However, latite porphyry dykes have been interpreted to trend north-south and dip moderately to shallow westward within the Cathedral Area. As a result, both are likely offset by faults and shears post dyke emplacement.

### **Fault Zones, Shears, & Joint Planes**

Chlorite shears have been identified as the dominant host to mineralization at Pinnacle. The shears generally have a north-south trend relative to brittle frequently quartz-carbonate infilled and healed fault structures which are more east-west trending. Table 7 presents structural interpretations for both ductile shears and brittle faults based on outcrop observations and review of LiDAR over the Pinnacle area. Jointing within the diorite seems to reflect larger scale north-south trending shears, which may suggest shearing initiates along joint planes.

Table 7: Structural measurements from the Pinnacle area

<b>Type</b>	<b>Trend Class</b>	<b>Strike/Trend</b>	<b>Dip</b>
Shear	N-S	190	44
Shear	N-S	189	59
Shear	N-S	188	57
Shear	NW-SE	127	-
Shear	N-S	198	59
Shear	NE-SW	206	88
Shear	NE-SW	201	69
Shear	N-S	170	57
Shear	N-S	184	64
Fault	E-W	105	-
Fault	E-W	270	69
Fault	NE-SW	060	-
Fault	E-W	290	87

Table 7: Structural measurements from the Pinnacle area (*cont'd*)

Type	Trend Class	Strike/Trend	Dip
Fault	E-W	290	-
Fault	E-W	115	60
Fault	N-S	160	-
Fault	N-S	170	-
Fault	E-W	104	67
Fault	NW-SE	143	46
Joint	N-S	348	36
Joint	N-S	020	38
Joint	N-S	172	50
Joint	N-S	020	32
Joint	NW-SE	150	50
Joint	N-S	178	63
Joint	N-S	185	66

Note: Strikes/trends within 20° of 000/180 are considered N-S; trends within 20° of 090/270 are considered E-W.

### 6.3.5 Gail Geology

#### **Diorite**

Equigranular, medium-coarse grained diorite of the early Jurassic Thane Creek suite is observed as the dominate intrusive phase within the Gail Area. Frequently, medium-coarse hornblendite (see below) is observed occurring as small pods with gradational contact margins, or as xenoliths within. Broad, propylitic alteration is dominated by mafic replacement, joint infilled and shear hosted chlorite as well as veins and micro-fractures of calcite epidote and quartz. Contact related K-feldspar and minor biotite alteration appears frequently within the diorite proximal to quartz monzonite contacts. Silicification and an increase in mafic replacement biotite alteration (likely as hornfelsing) is locally observed proximal to granodiorite contacts. Additionally, increased silica is observed proximal to 0.15-0.20 meter quartz veins. Significant mineralization is restricted to localized quartz veins containing fine-medium grained, blebby molybdenite, chalcopyrite and pyrite with lesser supergene enriched native copper in fractures within the southern areas. Otherwise, mineralization is rare within the diorite, typically occurring as trace disseminated pyrite concentrated within or on the margins of primary mafics likely related to the broad propylitic alteration observed.

#### **Hornblendite**

The hornblendite appears to co-mingle with the diorite commonly containing gradational contact margins. Small sub-angular to sub-rounded centimeter sized xenoliths are also observed within the diorite. Below cliffy ridgelines within the southern area, large hornblendite float boulders are observed. In outcrop, chlorite and possibly biotite alteration are noted to replace primary hornblende. Late, weak to moderate silica and carbonate (calcite) alteration appears concentrated proximal to late microfractures. Pyrite mineralization, often moderate to strongly oxidized, typically occurs in abundance of 3-8% along fractures, and 1-2% as mafic.



### Granodiorite to Quartz Monzonite

Equigranular, fine-medium grained granodiorite to quartz monzonite intrusive phases of the Mesilinka suite dominate the Southeastern area. In outcrop, they are finer grained, largely unaltered, and contain an increase in primary quartz relative to the diorite intrusive phases. Contact relationships with the earlier diorite are frequently observed as sharp and inter-fingered and both are crosscut by late minor faulting and quartz and quartz-carbonate veining

### Latite Porphyry

Relatively fresh, north-south to northwest-southeast trending latite porphyry dykes, typically 2-4 meters in width, were observed to crosscut both the Thane Creek and Mesilinka suite of rocks (Plate 4A and 4B). They are easily identifiable by their porphyritic texture and frequent trachytic mineral alignment of primary plagioclase on contact margins. Fine-medium grained, sub-euhedral, often lathe-like variable carbonate and epidote altered plagioclase and fine grained acicular variable chlorite altered amphibole phenocrysts occur within a brown-green fine grained aphyric groundmass. The dykes are traceable for up to 100 meters on strike, often containing significant quartz veins with copper mineralization proximal to them.



Plate 4: Field photographs of the complex intrusive contact relationships. **A)** Contact between fine-medium grained granodiorite (top), latite porphyry dyke (left), and coarse-grained diorite (right); location [342826 E, 6223788 N]. **B)** Dark green hornblendite hosted within diorite, notice the sharp xenolith-like contact with diorite (below hammer) compared to the diffuse contact margin (right of hammer), the granodiorite crosscuts the diorite and hornblendite (easily seen at the bottom of the photo); location [342328 E, 6223425 N].

### 6.3.6 Gail Alteration

#### Propylitic

Propylitic alteration is well developed and ubiquitous within Thane Creek diorite and hornblendite intrusive phases throughout the entire mapped area. It decreases in intensity, with a slight increase in silicification, towards the north. Rarely is it noted within the Mesilinka granodiorite to quartz monzonite intrusive phases, even when they are observed adjacent to propylitic altered diorite.

#### Potassic

Potassic alteration at Gail is defined by the increased presence of patchy K-feldspar, and locally mafic replaced biotite and increased patchy interstitial silicification. At this stage, secondary magnetite, albite and or anhydrite are absent. As with propylitic alteration, potassic alteration occurs within the diorite and is absent within the granodiorite to quartz monzonite. Minor secondary K-feldspar alteration is noted as vein selvage alteration proximal to late quartz veins (Plate 5A and 5B). At the Gail Showing (342310E, 6223431N), potassic alteration appears to overprint propylitic alteration and is most concentrated as a north-south trending elliptical body. Westward from the Showing, the alteration appears bound by a north-south trending fault structure along the west side of the lake, roughly parallel to line 342130E. The fault seems to follow an ~ 800-meter-long drainage valley that continues to cut through the lake. As was seen with the propylitic alteration, the potassic alteration decreases in intensity further north and eventually pinches out along a north-south trend.

Outside of the Gail Showing, most potassic related alteration (K-feldspar, biotite and increased silica) appears to occur as contact alteration and likely as biotite hornfels proximal to quartz monzonite and granodiorite intrusive phases.



Plate 5: Field photos highlighting two quartz vein styles. **A)** 2cm. quartz vein with pink K-feldspar vein selvage utilizing the contact between coarse-grained diorite and medium-grained granodiorite; Primary hornblende in the diorite is weakly replaced by biotite±chlorite (342326E, 6223778N). **B)** 17cm. barren bull quartz vein within coarse-grained diorite near the Gail Showing. Veins contain increased silica±sericite alteration selvages and lack K-feldspar alteration selvages (342311 E, 6223393 N).

### 6.3.7 Gail Mineralization

#### **Porphry-Type Mineralization**

Trace disseminated pyrite occurs as mafic replacement within diorite and hornblendite likely related to or associated with a broad outer propylitic alteration assemblage. Increased concentrations are also noted along or within small chloritic fractures. Frequently, along the western side of the mapping area, joint planes within the diorite also tend to host greater concentrations of pyrite and are usually accompanied with increased secondary silica, carbonate, epidote, chlorite, and in rare instances minor malachite (Plate 6).

#### **Vein Hosted Mineralization**

Sulphide mineralization of molybdenite, chalcopyrite, and higher concentrations of pyrite is restricted to late north-south and northwest-southeast trending sub-vertical quartz veins. Locally, supergene enrichment is noted as native copper within hairline fractures of quartz. Mineralization within the veins is typically seen along small fractures and is blebby to disseminated throughout the vein and on altered vein selvages. A total of ten quartz veins were sampled at the Gail Area, seven of which fall within the potassic alteration zone as described above within the Gail Showing.

Sample 3288, taken from a 20 cm wide quartz vein of the Gail Showing, contained trace native copper, ~5% molybdenite, and ~5% chalcopyrite. Two additional 15 cm and 6 cm quartz veins collected from the Showing contained 1-2% molybdenite and pyrite, sampled as 3277 and 3278 respectively. One 5 cm quartz vein approximately 400 meters due north, along strike of Showing, contained 1-2% molybdenite, chalcopyrite, and pyrite (3286, Plate 6). Three 15 cm quartz veins containing 2-5% chalcopyrite and 2-20% pyrite were sampled approximately 250 meters due north of the Showing, and within 40 meters of each other were observed and sampled (3280, 3281, and 3283).

Sample 3288, a quartz vein defining the Gail Showing, was submitted for Re-Os age dating (Appendix III d). The Re-Os date of (202.8 +/-0.8Ma) from molybdenite is within the alkalic porphyry Cu-Au age of mineralization cluster of 205-200Ma observed within porphyries located throughout British Columbia. Additionally, it post-dates the recently dated Diorite intrusive host in the Gail area which has an emplacement date of 206.6 +/-0.9 Ma (Duuring, *et al*, 2009).



Plate 6: 5cm. quartz vein with K-feldspar alteration selvage containing trace disseminated and predominately fracture-fill molybdenite and lesser chalcopyrite mineralization within the vein (Sample 3286)

### 6.3.8 Gail Structure

#### Geological Contacts

The granodiorite intrusive contact with diorite is frequently fractured and displaced as a result of multi-directional faulting. Where preserved, they commonly appear as splays or tails that pinch out in random directions. As a result, accurate or consistent structural contact measurements were difficult to define. Late quartz veins frequently appear to utilize the contacts (Plate 4A), indicating a potential north-south to northwest-southeast trend between the two bodies. Quartz vein dips are not unidirectional. East-dipping measurements predominate to west-dipping and may indicate an easterly dip to the granodiorite.

Two latite porphyry dykes were identified; one at the Gail Showing and the other along the base of an eastern ridgeline. The orientation at the showing indicates a northwest trend dipping moderately to the west that is parallel to many quartz veins in the area. A definitive structural measurement could not be captured on the other latite dyke location along the eastern ridge.

#### Hydrothermal Vein Geometry

Quartz veins are the most common vein type at the Gail Area. The quartz veins tend to pinch and swell throughout the area, with up to 15cm of dilation/contraction. Two localized calcite veins were identified along chloritic shear planes approximately 600 meters east of the lake. Trends for the measured quartz veins (Table 8) include:

- northwest-southeast trending with moderate to steep westerly dips;
- north-south trending, steeply east dipping;
- a single northeast-southwest trending vein with a moderate westerly dip and;
- One calcite vein is north-south trending dipping 62° and the other is northwest-southeast trending dipping 82°.

Table 8: Vein structure – Gail Area

Vein Type	Strike	Dip	Width (cm)
Quartz	155	70	6
Quartz	158	84	15
Quartz	168	87	15
Quartz	320	42	20
Quartz	331	74	15
Quartz	340	69	10
Quartz	345	76	15
Quartz	000	72	17
Quartz	000	79	5
Quartz	220	62	8
Calcite	112	82	2
Calcite	198	62	2

## **Faults and Joints**

Two major north-south to northeast-southwest trending faults cut through the Gail area. The north-south trending structure occurs along the western side of the lake following an 800-meter topographical incision. Only limited evidence for this fault is observed in the field due to widespread talus and boulder field cover. The northeast-southwest trending moderately west dipping fault is located approximately 600 meters to the east of the north-south trending structure and is traceable along a 1,400-meter topographical incision that is continuous across north and south facing slopes. The structure appears to be a silicified chloritic shear and contains significant late carbonate flooding within, and proximal to it, appear to overprint an earlier K-feldspar event. As a result, it appears to be a major hydrothermal fluid pathway for multiple hydrothermal events.

A consistent northwest-southeast trending steeply west dipping joint plane occurs within the diorite along the base of the eastern ridgeline (Plate 7A and 7B). Considering the northwest-southeast trend, it is likely the mineralizing vein system is utilizing the joint planes within the diorite.



Plate 7: Mineralized (predominately pyritic) quartz-carbonate-chlorite filled joints observed within coarse-grained diorite at the base of the western ridgeline of the Gail cirque may contribute to increased chargeability noted within the southwestern area of the lake. (342056 E, 6223556 N).

## 6.4 ROCK SAMPLING

A total of 69 rock samples were collected from outcrop and float sources. Included within outcrop sampling, are selective chip sampling across specified lengths. All samples were cut by rock saw, with one half delivered to ALS Minerals of Kamloops, BC for sample preparation and analysis and the other half retained as a reference. Analysis consisted of multi-element ICP-MS with aqua regia digestion and gold by fire assay. Assays were performed on all samples returning over limits in base and precious metals. Methodology for sample preparation and analysis is presented in sections 7.1 and 7.2, respectively.

### Results

Sample details, including location coordinates, descriptions and selected analytical results, are presented in Appendix IIc and certificates of analysis are presented in Appendices IIIb.

Rock sample locations with selected geochemical results are presented for the Pinnacle Area in Figure 5 (1:10,000) and Figure 10 (1:2,000), for the Gail Area in Figure 6 (1:10,000) and Figure 11 (1:2,000), for the Mat Area in Figure 7 (1:10,000) and for the Aten Area in Figure 12 (1:10,000).

#### 6.4.1 Pinnacle Area

Of the 18 samples collected from the Pinnacle Area, 8 returned greater than 0.1% Cu, of which 4 returned greater than 0.5% Cu (Table 9).

Table 9: Selected grab sample results >0.5% Cu, Pinnacle Area

Sample	UTM		Sample Type	Rock Type	Results			
	Easting	Northing			Ag (ppm)	Au (ppm)	Cu (%)	Mo (ppm)
3260	347311	347311	float	fault zone	21.0	0.176	3.800	55.00
3263	347294	347294	outcrop	monzonite	5.6	0.125	1.365	2.88
3271	347128	347128	outcrop	diorite	12.2	0.336	1.345	3.25
3274	347655	347655	outcrop	quartz vein	11.8	3.740	0.690	303.00

#### 6.4.2 Gail Area

Of the 17 samples collected from the Gail Area, 12 returned greater than 0.1% Cu, of which 9 returned greater than 0.3% Cu (Table 10).

Table 10: Selected grab sample results >0.3% Cu, Gail Area

Sample	UTM		Sample Type	Rock Type	Results			
	Easting	Northing			Ag (ppm)	Au (ppm)	Cu (%)	Mo (ppm)
3275	342631	6223660	float	diorite	4.02	0.041	0.397	9.97
3276	342384	6223517	float	diorite	1.61	0.029	0.302	5.59
3280	342304	6223672	outcrop	quartz vein	5.06	0.029	0.446	19.15
3281	342315	6223677	outcrop	quartz vein	9.68	0.414	0.531	15.9
3282	342315	6223683	float	quartz vein	8.61	1.335	1.105	1270
3283	342291	6223638	outcrop	quartz vein	4.84	0.168	0.423	6.67
3284	342124	6223600	float	hornblendite	8.15	0.143	1.005	49.5
3287	342348	6223406	float	quartz vein	2.51	0.169	0.339	12.05
3901	345176	6222627	outcrop	diorite	8.61	0.062	0.408	19.6

### 6.4.3 Mat Area

A total of 5 chip samples were collected from the main vein of the Mat Showing (Table 11). Samples 3215 and 3216 were taken from the quartz-carbonate vein. Sample 3213 and 3214 were collected from the hanging wall and foot wall, respectively, of sample 3215. Sample 3217 was collected from the footwall of sample 3216 (Figure 7).

Table 11: Chip samples, Mat Area

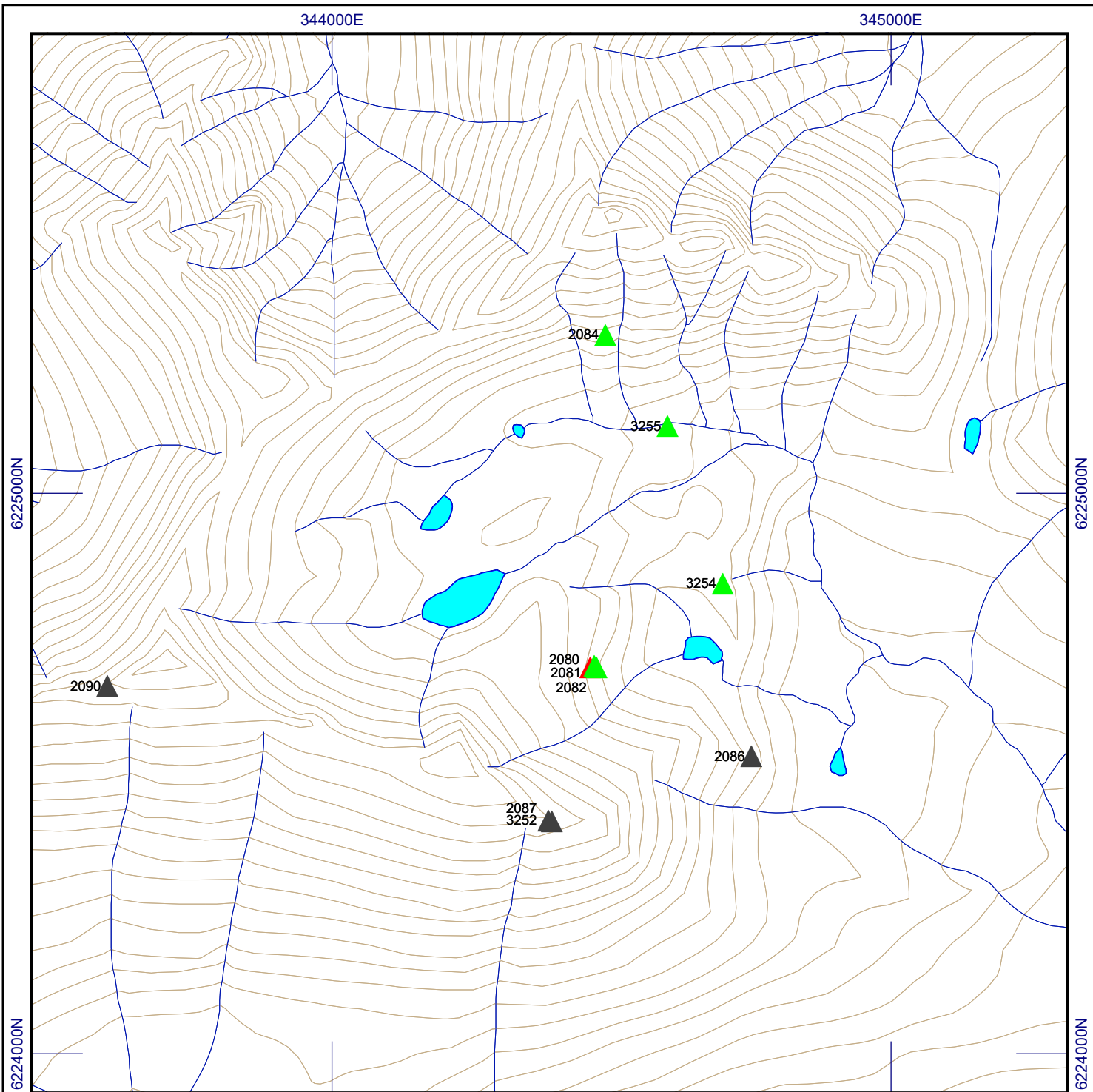
Sample	UTM		Sample Type	Rock Type	Results			
	Easting	Northing			Ag (ppm)	Au (ppm)	Cu (%)	Mo (ppm)
3213	340371	6235465	chip/0.4m	andesite tuff	53.6	0.013	0.016	0.93
3214	340371	6235465	chip/0.3m	andesite tuff	0.24	<0.001	0.006	0.17
3215	340371	6235465	chip/0.35m	quartz-carb vein	476	0.056	0.338	2.58
3216	340377	6235459	chip/0.35m	quartz-carb vein	401	0.038	0.104	2.75
3217	340377	6235459	chip/0.3m	andesite tuff	4.07	0.017	0.009	1.08

### 6.4.4 Aten Area

Of the 27 samples collected from the Aten Area, 17 returned greater than 0.1% Cu, of which 6 returned greater than 0.5% Cu (Table 12). Figure 12 shows rock sample results from the northern section of the Aten Area.

Table 12: Selected grab sample results >0.5% Cu, Gail Area

Sample	UTM		Sample Type	Rock Type	Results			
	Easting	Northing			Ag (ppm)	Au (ppm)	Cu (%)	Mo (ppm)
2080	344462	6224690	outcrop	diorite	6.82	0.57	3.28	8.76
3205	344792	6222504	outcrop	diorite	3.01	0.02	1.02	2.82
3206	344846	6222558	outcrop	diorite	11.2	0.076	1.345	365
3209	344987	6222866	outcrop	diorite	14.85	1.775	4.13	19.2
3210	344869	6222933	outcrop	diorite	19.15	0.565	2.18	7.72
3211	344599	6222408	outcrop	diorite	2.01	0.007	0.563	2.86



**LEGEND**

**TOPOGRAPHY**

- Contour (20m interval)
- Watercourse
- Waterbody

**SAMPLING**

- Soil
- Soil (100m station mark)
- Soil: no sample
- Rock: outcrop - grab
- Rock: outcrop - chip (m)
- Rock: float

**GEOCHEMISTRY**

**ROCK - Cu (ppm)**

- < 0.1
- 0.1 to 0.5
- 0.5 to 1.0
- > 1.0



NAD83, UTM Zone 10 North  
94C/03, 04, 05, 06

**INTERRA COPPER CORP.**

**GEOCHEMISTRY PLAN MAP**

**ATEN AREA**

**Copper (Cu)**

Thane Property  
Omineca M.D. British Columbia, Canada

Project No.:	P72	By:	CN
Scale:	1:10000	Drawn:	CN
Figure:	12	Date:	March 2022





## 6.5 DIAMOND DRILING

A total of 2,783.24 metres of diamond drilling was completed in 12 drill holes from 9 drill setups (TH21-1 through TH21-12). Drill hole locations were established to test accessible high priority targets at the Cathedral Area (Cathedral Main & South, Gully and Pinnacle).

Drilling was carried out by Atlas Drilling Ltd. of Kamloops, BC, using two Hydracore 2000 fly diamond drills. Drill core size was NQ. Coordinates for all collar locations were surveyed by CME using a GeoExplorer XH GPS receiver. A tabulation of drilling specifications is presented in Table 13. A plan of the drill hole locations is presented in Figure 13.

Downhole surveying was carried out by the drill crew using a single shot Flex-It survey instrument provided by Atlas Drilling. Readings were taken during the drilling of the hole and at the end of the hole during rod pull out. Erroneous readings were discarded, which was attributable to the drill string still in motion at time of survey, or magnetic deflection due to the presence of pyrrhotite, magnetite or steel from the drill string.

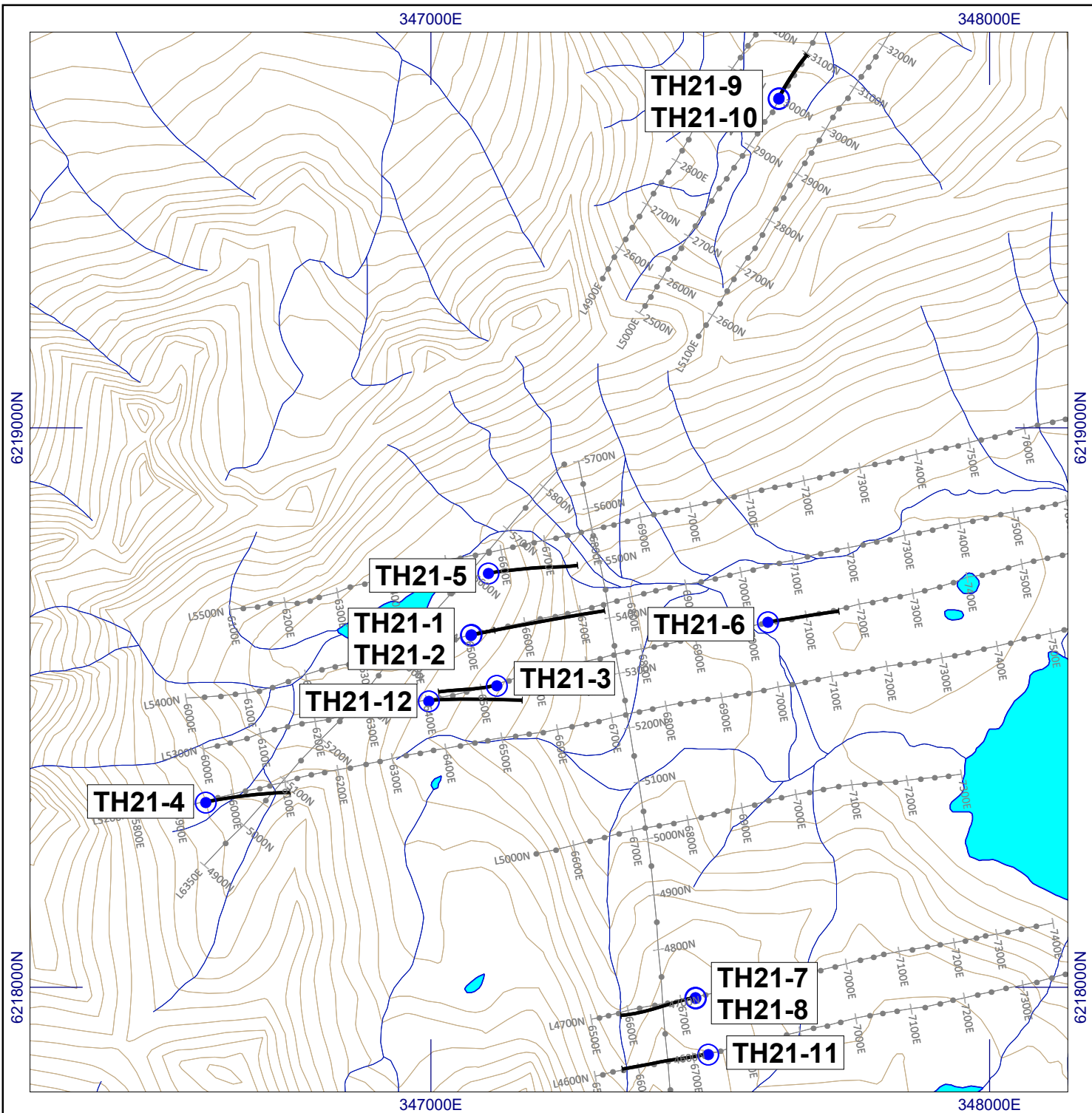
Core for geochemical analysis was cut by rock saw, with one half delivered to ALS Minerals of Kamloops, BC for sample preparation and analysis and the other half returned to the core box for reference. A total of 2,389 samples were submitted for analysis, which consisted of multi-element ICP-MS with a four-acid total digestion and gold by fire assay. Assays were performed on all samples returning over limits in base and precious metals. Methodology for sample preparation and analysis is presented in sections 7.1 and 7.2, respectively.

Detailed core logs, results of core analyses (recovery, rock quality, magnetic susceptibility), strip logs and cross sections are presented in Appendix Va to Vd, respectively. Certificates of analyses for the drill core are presented in Appendices IIIc.

All drill core is currently stored at CME's field office in Vavenby, BC (51°35'N Latitude and 119°44'W Longitude).




Table 13: Drill hole specifications

Hole	Location (NAD 83 UTM Zone 10 North)			Orientation (°)		Length (m)	Area
	Easting	Northing	Elevation (m)	Dip	Azimuth		
TH21-1	347070.74	6218629.20	1736.94	80	-80	234.00	Cathedral Main
TH21-2	347071.58	6218630.29	1735.16	80	-50	381.00	Cathedral Main
TH21-3	347116.64	6218539.89	1696.32	260	-70	296.00	Cathedral Main
TH21-4	346595.83	6218331.17	1861.04	80	-55	243.00	Cathedral South
TH21-5	347101.73	6218740.03	1734.75	80	-50	253.60	Cathedral Main
TH21-6	347602.06	6218652.69	1599.57	80	-50	204.00	Cathedral Valley
TH21-7	347472.50	6217981.96	1736.80	260	-50	240.00	Gully
TH21-8	347472.80	6217981.43	1738.09	260	-88	150.00	Gully
TH21-9	347621.88	6219589.25	1677.27	30	-50	144.50	Pinnacle
TH21-10	347621.48	6219588.13	1677.45	30	-55	163.14	Pinnacle
TH21-11	347495.55	6217880.98	1750.21	260	-50	240	Gully
TH21-12	346994.74	6218512.64	1723.61	80	-45	234	Cathedral Main







**LEGEND**

**TOPOGRAPHY**

-  Contour (20m interval)
-  Watercourse
-  Waterbody

**SYMBOLS**

-  Grid line with line number
-  Grid station
-  Grid station (100m station number)
-  Diamond drill hole collar location and trace with number



NAD83, UTM Zone 10 North  
94C/03, 04, 05, 06

**INTERRA COPPER CORP.**

**DDH COLLAR LOCATION MAP  
CATHEDRAL AREA**

Thane Property  
Omineca M.D. British Columbia, Canada

Project No.: P72	By: CN
Scale: 1:10000	Drawn: CN
Figure: 13	Date: March 2022



### **6.5.1 Cathedral Main**

Five drill holes, TH21-01, TH21-02, TH21-03, TH21-05, and TH21-12 were collared within the Cathedral Main area.

Drilling targeted the porphyry related extent of the hydrothermal alteration and mineralization system proximal to and outboard of the north-south trending Duckling Creek (quartz) monzonite to syenite complex that intruded Thane Creek diorite to (quartz) monzodiorite intrusive phases.

Drill holes oriented easterly and sub-vertical, targeted the width and depth extent of the interpreted north-south trending, sub-vertical to moderate westerly dipping porphyry system and the correlation to the surface and sub-surface modeled chargeability and resistivity high areas observed on the IP/Soil lines (L5200N-L5500N). Drilling was oriented to intersect and provide information related to structural continuity and control related to several south to southeast trending and sub-vertical to south and southwesterly dipping structures previously mapped within the area. Low to moderate increased copper, gold, molybdenum and local areas of arsenic values were observed from collected rock samples and soil geochemistry throughout the area. The drill target included coincident chargeability high with anomalous chalcopyrite±arsenopyrite mineralization in rock and soil samples.

#### **TH21-1**

##### ***Objective***

TH21-1 was collared proximal to Station 6500E on line 5400N. The hole was oriented to intersect the centre of a bulbous to bullseye chargeability high contained within a sub-surface, sub-vertical resistivity high and a section of a low resistivity features within a airborne magnetic high. The chargeability anomaly was targeted from 50 to 120 meters depth (Figure 14) within OCP altered and mineralized diorite and (quartz) monzonite cross-cut by syenite.

##### ***Results***

The drill hole is structurally separated into an upper diorite dominate and a lower (quartz) monzonite dominate section. The upper section intersected predominately medium to course grained diorite (Plate 8) cross-cut by fine-medium grained (quartz) monzonite (Plate 9), fine to medium grained and coarse grained (quartz) syenite dykes (Plate 10). Alteration of the diorite is dominated by weak to moderate, intrusion related contact K-feldspar alteration associated with both the (quartz) monzonite and (quartz) syenite intrusive phases. Porphyry related OCP K-feldspar dominate alteration is associated with localized areas of increased magnetite veining and brecciation that define the magnetic high observed within the airborne magnetics. Both are overprinted by subtle to moderate patchy zones of IPZ alteration related to actinolite-chlorite veins and fractures commonly with albite alteration selvages. The interpreted intersection of increased chargeability correlates with an increase in disseminated, mafic and magnetite replaced sulphides as a result of hairline fractures and localized veins of late quartz-epidote-calcite±sulphide with K-feldspar alteration selvages. This hydrothermal fluid pulse appears to predominately occur as south-southeast trending and moderate to steeply west dipping fractures and veins of quartz-epidote-calcite±sulphides that post date

porphyry alteration assemblages and most structures, frequently infilling chloritic shears, breccias, and porphyry related magnetite and actinolite-chlorite veins and fractures. Sulphides observed within the veins and fractures include pyrite-chalcopyrite-molybdenite-bornite. The interpreted increased chargeability occurs within the sub-surface resistivity low that correlates with the presence of an increase in K-feldspar dominated OCP alteration overprinted by a patchy to pervasive increase in albite and actinolite related IPZ alteration. A moderately silicified chlorite shear containing semi-massive magnetite is replaced by semi-massive granular pyrite+chalcopyrite and marks the center of the bulbous bullseye chargeability.

Localized chloritic ductile shears and later brittle shear brecciation contain interstitial, veins and fractures of quartz, calcite and lesser magnetite hydrothermal events throughout the upper section of the diorite and on contact margins of the dykes. Typically, these areas appear to be focal points of increased resistivity likely as a result of increased silica within the structures. A significant fault zone (144.15-169.00m) is interpreted to represent an area of intersecting south-southwest trending west-northwest (50-60°) dipping and south-southeast trending southwest (60-70°) dipping chloritic shears and brittle brecciation. Quartz-epidote-calcite-sulphide bearing veins and fractures appear to utilize the latter structure and bleed into the former. Brittle reactivation of the structure observed typically with increased calcite veining and breccia infill and remobilized copper potentially related to a southeast trending (60-80°) southwest dipping structure. Additionally, this zone marks the transition to increased resistivity associated with an increase in structure related silicification and a transition to OPZ alteration within the lower section of the drill hole.

An increase in visible sulphide mineralization and the geochemical presence of increased Cu, Au, Ag, As and Mo correlate with the sub-surface chargeability high feature. A representation of mineralization within the feature occurs as quartz veins (Plate 11) and structures proximal to contact margins (Plate 12), the latter grading 0.14% Cu, 0.04g/t Au, 0.50g/t Ag and 4.5ppm Mo over 5.07 metres (59.70 to 64.77 metres). A lower shear zone containing a polythitic breccia (Plate 13) located on the outer margin of the chargeability returned 0.57% Cu, 0.29g/t Au, 3.90g/t Ag and 4.50ppm Mo over 1.00 meters (110.00-111.00m).

The bottom section of the drill hole intersected predominately fine to medium grained (quartz) monzonite (Plate 14) and lesser (quartz) syenite (Plate 15) intrusive phases with minor intersections of diorite. A single late weakly chlorite+epidote altered latite porphyry (Plate 16) is observed to crosscut the (quartz) monzonite. The interpreted high resistivity combined with a gradual decrease in chargeability is observed throughout the entire lower section of the drill hole as shown on Figure 14. The increase in resistivity likely occurs as a result of a slight increase in both primary and secondary silica within pervasive weak to moderate porphyry related OPZ and localized SA alteration assemblages. The decrease in chargeability is directly correlated to the decrease of appreciable sulphides ( $\leq 1\%$  pyrite) intersected within the lower section of the drill hole. OPZ alteration was confirmed by thin section analysis of samples collected at depth associated with increased chlorite + albite + actinolite + calcite  $\pm$  quartz  $\pm$  sericite  $\pm$  pyrite alteration of primary felsic and mafic minerals within intrusive phases. Patchy vein selvage K-feldspar alteration and silicification is noted proximal to quartz-epidote-calcite $\pm$ sulphide veins and fractures that appear to overprint OPZ alteration. Near the basal sections of the drill hole, SA alteration occurs as patchy to pervasive and locally

texturally destructive albite with actinolite+quartz veining within both diorite and (quartz) monzonite. The SA alteration, also confirmed by thin section analysis (Plate 17) appears to overprint contact related potassic and or biotite hornfels within the diorite. No significant mineralization is noted within the lower sections of the drill hole.

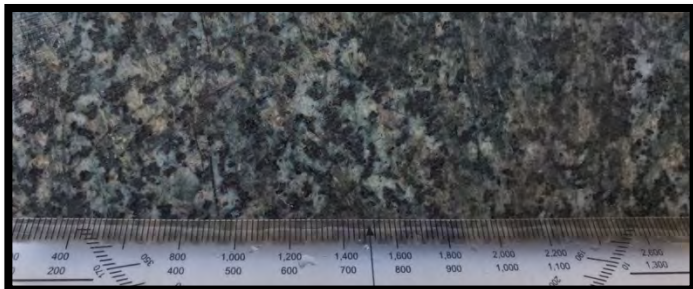


**Plate 8:** Barren, medium-coarse grained diorite @19.64m. Contains pervasive IPZ alteration related to actinolite+chlorite±magnetite fractures with albite alteration selvages overprinted by patchy weak-moderate silica and K-feldspar alteration as selvages to late quartz±epidote fractures.

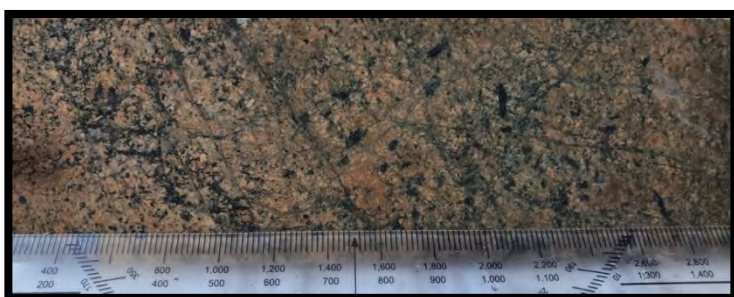


**Plate 9:** Barren, fine-medium grained (quartz) monzonite dyke @39.00m. proximal to diorite-monzonite contact. Contains weak chlorite filled shear brecciation textures that post-date pervasive strong K-feldspar dominate OCP alteration. Fractures and veinlets of quartz-calcite post date and infill shear related textures.

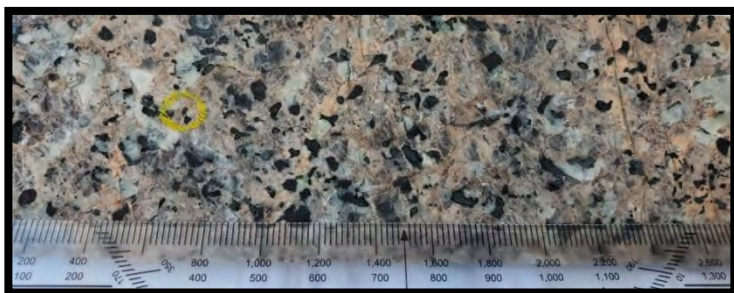


**Plate 10:** Barren, coarse grained to Pegmatitic (quartz) syenite dyke @29.62m. Thin section analysis of this sample #76077 confirms quartz syenite as protolith containing subtle-weak actinolite-chlorite-epidote-sericite and carbonate alteration. Trace bornite-chalcocite-chalcopyrite observed in thin section are associated with thin quartz-epidote-calcite filled fractures. Close similarity compositionally suggests it may represent a coarse (unchilled) version of Plate 9.



**Plate 11:** Isolated 10cm quartz-calcite±magnetite vein @60.33m contains coarse grained blebs of chalcopyrite+pyrite. Sample# 76109 containing 0.64% Cu, 0.026g/t Au, 1.20g/t Ag and 1.69ppm Mo over 1.00m.

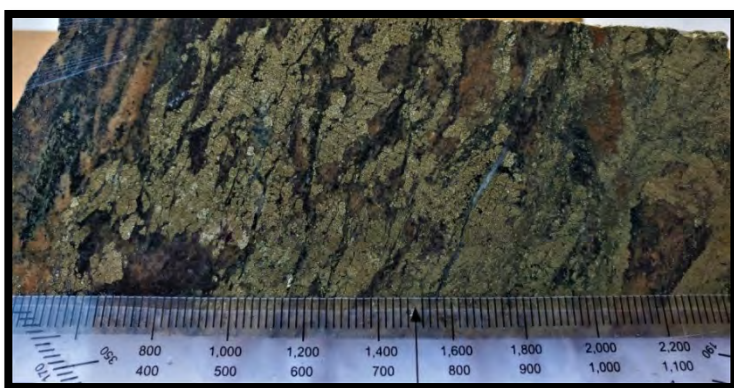


**Plate 12:** Semi-massive, shear elongated, granular pyrite±chalcopyrite with secondary interstitial quartz+calcite appear to replace magnetite within ductile shear on the contact margin of a (quartz) monzonite dyke @64.12m. Sample #76114 containing 0.025% Cu, 0.26g/t Au, 2.07g/t Ag and 37.7ppm Mo over 0.65m.



**Plate 13:** Polyolithic breccia (30cm) @110.50m with chloritic matrix containing interstitial and blebby quartz-calcite-chalcopyrite-pyrite. Sample# 76161 containing 0.57% Cu, 0.29g/t Au, 3.94g/t Ag and 4.52ppm Mo over 1.00m.

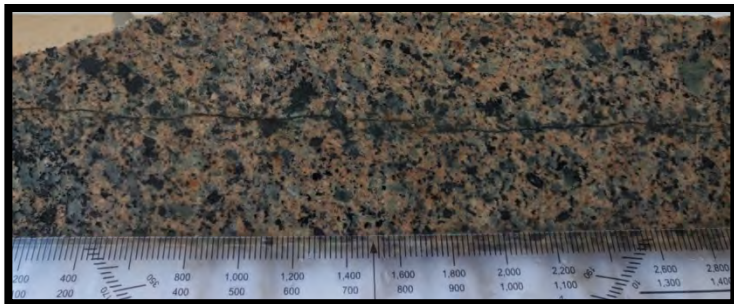


**Plate 14:** Barren, weak K-feldspar (deuteric.) and OPZ altered fine to medium grained (quartz) monzonite @179.06m.

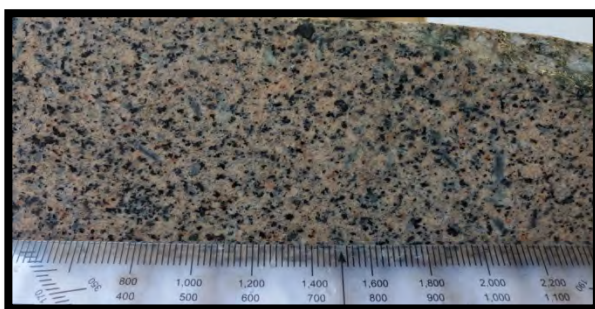


**Plate 15:** Typical weak OPZ altered fine-medium grained (quartz) syenite @190.80m.

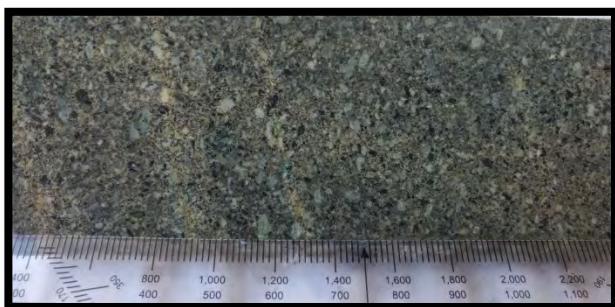


**Plate 16:** Barren, typical weak OPZ altered Latite Porphyry @201.00m.

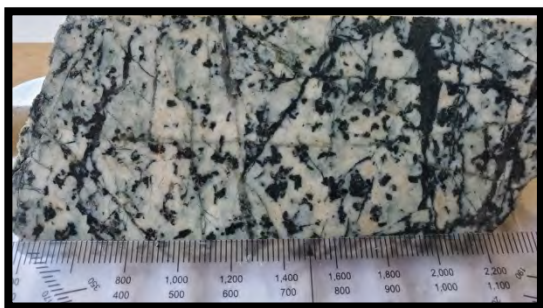


**Plate 17:** Pervasive SA within diorite @222.83m.

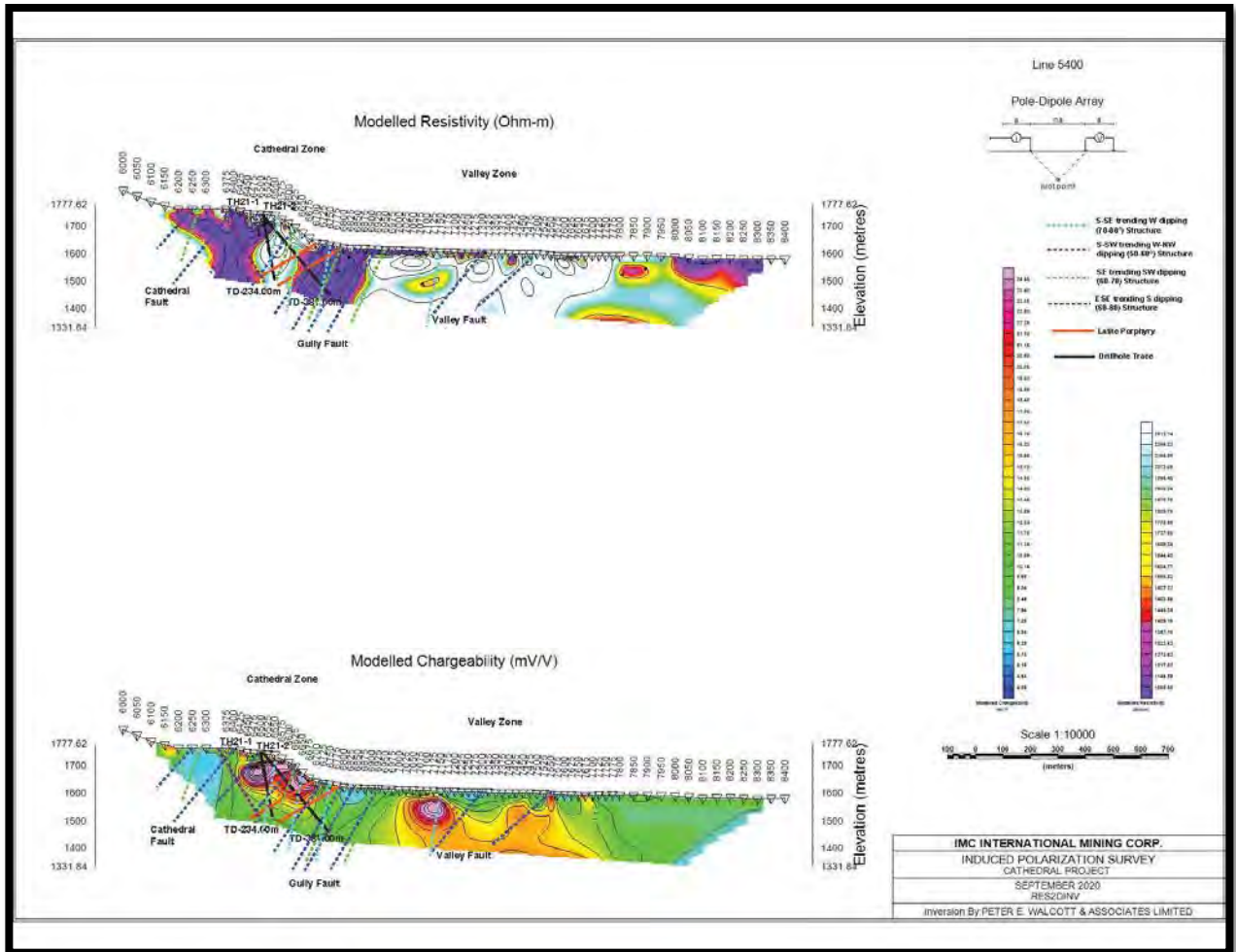


Figure 14: Drill hole trace with IP, TH21-1 and TH21-2 (schematic)

## TH21-2

### **Objective**

TH21-2 was collared from the same pad as TH21-1 proximal to Station 6500E on line 5400N with a shallower angle to intersect the extension of the interpreted upper sub-surface chargeability high from 29 to 90 meters depth and a second bulbous chargeability high just to the east within an area of high resistivity from 140 to 190 meters depth (Figure 14). The chargeability anomalies were targeted within OCP and IPZ altered and mineralized diorite and (quartz) monzonite cross-cut by syenite. Additionally, the drill hole targeted OCP related magnetite veining and brecciation that defines the airborne magnetic high in the area. The south-southeast trending steeply west dipping and the southwest trending moderately west dipping significant structures were also targeted at depth.

### **Results**

The drill hole is separated into an upper and lower section of a diorite dominate host and a middle section of (quartz) monzonite and (quartz) syenite. The upper section down to 145m intersected predominately medium to coarse grained diorite cross-cut by three fine-medium



grained (quartz) monzonite and (quartz) syenite dykes <5 meters in width. Alteration within the upper section of the diorite particularly within the area of lower resistivity, that extends from TH21-1, is dominated by weak to moderate pervasive IPZ alteration consisting of predominately chlorite-actinolite-albite-magnetite±epidote and quartz. Abundant barren magnetite veining and localized brecciation are also present within IPZ alteration, containing both albite±actinolite and K-feldspar alteration halos, the latter seemingly appears to increase with depth. Within the interpreted area of decreased resistivity and increased chargeability, only trace fractures of pyrite and chalcopyrite are noted. As a result, it is likely the presence of magnetite throughout the zone may contribute to the increased chargeability IP response modeled within this zone as well as the magnetic high observed within the airborne magnetics. K-feldspar dominate contact alteration occurs proximal (<5m width) to (quartz) monzonite and (quartz) syenite dykes. OCP alteration defined primarily as K-spar alteration with magnetite is weakly distributed throughout the upper section (Plate 18). Patchy, localized moderate to strong SCA containing epidote+albite and weak to moderate silica alteration (Plate 19) representing a SCA overprint of the IPZ alteration phase occurs locally and most K-spar alteration occurs as vein selvage alteration to quartz+epidote+calcite veins fractures and veins rarely containing sulphides.

Two significant structural zones were intersected within the upper section of diorite within the interpreted area of increased resistivity. The first marks the transition from low to high resistivity occurring as a south-southeast (70-80°) west dipping weakly magnetite filled chloritic shear. A slight increase in quartz-epidote±calcite veining increases below this upper structure. The second is a zone containing intersecting south-southwest trending west-northwest (50-60°) dipping shear and a south-southeast trending southwest (60-70°) dipping chloritic shear. The up-dip projection of the latter shear marks the transition from interpreted moderate to high chargeability and the on-set of the lower bulbous chargeability zone. Both structural zones occur with IPZ alteration, appear to be weak to moderately silicified and contain magnetite infill and minor quartz-calcite veining.

The middle section of the drill hole contains the lower interpreted bulbous chargeability high that occurs within an upper and lower sub-vertical (quartz) monzonite to (quartz) syenite intrusive phase (<21meters) separated by diorite. The upper (quartz) monzonite contains xenolithic pods of diorite and both contain OCP and IPZ alteration dominated by K-feldspar-albite-chlorite-±actinolite and quartz. The upper contact contains a centimeter scale magnetite and quartz+calcite+pyrite veined chloritic shear. Significant magnetite veins and brecciation (Plate 20) occur throughout associated with K-feldspar±albite±silica vein selvage alteration. As a result, the interval has been interpreted to contain OCP alteration rather than IPZ, although it is likely much of the K-feldspar within is primary and deuteric. The lower contact contains a south-southeast trending (70-80°) west dipping shear structure that cuts through the center of the interpreted high chargeability and marks the transition from high to low resistivity. This also occurs at the transition from the high to low airborne magnetics. The structure has been reactivated and overprinted by structural related phyllic and carbonate (calcite) alteration. The increase in the interpreted chargeability is attributed to the gradual increase of pyrite+chalcopyrite mafic replacement disseminations, fractures and veins frequently noted to cut and seemingly replace earlier magnetite veins and brecciation (Plates 20 and 21) on contact boundaries. Higher grades of copper, gold, silver molybdenum and

arsenic occur within the center area of the interpreted chargeability high where pyrite and chalcopyrite occur (1-3% in abundance). The veins are sub-parallel to the south-southeast trending westerly dipping structure and trail off immediately below the structure and occur at the lower boundary of interpreted chargeability. Mineralization within this zone returned 0.17% Cu, 0.05 g/t Au, 0.60 g/t Ag and 16.9 ppm Mo over 14.90 metres (154.00 to 168.90m).

The middle section of diorite between the upper and lower (quartz) monzonite dykes continues to be dominated by IPZ that appears to overprint both contact related and OCP K-feldspar±magnetite alteration. The transition to the interpreted broad low resistivity that continues to the end of the drill hole correlates to the increase in albite+actinolite, K-feldspar and carbonate (calcite) alteration as well as the reduction in both primary and secondary quartz. A carbonate (calcite) and weak to moderately PAZ altered west dipping latite porphyry cross-cuts the diorite within this section and is the up-dip equivalent of the latite intersected within TH21-1 at 199.00m. A significant south-southeast trending (70-80°) west dipping shear structure is intersected and is interpreted as a major structure that transgresses through the Cathedral area to the south, towards the Gully area, on the western side of the gully. No mineralization is associated within or proximal to this structure.

The lower sub-vertical (quartz) monzonite is cut by a south-southwest trending (50-60°) west-northwest dipping major structure. The structure and associated PAZ and pervasive fractured controlled carbonate (calcite) alteration as well as hematite to overprint OCP K-feldspar+magnetite veining and brecciation within and continue at depth below the structure within the lower diorite. The magnetite is barren and no significant mineralization is associated within or proximal to the structure nor within the altered host reflecting a decrease in the interpreted chargeability in conjunction with low resistivity.

The diorite within the lower section of the drill hole appears to be predominately IPZ and patchy K-feldspar+magnetite OCP dominate altered with a significant overprint of both PAZ and carbonate (calcite)+hematite alteration as a result of significant faulting. A lower westerly dipping carbonate altered latite porphyry is intersected just below the lower (quartz) monzonite is also significantly altered. A major structural zone occurs within the core of the interpreted resistivity low. It is characterized by localized chlorite-hematite shears and pervasive locally texturally destructive intense PAZ alteration and late carbonate (calcite) alteration throughout the base of the drill hole. Currently, this zone is potentially indicative of intersecting south-southwest trending (50-60°) west-northwest dipping, southeast trending (60-70°) southwest dipping and south-southeast trending (70-80°) westerly dipping structures. Late, interstitial, fractures, veins and vein breccia calcite and associated carbonate alteration occur throughout the structural zone and overprints all alteration assemblages, localized mineralization. It's abundance is unusual for structures intersected at this stage and may occur due to another structural component not yet identified in the area or may potentially be the down-dip extension related to the Gully structure system. Within the structure, a significant zone of magnetite veining and vein brecciation with associated vein selvage K-feldspar alteration similar to the upper section of mineralization occurs. Quartz + calcite + pyrite + chalcopyrite mineralization cuts and locally appears to replace magnetite throughout the zone and is likely related to the south-southeastern steeply west dipping mineralization trend observed in similar structures up hole. This lower zone of mineralization within the structure

returned 0.14% Cu, 0.08 g/t Au, 1.00g/t Ag and 13.10 ppm Mo over 5.50 meters (335.00-340.5m)

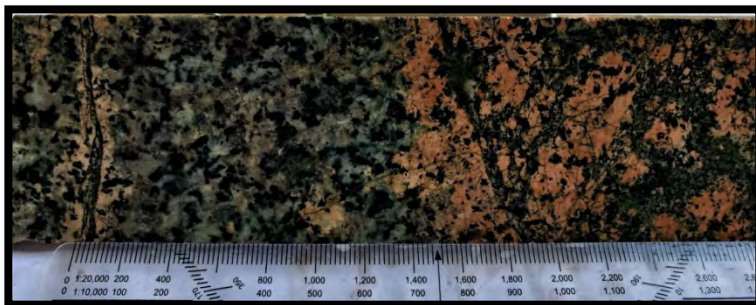


**Plate 18:** An example of patchy OCP alteration dominated by K-feldspar selvage on a local zone of biotite+magnetite fracturing now completely replaced by chlorite @56.00m.

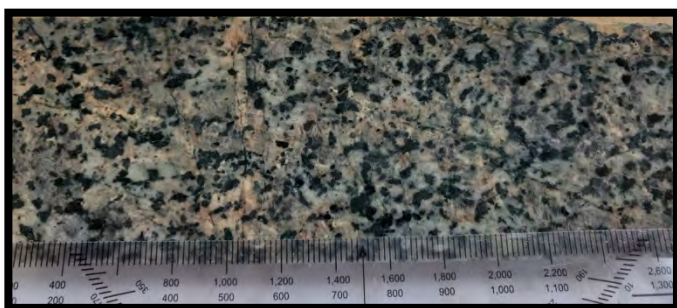


**Plate 19:** Weak-moderate SCA to SA diorite containing discontinuous hairline actinolite fractures and late quartz+epidote fractures with K-feldspar alteration selvages @62.50m.



**Plate 20:** Semi-massive magnetite breccia with associated K-feldspar alteration of (quartz) monzonite and late pyrite+chalcopyrite fractures, blebs and disseminations cutting and replacing magnetite @165.80m. Sample #76505 containing 0.34%Cu, 0.09g/t Au and 0.97g/t Ag and 3.47ppm Mo over 0.68m.

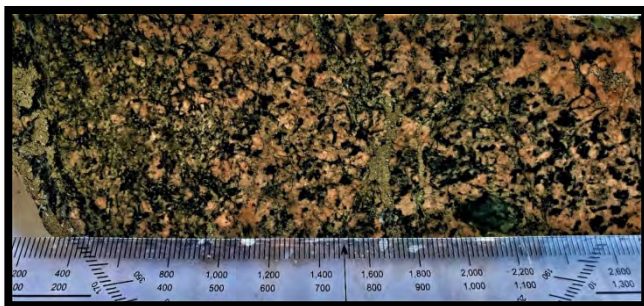


**Plate 21:** Vein and disseminated pyrite+chalcopyrite mineralization within K-feldspar altered (quartz) monzonite within TH21-02 @165.20m. Sample# 76504 containing 0.89%Cu, 0.31g/t Au and 2.52 g/t Ag over 0.72m.

## **TH21-5**

### ***Objective***

TH21-5 was collared 125 metres to the northeast of drill holes TH21-1 and TH21-2, between lines 5400N and 5500N in the vicinity of stations 6550 respectively of these lines. The location is directly above the northern extension of the interpreted upper chargeability high from TH21-1 and TH21-2. The hole was drilled eastward to target the northern extension of the interpreted lower bullseye chargeability within high resistivity (Figure 15). The location of the chargeability was interpreted to occur from 110 to 170 meters down hole. The drill hole targeted upper and lower sections of medium to coarse grained OCP and IPZ altered diorite and fine to medium grained (quartz) monzonite. OCP alteration associated with the reduced airborne magnetic high northern extension of the westerly dipping latite porphyry dyke was also targeted. Northern extensions of south-southwest trending and south-southeast trending structures were also projected to be intersected within this drill hole.

### ***Results***

Both the diorite and the (quartz) monzonite to (quartz) monzonite are separated into upper and lower sections. The upper section of the drill hole down to 93 m intersected predominately medium to coarse grained diorite cross-cut by two fine-medium grained (quartz) monzonite and (quartz) syenite dykes <3 meters in width. Alteration within the diorite is predominately weak to moderate OPZ alteration that increases with depth and is accompanied by subtle to strong IPZ alteration. Both assemblages include albite-quartz-sericite - chlorite ± actinolite ± epidote. Barren magnetite veining and breccias are present with increasing IPZ and rare patchy OCP alteration, with both containing albite and K-feldspar alteration selvages. Patchy K-feldspar contact alteration related to localized (quartz) monzonite dykes and vein selvages to late quartz+epidote+chlorite±calcite±sulphide veins and fractures overprints all the above. The presence albite and K-feldspar relative to quartz throughout the upper section appears to correlate to the interpreted low resistivity from the upper section of the drill hole. Low grade copper with moderate values of molybdenum mineralization is commonly associated with isolated hairline fractures and disseminations of pyrite+chalcopyrite with lesser molybdenite and arsenopyrite. They are frequently proximal to and often associated with quartz + epidote + chlorite ± calcite gangue veins. Two significant zones of mineralization are noted within the upper diorite. The first occurs within the small near surface upper chargeability high within

and proximal to a set of patchy silica and carbonate (calcite) healed, magnetite infilled and brecciated south-southwest trending (50-60°) west-northwest dipping chloritic shears (Plate 22). The upper zone returned 0.09% Cu, 0.05 g/t Au, 0.70 g/t Ag and 4.10 ppm Mo over 18.53 meters (20.87-39.40m). The lower zone (Plate 23), which occurs within the interpreted moderate chargeability, returned 0.54% Cu, 0.14g/t Au, 2.70g/t Ag and 20.6 ppm Mo over 2.80 meters (68.00-70.8m).

A major southeast trending (60-70°) southwest dipping chloritic shear structure marks an increase in the interpreted chargeability that occurs on the contact between the upper diorite and upper fine-medium grained (quartz) monzonite intrusive body. Pervasive OCP alteration associated with magnetite veins and breccias (Plate 24) is overprinted by patchy to pervasive IPZ alteration dominated by albite as vein selvage alteration to sheeted and weakly developed semi-stockwork actinolite veins and fractures that cut and infill earlier magnetite veining and brecciation (Plate 25). Similar to the upper diorite, low grade copper and molybdenum indicator mineralization occurs as rare sections (<2m) containing late pyrite ± chalcopyrite ± molybdenite veins, fractures and coarse disseminated blebs that cut, infill and replace magnetite (Plate 24) and actinolite. Unlike the veins within the upper section of diorite they lack quartz + epidote and are associated with calcite and minor quartz. Proximal to the interpreted bullseye chargeability high, the drill hole intersected barren magnetite + actinolite hairline fractures, veins and vein breccias with minor sections of trace-3% disseminated and blebby pyrite. A south-southwest trending (50-60°) west-northwest dipping chloritic shear combined with a south-southeast trending (70-80°) westerly dipping, brittle clay + carbonate structure occur on and just below the lower contact with the lower diorite. The presence of clay within the south-southeast trending structure may contribute to the interpreted chargeability. A low grade zone of mineralization occurs proximal to the upper (quartz) monzonite and southeast trending shear, located within the interpreted moderate chargeability. This zone returned 0.04% Cu, 0.03 g/t Au, 0.20g/t Ag and 38.80 ppm Mo over 5.34 meters (96.64-101.98m).

The lower section of medium to coarse grained diorite is cross-cut by the north-south trending and westerly dipping upper latite porphyry dyke. Alteration throughout is predominately OPZ alteration with patchy zones of moderate to strong K-feldspar dominate contact related and OCP alteration the latter related to magnetite veining. Patchy areas of weak to moderate IPZ and SCA alteration occur as increased albite + actinolite + epidote overprints both contact and OCP alteration. Within localized areas of increased magnetite fractures and veining, late sporadic quartz + calcite ± sulphide hairline fractures and veins contain localized indicator copper and molybdenum mineralization. The increase in quartz may contribute to the slight increase in the interpreted resistivity seen in the area.

Pervasive OCP alteration associated with a decrease in magnetite veins and breccias overprinted by patchy to pervasive IPZ alteration similar to the upper (quartz) monzonite occurs proximal to the upper contact within the lower (quartz) monzonite. Mineralization occurs as pyrite ± chalcopyrite late veins, fractures with minor quartz + actinolite ± calcite. Localized coarse disseminated blebs are also noted within, cutting and replacing magnetite proximal to the upper contact. The mineralized contact zone grades 0.01% Cu, 0.03 g/t Au, 0.40g/t Ag and 49.70 ppm Mo over 5.11 meters (221.64-226.75 m).

A significant zone of faulting occurs at the base of the drill hole and consists of intersecting south-southwest trending (50-60°) west-northwest dipping and southeast trending (60-70°) southwest dipping structures and is interpreted as part of the northern extent of the fault zone intersected within the base of TH21-2.

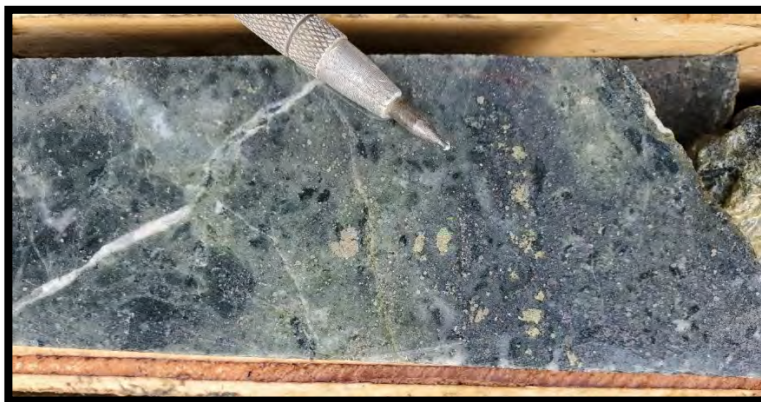


**Plate 22:** Disseminated and blebby pyrite±arsenopyrite±chalcOPYrite within upper mineralization zone contains interstitial silica+calcite+sericite healed polyolithic breccia @21.52m. Sample# 10208 containing 0.22% Cu, 0.25g/t Au, 12.85g/t Ag and 3.57ppm Mo over 0.60 meters.



**Plate 23:** Section of lower mineralization zone (40cm) within a moderately silicified and quartz veined chloritic shear containing semi-massive magnetite cut by quartz and sulphides, the latter replacing magnetite. Sample# 41340 containing 1.84% Cu, 0.45g/t Au, 9.49g/t Ag, and 73.70ppm Mo over 0.64 meters.

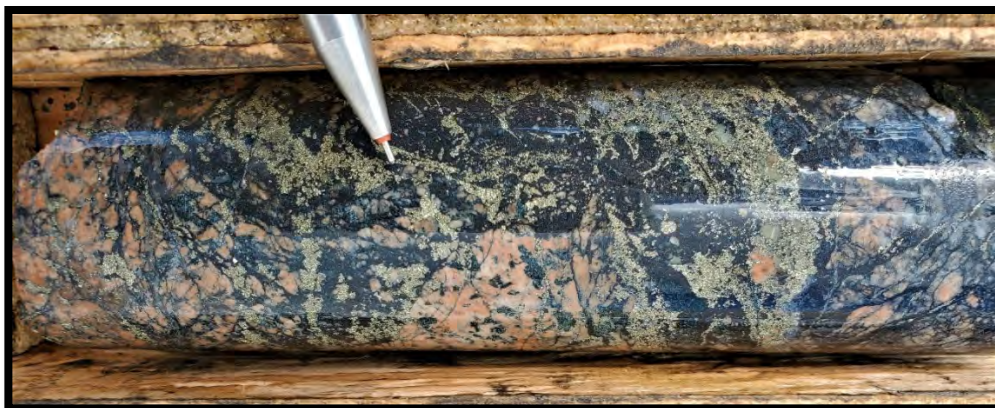


**Plate 24:** Semi-massive magnetite vein breccia and associated K-feldspar alteration cut and replaced by disseminated and blebs of pyrite and chalcopyrite @98.00m. Sample# 41375 containing 51.70ppm Mo over 0.28 meters.



**Plate 25:** Semi-stockwork to sheeted veins and fractures of magnetite and later actinolite with associated pervasive albite alteration and disseminated to blebby pyrite and chalcopyrite replacing magnetite @ 104.7m. Sample# 41385 containing 0.17% Cu, 0.04g/t Au, 0.50g/t Ag and 7.43ppm Mo over 0.46 meters.

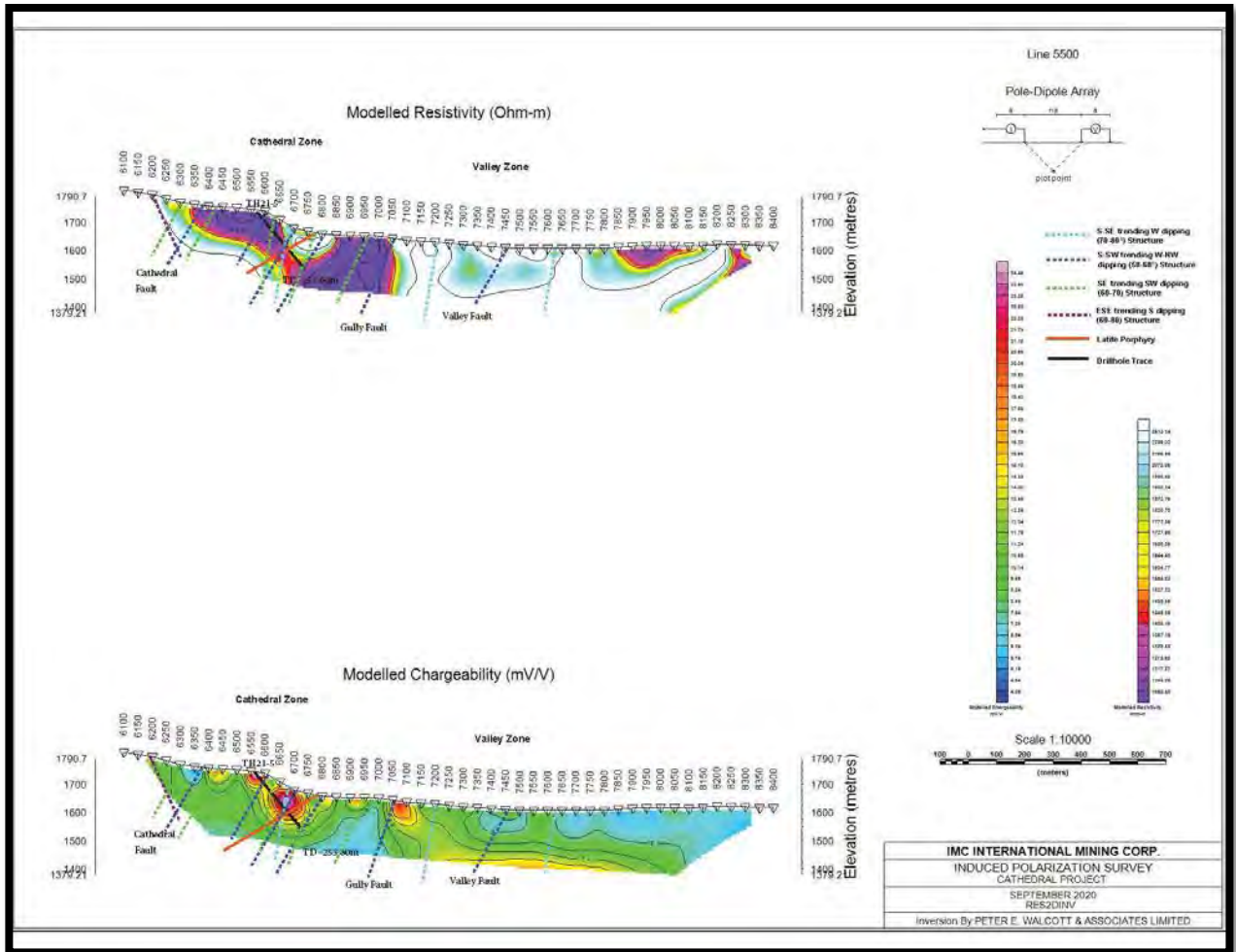


Figure 15: Drill hole trace with IP, TH21-5 (schematic)

### TH21-3

#### *Objective*

TH21-3 was collared 90 metres to the southeast of TH21-1 and TH21-2, proximal to Station 6526E on line 5300N. The hole was drilled westward to test the southern extent of the airborne magnetic high and the intersection of a large bulbous, sub-vertical chargeability high interpreted from 23 to 140 meters depth, contained within a large area of high resistivity (Figure 16). TH21-3 was targeted to intersect sections of medium to coarse grained OCP and IPZ altered diorite and fine to medium grained (quartz) monzonite to (quartz) syenite as well as the potential for the southern extension of the westerly dipping latite porphyry dyke and a south-southwest trending (50-60°) west-northwest dipping structure. Two other faults interpreted by mapping were projected to be intersected within the upper portion of the drill hole include a southeast trending (60-70°) southwest dipping structure and an east-southeast trending (60-80°) south dipping structure.



## **Results**

The majority of the drill hole is dominated by medium to coarse grained diorite cross-cut by sub-vertical fine-medium grained (quartz) monzonite to (quartz) syenite dykes ranging from <1 to 10 meters in width. A larger (quartz) monzonite dyke up to 30 meters cuts up through the diorite in the middle portion of the drill hole. Moderate to locally strong contact related K-feldspar alteration, OCP and IPZ alteration occurs throughout the upper section of diorite down to the larger intersection of (quartz) monzonite (164.20m). OCP alteration associated with localized increased hairline fractures, and veins of magnetite is typically noted proximal to diorite and (quartz) monzonite contact areas and overprints contact related K-feldspar alteration. Patchy areas of moderate IPZ alteration overprints both contact related and OCP alteration. IPZ alteration contains increased albite-quartz-sericite-actinolite  $\pm$ chlorite $\pm$ epidote. Albite and lesser silica alteration frequently occurs as an alteration selvage to actinolite  $\pm$  chlorite  $\pm$  quartz veins and fractures.

Several significant chloritic shear structures were intersected within the top 65 meters of the drill hole. They include a southeast trending (60-70°) southwest dipping structure, an east-southeast trending (60-80°) south dipping structure and a larger fault zone containing the intersection of a south-southeast trending (70-80°) westerly dipping structure with a south-southwest trending (50-60°) west-northwest dipping structure. All three are moderately silicified and contain abundant interstitial magnetite-actinolite-chlorite and lesser calcite with disseminated and blebby magnetite replaced pyrite $\pm$ chalcopyrite. The lower intersecting structure contains increased clay as gouge. It is interpreted the significant amount of moderately silicified chloritic shear structures combined with moderate amounts of secondary hairline fractures and veins of quartz throughout the upper section correlate to the interpreted high resistivity projected for the upper section of the drill hole

Low grade copper mineralization occurs within the structural zone above and the upper area of the interpreted chargeability high. Late quartz+epidote+chlorite $\pm$ calcite $\pm$ sulphide fractures, veins and small vein breccias with K-feldspar alteration selvages post dates all alteration assemblages above and frequently utilizes earlier actinolite fractures. In areas of increased secondary magnetite veining (Plate 26) and isolated chloritic shear breccias (Plate 27) late quartz+epidote+chlorite $\pm$ calcite $\pm$ sulphide are noted to cross-cut, infiltrate and replace earlier magnetite and most structures. Similar to mineralization intersected within TH21-2 these late mineralized veins appear associated with south-southeasterly trending and steeply west dipping structures. The extension of the chargeability to 140 meters depth appears to correlate to trace amounts of disseminated and hairline fractures of pyrite within and cross-cutting magnetite veins and fractures. A single low-grade mineralized zone intersected within the structural area of the upper section of the interpreted chargeability high returned 0.13% Cu, 0.06g/t Au, 0.24g/t Ag and 2.07 ppm Mo over 9.00 meters (31.75-40.75m).

The upper contact of the larger intersection of (quartz) monzonite (164.20-193.00m) contains a PAZ altered, east-southeast trending (60-80°) west dipping chloritic shear structure that marks the on-set of OPZ dominate alteration consisting predominately of quartz + chlorite + sericite. A significant gradual decrease in the interpreted chargeability is observed below this structure, corresponding to the decrease of both sulphides and magnetite. Beneath the (quartz) monzonite, diorite hosts patchy zones of IPZ alteration, dominated by albite+actinolite and

lessor magnetite and SCA alteration, containing increased patchy epidote are noted. A small intersection of latite porphyry clipped within the drill hole may correspond to the lower latite porphyry intersected within TH21-2.

A south-southwest trending (50-60°) west-northwest dipping, strongly PAZ altered chloritic shear intersected proximal to the base of the drill hole, is the down-dip extension of the structure intersected within TH21-2 (~267.00m). No significant mineralization is noted within the lower sections of the drill hole.



**Plate 26:** Veins and fractures of pyrite±chalcopyrite cross-cut, infill and replace earlier magnetite (K-feldspar selvage) and actinolite (albite selvage) veins and fractures within diorite @37.60m. Sample # 60430 containing 0.14%Cu, 0.03g/t Au, 0.29g/t Ag and 1.6ppm Mo over 1.00 meter.



**Plate 27:** Coarse, blebby chalcopyrite and lessor pyrite proximal to late calcite vein that cuts chloritic shear breccia infilled with magnetite (K-feldspar selvage) and silica. Host is diorite @59.00m just above shear zone. Sample# 60473 containing 0.15% Cu, 0.05g/t Au, 0.37g/t Ag and 1.87ppm Mo over 1.00m.

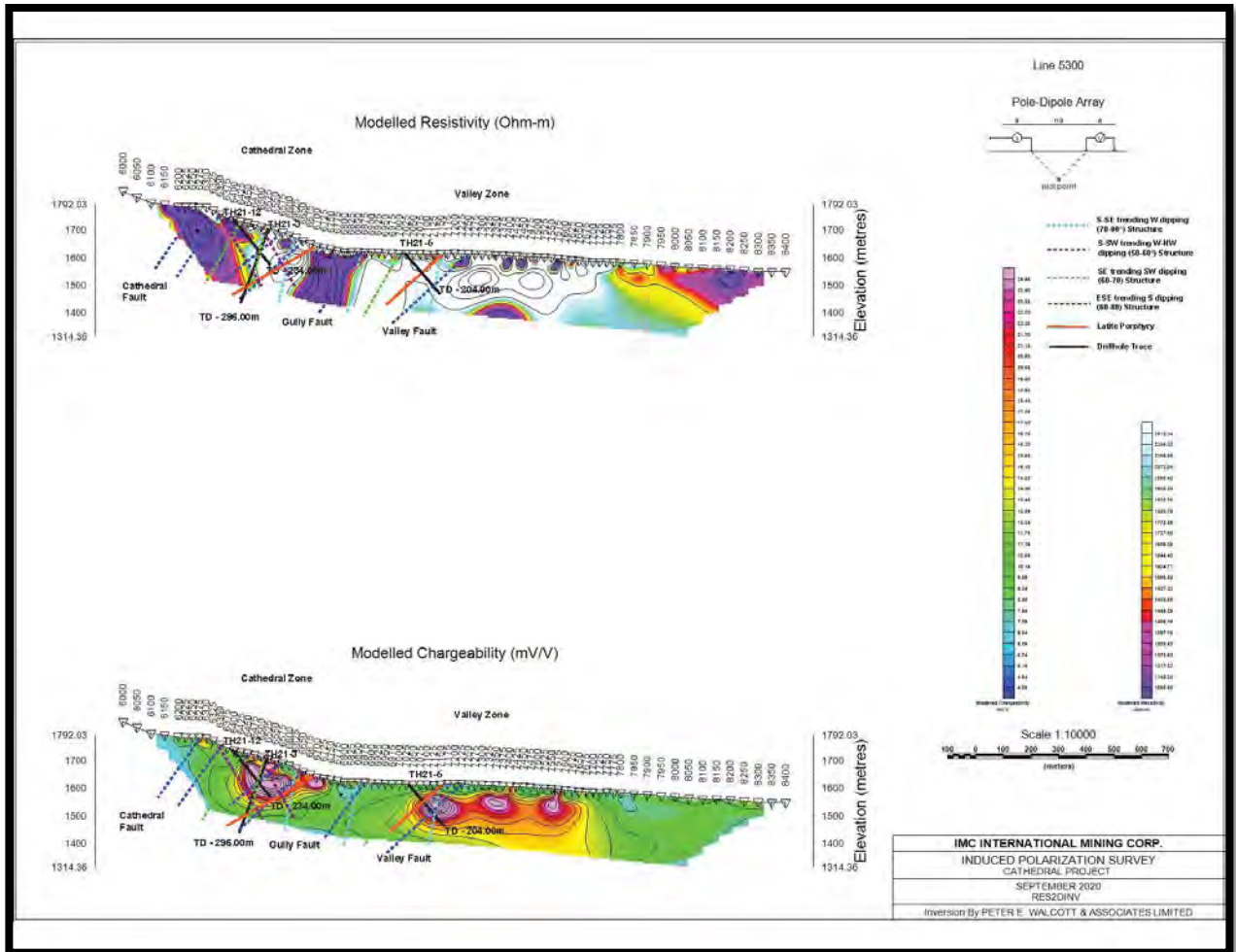


Figure 16: Drill hole trace with IP, TH21-1 TH21-12 and TH21-6 (schematic)

## TH21-12

### **Objective**

TH21-12 was collared 90 meters to the west of TH21-3, proximal to Station 6400E on line 5300N. The hole was drilled eastward within a moderate airborne magnetic signature to intersect the westward expansion of the bulbous chargeability high at approximately 72 meters depth within a resistivity which continues with depth (Figure 16). TH21-12 was targeted to intersect predominately OPZ altered medium to coarse grained diorite with patchy areas of overprinting K-feldspar dominate contact, OCP and IPZ alteration in addition to the up-dip extension of a sub-vertical OPZ altered fine to medium grained (quartz) monzonite to (quartz) syenite. The fault zone containing intersecting south-southwest trending (50-60°) west-northwest dipping and south-southeast trending west dipping (70-80) chloritic shears intersected within TH21-3 from 60-80 meters depth is anticipated to occur from 125 to 145 meters.

## Results

The upper section of the drill hole down to the intersection of (quartz) monzonite (80.96m depth) within the interpreted low chargeability and resistivity is dominated by medium to coarse grained OPZ altered diorite cross-cut by several localized (quartz) monzonite to (quartz) syenite dykes ( $\leq 3$ m) in width. K-feldspar dominated contact related and patchy areas of OCP and IPZ alteration ( $\leq 3$ m) in width are also noted throughout the former proximal to dykes. A significant zone of PAZ alteration correlates to a southeast trending ( $60-70^\circ$ ) southwest dipping shear structure containing brittle reactivation and increased carbonate (calcite) alteration. Pyrite±chalcopyrite ( $\leq 1\%$ ) occurs as disseminations frequently replacing chlorite altered mafics and rare fine-coarse blebs within quartz+calcite hairline fractures and veins with K-feldspar alteration selvages.

The (quartz) monzonite intersected (80.90 -111.25) is interpreted as the sub-vertical, up-dip extension from within TH21-3 (~163.47m). Proximal to the upper contact, a gradual increase from hairline fractures to semi-massive veins of magnetite occur in conjunction with a gradual increase from wispy disseminated to hairline fractures and veins of quartz + pyrite ± chalcopyrite cross-cutting and often replacing magnetite. The onset of both correlate to the location of the interpreted increase chargeability. Proximal to the base of the (quartz) monzonite lower contact and within the lower portion of the diorite, a shear zone consisting of several silica+calcite±magnetite infilled and healed chloritic shears and shear breccias occur (115.35-144.67). This zone appears to represent the fault zone containing intersecting south-southwest trending ( $50-60^\circ$ ) west-northwest dipping and south-southeast trending west dipping ( $70-80^\circ$ ) chloritic shears intersected within TH21-3 from 60-80 meters depth. A single low to moderate mineralized zone (Plate 28) was intersected within a magnetite filled chloritic shear breccia, which returned 0.31% Cu, 0.10g/t Au, 0.89g/t Ag and 28.05 ppm Mo over 3.00 meters (113.35-116.35m).

Below the shear zone, medium to coarse grained diorite contains alternating weak to moderate OCP with overprinting IPZ alteration, The IPZ is associated with magnetite veins and breccias that are cross-cut, infilled and frequently replaced by pyrite. Several isolated shear zones ( $\leq 1$  meter) are frequently proximal to small dykes of (quartz) monzonite. Late hairline fractures and small veins of quartz ± epidote + calcite + pyrite ± chalcopyrite containing K-feldspar alteration selvages and minor disseminated blebs of sulphides down to the base of the drill hole reflecting a potential chargeability and resistivity highs.



**Plate 28:** Moderately silicified chloritic shear zone on the lower (quartz) monzonite contact (113.35-115.35m) contains magnetite veining cut by and replaced with pyrite and chalcopyrite. Sample #'s 42261 and 42263 containing 0.45% Cu, 0.14g/t Au, 1.27g/t Ag and 40.78ppm Mo over 2.00m.

## 6.5.2 Cathedral Valley

A single drill hole was collared in the Cathedral Valley proximal to Station 7025E on line 5300N.

### **TH21-6**

#### ***Objective***

The hole was drilled eastward and targeted the western most series of bullseye to bulbous shaped chargeability highs on the margin of an airborne magnetic low. The increase in chargeability was targeted from 60 to 180 meters depth within a significant broad high resistivity (Figure 16). The Valley area, with associated chargeability, is interpreted as a potential structurally displaced extension of the porphyry related hydrothermal system similar to the Cathedral Area. Due to lack of outcrop within the swampy, overburden covered surface, the drill hole was interpreted to intersect medium to coarse grained diorite and fine to medium grained (quartz) monzonite in addition to several south to southeast trending moderate to steeply westerly dipping chloritic shear structures. Both intrusive phases and structures were extrapolated through the Valley area from previous mapping completed to the north within the eastern end of the Gully area and immediately to the south both at the base and tops of the east west trending mountains.

#### ***Results***

The drill hole consisted predominately of a pervasive weak to moderate OPZ altered fine to medium grained (quartz) monzonite (Plate 29). Two late, barren dykes consisting of an alkali-granite (Plate 30) and an OPZ altered latite porphyry (Plate 31) were also intersected within the drill hole. Local areas of OCP were observed associated with increased minor hairline fractures and veins of magnetite. Vein selvage K-feldspar alteration with accessory silica is noted throughout most of the hole associated with hairline fractures and rare veins of quartz+calcite±epidote±sulphides.

Several southeast trending (60-70°) southwest dipping chloritic shears, frequently infilled and or healed with interstitial quartz and rare epidote occur throughout the drill hole. Rarely, secondary amorphous grey quartz and magnetite veining (Plate 32) occur as infill or on margins of shears. Brittle reactivation and associated PAZ alteration and secondary calcite infill and veining are observed within and proximal to shears.

The zone of interpreted high chargeability correlates to a gradual increase in disseminated and blebs of pyrite + chalcopyrite ± arsenopyrite associated with hairline fractures and veins of quartz + calcite ± epidote. Low grade indicator copper mineralization, proximal to the interpreted bullseye chargeability occurs within and proximal to the intersection of the south-southwest trending (50-60°) west-northwest dipping Valley Fault and a south-southeast trending (70-80°) westerly dipping chloritic shear structure. Where quartz + calcite ± epidote + sulphide veins intersect localized OCP related magnetite ± specularite veins and fractures, an increase in coarse granular blebby sulphides are noted to replace magnetite (Plates 33 and 34). A gradual decrease in sulphides with depth correlates to the gradual decrease in the interpreted chargeability outside of this structural zone. Similar to the Cathedral area,

mineralization appears to be associated with the south-southeast trending (70-80°) westerly dipping chloritic shear structures. The presence of minor primary quartz within the (quartz) monzonite, increased secondary silica as a result of hairline fractures and veins, combined with silica healed chloritic shears, may be responsible for the broad resistivity high observed within the Valley area. Additionally, the near absence of both primary and secondary magnetite supports the magnetic low observed within the airborne magnetics. A low-grade intersection of indicator mineralization within the interpreted chargeability high returned 0.07% Cu, 0.03g/t Au, 0.50g/t Ag and 5.00 ppm Mo over 36.71 meters (120.00-156.71 m).

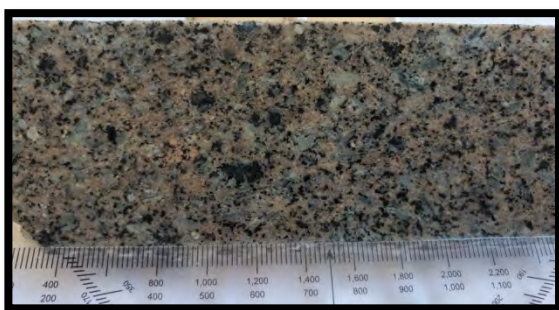


**Plate 29:** Confirmed via thin section analysis as a weak deuteric and OPZ altered (quartz) monzonite @34.84m containing subtle to weak, actinolite, chlorite and sericite alteration of primary minerals.

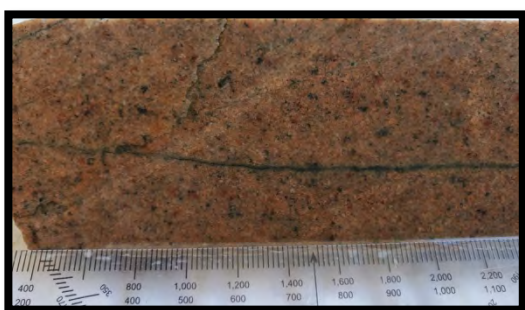


**Plate 30:** Barren, alkali-granite (Aplite) containing quartz-chlorite fracture with subtle silica+sericite alteration selvage @74.36m.

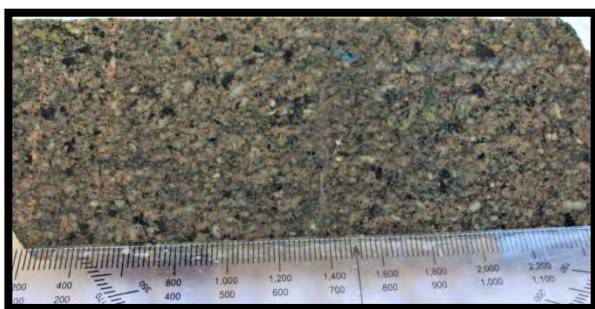


**Plate 31:** Barren, subtle to weakly OPZ altered latite porphyry @104.58m.



**Plate 32:** Magnetite vein within isolated, moderately silicified chloritic shear both cut by late, hairline fractures of quartz-epidote-pyrite and lesser calcite @25.26m.



**Plate 33:** Localized OCP alteration related to magnetite veining within (quartz) monzonite shows granular pyrite±chalcopyrite replacing magnetite @121.00m. Sample# 43070 containing 0.35% Cu, 0.07g/t Au, 1.66g/t Ag and 6.72ppm Mo over 1.00 meters.

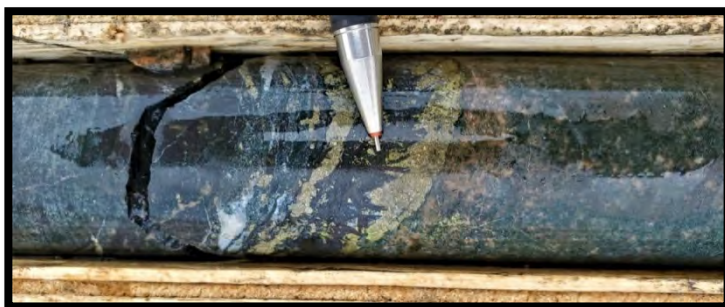


**Plate 34:** Bladed, secondary magnetite±specularite vein with blebby granular pyrite and lesser chalcopyrite on the margins with calcite @130.72m. Sample # 43081 containing 0.07% Cu, 0.03g/t Au, 0.41g/t Ag and 9.04ppm Mo over 1.00 meters.

### 6.5.3 Gully

Three drill holes, TH21-07, TH21-08 and TH21-11 were collared within the Gully area.

As with the Cathedral Main area, drill holes targeted the southern extent of the porphyry related hydrothermal alteration and mineralization system proximal to and outboard of the

north-south trending Duckling Creek (quartz) monzonite to (quartz) syenite complex that intruded Thane Creek diorite to (quartz) monzodiorite intrusive phases. These holes were also designed to test the potential for upper-level auriferous pyrite + arsenopyrite ± chalcopyrite fracture-controlled and vein hosted mineralization and associated increase in silicification identified during previous mapping campaigns.

Drill holes were oriented westerly and sub-vertical, targeted the width and depth extent of the interpreted porphyry system, the potential correlation with the interpreted chargeability and resistivity high areas (Figure 17) and an airborne magnetic high. The holes were also designed to provide information related to structural continuity and control related to several south to southeast trending and sub-vertical to south and southwesterly dipping structures previously mapped within the area. Throughout the area and along the IP lines, low to moderate increased copper, gold, molybdenum and local areas of arsenic values were observed within soil geochemistry and potassic to silica altered diorite and (quartz) monzonite surface samples containing pyrite + chalcopyrite ± arsenopyrite mineralization.

### **TH21-7**

#### ***Objective***

TH21-7 was collared proximal to Station 6725E on line 4700N. The hole was drilled westward and targeted a subvertical to easterly dipping chargeability high targeted from 48 to 125 meters depth within a resistivity and airborne magnetic high (Figure 17). The drill hole was expected to intersect alternating OPZ and IPZ altered medium to coarse grained diorite crosscut by OCP altered fine to medium grained (quartz) monzonite to (quartz) syenite dykes. Several significant moderate to strongly SIL and brittle reactivated CRB healed and altered southeast trending southwest dipping chloritic shears potentially controlling mineralization were also expected to be intersected at depth.

#### ***Results***

The upper section of the drill hole, down to 80 meters depth contains equal proportions of medium to coarse grained diorite cross-cut by sub-vertical (quartz) monzonite to (quartz) syenite dykes interpreted to be a branching singular body. Alteration within this area of intrusive phases is dominated by moderate to strong, locally pervasive IPZ alteration that overprints significant and frequently barren magnetite veining (Plate 35) and brecciation and associated OCP alteration that occurs frequently proximal to (quartz) monzonite to (quartz) syenite contact margins. Alternating IPZ and OCP alteration however, extends below the upper (quartz) monzonite down to the faulted contact with (quartz) monzodiorite (155m). The interpreted increased chargeability occurs as a result of an increase in pyrite with lesser chalcopyrite, molybdenite and arsenopyrite mineralization associated with late phase quartz±epidote+calcite veins and fractures containing K-feldspar alteration selvages. Where these veins intersect and frequently brecciate OCP magnetite, an increase in coarse grained blebs of sulphides appear to replace magnetite (Plates 37-39). Increased veining and associated mineralization occurs within and proximal to increased moderate to strong, patchy SIL, CRB and localized veins of tourmaline (Plate 40) AKL alteration. The increased frequency and abundance of veining and silicification occurs within and proximal to an area of brittle reactivated, frequently carbonate infilled, south-southeast trending (70-80°) westerly



dipping chloritic shears within the interpreted zone of high chargeability and resistivity. A gradual decrease in quartz ± epidote + calcite veining and associated mineralization as well as magnetite veining is consistent with an interpreted decrease in chargeability with depth and is truncated within a south-southeast trending (70-80°) westerly dipping chloritic shear on the upper contact with medium to coarse grained (quartz) monzodiorite (Plate 41). Within the interpreted area of increased chargeability, a 24.50 meter intersection of indicator low grade copper-gold mineralization occurs from 70.0 m to 94.5 m, with an average grade of 0.13% Cu, 0.03 ppm Au, 0.3 g/t Ag and 4.1 ppm Mo.

The shear located on the upper contact with medium to coarse grained (quartz) monzodiorite marks the transition to predominately OPZ alteration with depth as well as a decrease in the airborne magnetic signature. OPZ alteration is locally overprinted by patchy areas of contact K-feldspar and OCP alteration related to localized magnetite veining proximal to (quartz) monzonite dykes. Additionally, it marks the depth extent of the interpreted chargeability and resistivity. An east-southeast trending (60-80°) southerly dipping structure occurs on the lower (quartz) monzodiorite contact with (quartz) monzonite. Below this structure is predominately diorite cross-cut by several (quartz) monzonite to (quartz) syenite dykes (<6m) in width that together form the lower sub-vertical (quartz) monzonite that is interpreted to trend northwards into the Cathedral Main area. The dykes appear relatively fresh with rare K-feldspar alteration selvages to quartz + epidote ± calcite ± sulphide and magnetite hairline fractures. Where trace sulphides are noted they appear associated with sharp contact margins absent of chloritic shearing. No significant mineralization is noted within the lower section of the drill hole.



**Plate 35:** Barren, semi-massive magnetite veining with interstitial secondary chlorite, actinolite, calcite and quartz @15.40m.



**Plate 36:** Late quartz+calcite vein utilizes and replaces magnetite with blebs of pyrite+chalcopyrite within OCP altered (quartz) monzonite @23.80m. Sample# 42537 containing 0.14% Cu, 0.04g/t Au, 0.28g/t Ag and 6.98ppm Mo over 1.00m.



**Plate 37:** Blebs of pyrite+chalcopyrite within silica brecciated magnetite vein containing late coarse calcite proximal to increased mineralization @72.50m. Sample# 42580 containing 3.42% Cu, 0.75g/t Au, 7.03g/t Ag and 1.13ppm Mo over 0.50m.



**Plate 38:** Blebs of pyrite+chalcopyrite within silica brecciated magnetite vein containing late coarse calcite proximal to increased mineralization @123.60m. Sample# 42626 containing 0.56% Cu, 0.14g/t Au, 0.85g/t Ag and 2.10ppm Mo over 0.60m.

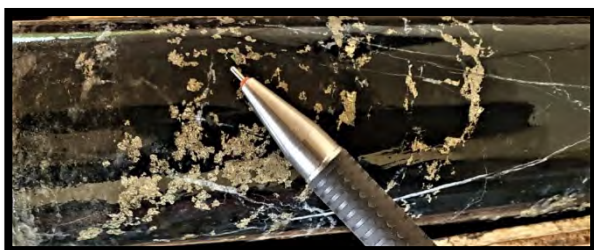


**Plate 39:** Tourmaline+quartz vein (AKL alteration) within and proximal to chloritic shear cut by late pyrite±chalcopyrite and later hairline fractures of calcite @69.50m.

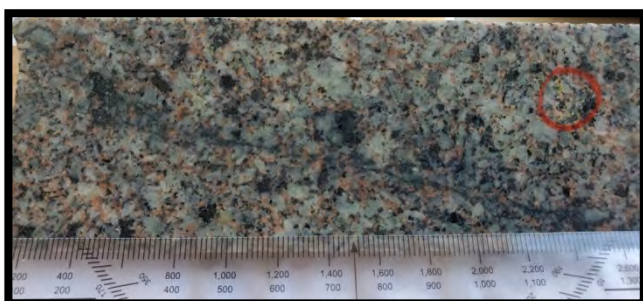


**Plate 40:** Confirmed via thin section analysis as an OPZ and weakly SA altered (quartz) monzodiorite with rare fine grained mafic replacement chalcopyrite and bornite (circled) @173.33m.

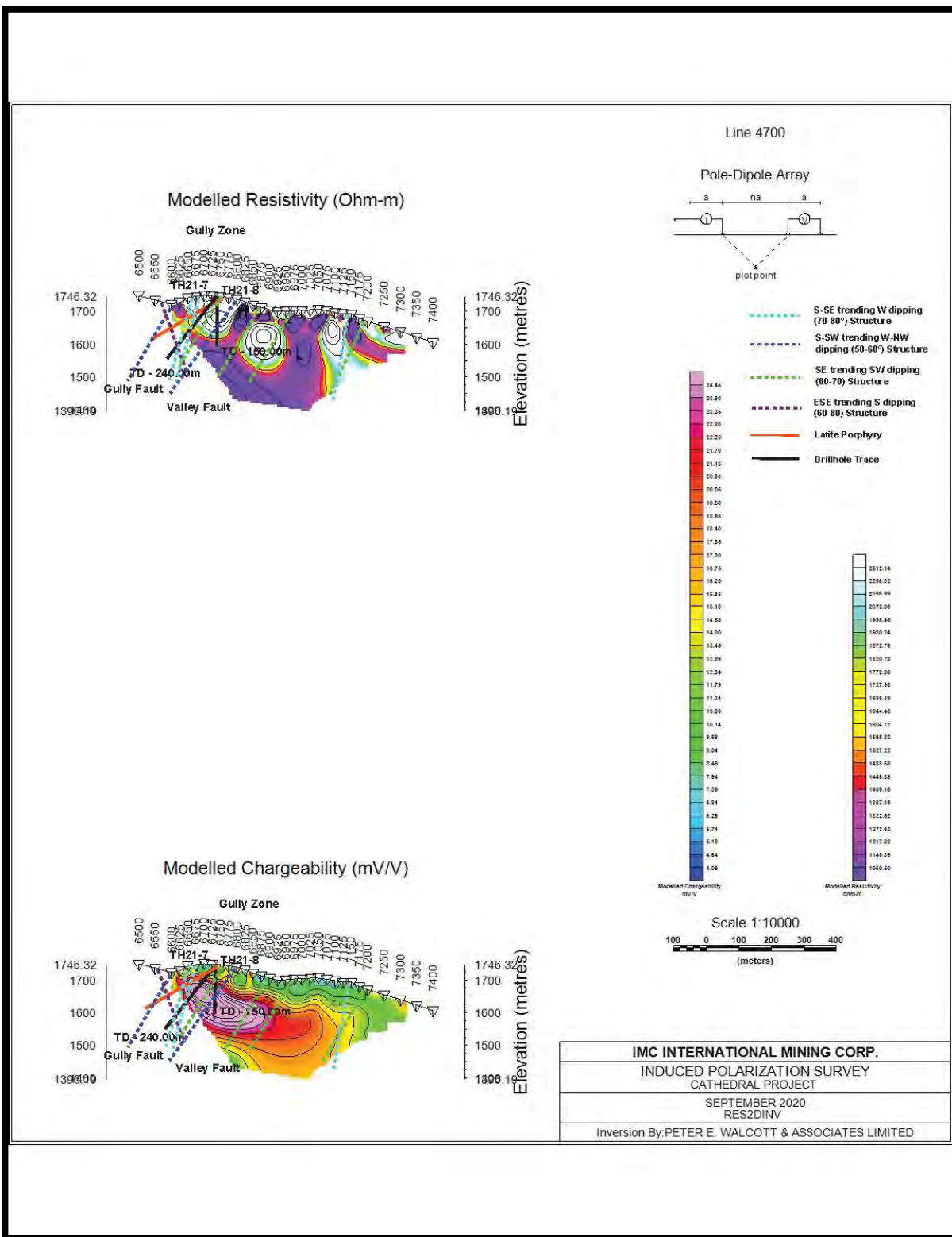


Figure 17: Drill hole trace with IP, TH21-7 and TH21-8 (schematic)

## **TH21-8**

### ***Objective***

TH21-8 was collared from the same pad as TH21-7 proximal to Station 6725E on line 4700N with a sub-vertical angle to test the depth and easterly extension of the sub-vertical to easterly dipping chargeability high expected to from 50 to 170 meters depth within a resistivity and airborne magnetic high (Figure 17).

### ***Results***

The upper section of the drill hole, from top of hole to 114 metres, is dominated by medium to coarse grained diorite cut by several small (<6m) (quartz) monzonite dykes. Similarly to TH21-7, alteration is dominated by moderate to strong, locally pervasive IPZ alteration that overprints significant and frequently barren magnetite veining (Plate 41) associated with OCP. Magnetite veins and breccias occur frequently however not exclusively proximal to (quartz) monzonite to (quartz) syenite contact margins and, which can explain the strong magnetic signature observed within the airborne magnetics. Localized weakly silica healed and frequently magnetite filled chloritic shears and dilational shear brecciation are noted throughout the upper section of the drill hole within both the diorite and the (quartz) monzonite dykes. Localized tourmaline ± quartz veins (Plate 41) occur as fractures and rare veins. Calcite + pyrite hairline fractures occur sporadically throughout and are noted to cause mafic replaced disseminated and magnetite replaced pyrite ± chalcopyrite that ranges from 1-2% and gradually increase with depth. Immediately below a southeast trending (60-70°) southwest dipping chloritic shear an increase in calcite + pyrite veining and disseminations is noted proximal to the onset of the interpreted chargeability high and continues throughout the drill hole ranging from 1-10% pyrite with trace amounts of chalcopyrite replacing both chlorite + actinolite altered mafics and magnetite. The south-southwest trending (50-60°) west-northwest dipping Valley Fault occurs as a weakly SIL and moderately CRB altered shear zone at 73m depth.

The lower section of the drill hole is dominated by a moderately OCP altered, fine-medium grained (quartz) monzonite. K-feldspar dominate OCP alteration occurs predominately as vein selvage alteration to local weakly developed magnetite fractures and crackle breccias and rare late quartz ± epidote hairline fractures with calcite infill. Frequently, where increased calcite is noted, an increase in disseminated wispy to blebby pyrite ± chalcopyrite is noted predominately as magnetite replacement. Significant zones of chloritic shearing is more represented as vein style chloritic micro-shears infilled with calcite and minor magnetite within the (quartz) monzonite.

No significant zones of mineralization were intersected within the drill hole.

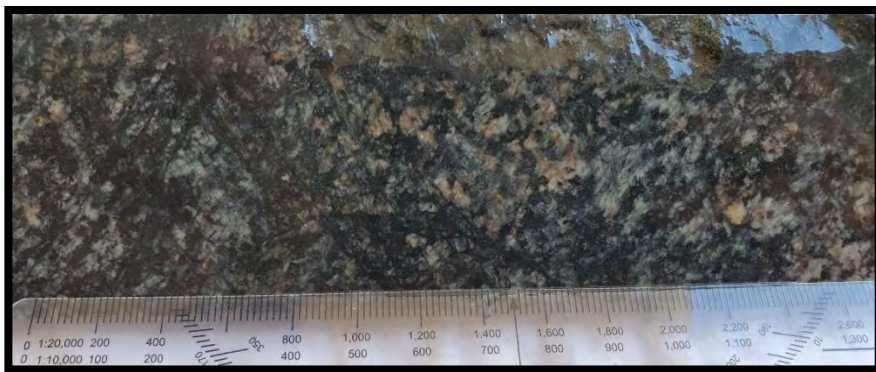


**Plate 41:** Logged as a medium to coarse grained diorite containing fracture fill weakly chlorite altered biotite with K-spar alteration selvages and magnetite+tourmaline fractures @65.40m.

## **TH21-11**

### ***Obejctive***

TH21-11 was collared proximal to Station 6725E on line 4600N approximately 100 meters north of TH21-7 and TH21-8. The hole was drilled westward and targeted the southern extension of the airborne magnetic high and the sub-vertical to easterly dipping chargeability that is interpreted to occur from the collar down to a minimum depth of 120 meters (Figure 18). The chargeability high occurs within a resistivity high that decreases with depth. The drill hole targeted alternating OCP, IPZ and OPZ altered medium to coarse grained diorite crosscut by the northern extensions of the upper and lower sub-vertical to easterly dipping OCP altered fine to medium grained (quartz) monzonite to (quartz) syenite dykes, which were intersected within drill holes TH21-7 and TH21-8. Additionally, the northern extension of several south-southeast trending (70-80°) westerly dipping and potentially mineralization controlling structures were targeted at depth.

### ***Results***

The upper section of the drill hole, down to 63 meters depth, contains medium to coarse grained diorite cross-cut by a moderate westerly dipping latite porphyry. Alteration is dominated by moderate to strong, locally pervasive IPZ alteration that overprints OCP alteration related to hairline fractures and veins of magnetite that also infiltrate localized south-southeast trending (70-80°) westerly dipping chloritic shears and dilational shear breccias. OCP alteration is also noted within and along the lower contact margin of the latite porphyry and the upper section of the (quartz) monzonite. Patchy moderate to strong SIL alteration locally with an increase in mafic replaced biotite alteration potentially represents biotite hornfelsing of the diorite related to the upper (quartz) monzonite dyke at depth. Late quartz + epidote + calcite + pyrite ± chalcopyrite ± arsenopyrite hairline fractures and veins with K-feldspar alteration selvages increase in frequency and abundance with depth and overprints all alteration above (Plates 42 and 43). The interpreted chargeability is conducive to the increase in quartz + epidote + calcite + pyrite ± chalcopyrite hairline fractures and veins and associated mafic and magnetite replacement that increases typically from 1-3% in abundance to 3-5%.

Within TH21-11, the northern extension of the upper (quartz) monzonite contains moderate OCP and localized AKL (tourmaline + quartz veins, fractures and blobs) alteration overprinted by weak to moderate interstitial SIL alteration. Late CRB alteration is also observed and appears to post date SIL alteration related to a significant increase in quartz + epidote + calcite + pyrite ± chalcopyrite ± arsenopyrite hairline fractures and veins. Both SIL and CRB alteration occur proximal to intersecting south-southeast trending (70-80°) west dipping and an east-southeast trending (60-80°) south dipping structure at 86 meters depth. It is interpreted the SIL alteration and related quartz+sulphide veins and fractures are associated with south-southeast trending (70-80°) west dipping structures whereas the CRB alteration and related calcite veins are related to the east-southeast trending (60-80°) south dipping structures. An increase in arsenic appears associated with the latter structural set. The intersection of these structures also marks a potential decrease in resistivity, as a result of increased secondary and primary K-feldspar and albite in conjunction with a decrease in secondary silica. Within the area of intersecting structures, a low-grade mineralized zone returned 0.14% Cu, 0.07 g/t Au, 0.7 g/t Ag and 5.5 ppm Mo over 10.50 meters (82.50-93.00m).

Between the upper and lower (quartz) monzonite dykes, medium to coarse grained diorite is dominated by OPZ alteration locally overprinted by patchy OCP related to magnetite ± biotite veins and fractures (Plate 44). Quartz ± epidote + calcite + pyrite ± chalcopyrite fractures and veins and associated low-grade indicator style copper gold intercepts occur proximal to and within several south-southeast trending west dipping (70-80°) chloritic shears. Where PAZ and CRB alteration is noted to increase within these structures, intersecting east-southeast trending (60-80°) south dipping structures are suspected.

The northern extension of the lower sub-vertical (quartz) monzonite to (quartz) syenite is intersected within the base of the drill hole. It occurs as a series of dykes containing moderate to strong OCP alteration related to magnetite veining. Late quartz + epidote + calcite ± sulphide veins and fractures are frequently noted proximal to contacts replacing magnetite.

Sulphides below the interpreted level of chargeability (~120m depth) throughout the diorite and into the lower (quartz) monzonite are recorded to range from 1-10%.

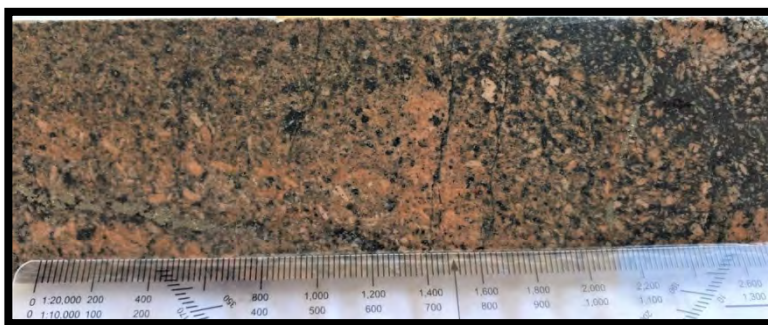


**Plate 42:** Vein selvage K-feldspar alteration related to OCP magnetite cross-cut by granular veins of pyrite and lesser chalcopyrite within latite porphyry @27.55m. Sample# 41891 containing 0.21% Cu, 0.02g/t Au, 0.73g/t Ag and 0.55ppm Mo over 1.00m.

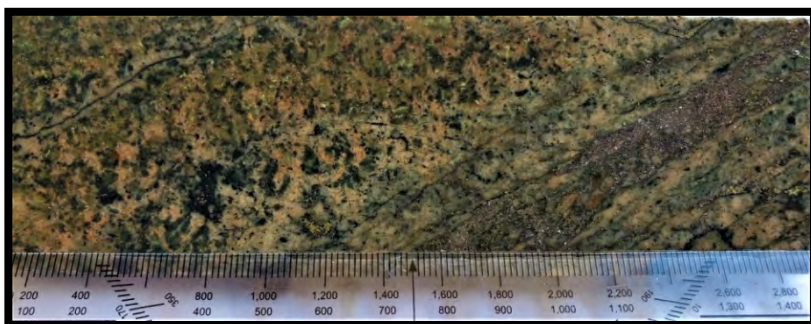


**Plate 43:** Quartz-arsenopyrite-pyrite-chalcopyrite vein with sericite altered margins cuts (quartz) monzonite @83.00m. Arsenopyrite is potentially related to east-southeast trending southerly dipping structures often containing increased CRB alteration (calcite). Sample# 41958 containing 0.19% Cu, 0.20g/t Au, 0.92g/t Ag and 13.70ppm Mo over 0.50m.

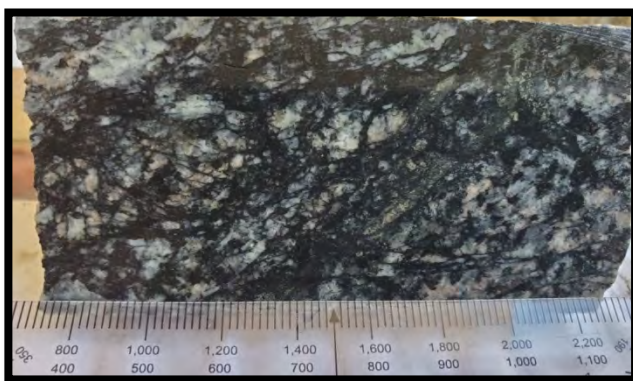


**Plate 44:** Pervasive K-feldspar and silica alteration associated with biotite+magnetite and lesser actinolite veins cuts and alters medium-coarse grained diorite @204.00m.

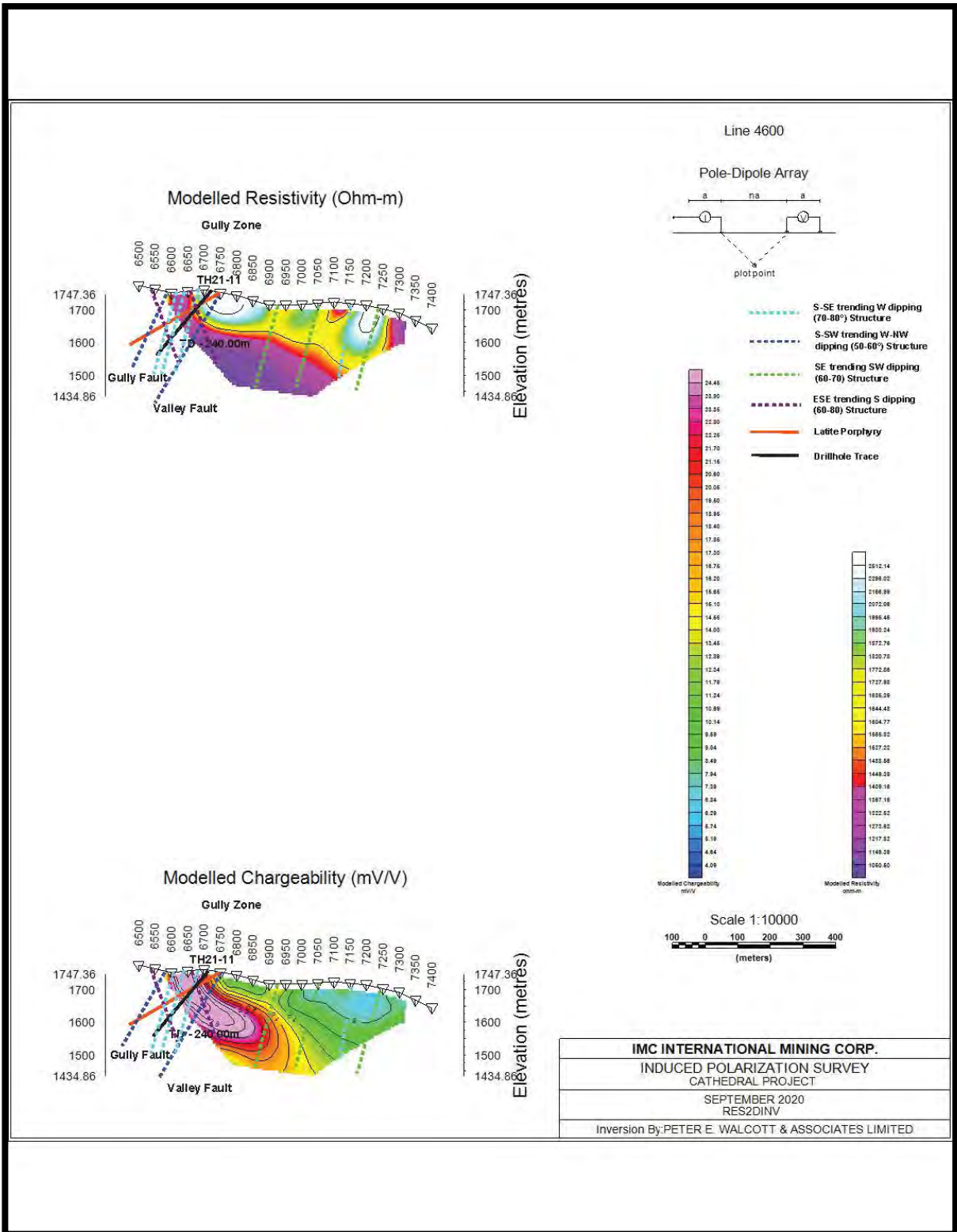


Figure 18: Drill hole trace with IP, TH21-11 (schematic)



#### 6.5.4 Cathedral South

A single drill hole was collared in the Cathedral South area proximal to Station 5950E on line 5200N

##### **TH21-4**

###### ***Objective***

The hole was drilled eastward within a low airborne magnetic signature and moderate to low resistivity and chargeability (Figure 19). The hole targeted IPZ hydrothermal porphyry alteration and associated sheeted to stockwork actinolite-magnetite-pyrite-chalcopyrite mineralization as well as peripheral SCA to SA at depth. Targeted rock types included altered diorite to (quartz) monzonite and a potential north-south trending westerly dipping latite porphyry intrusive phase. Additionally, alteration and mineralization controlled by east-southeast trending and south to southeast trending chlorite shear related structures were targeted at depth.

###### ***Results***

The upper section of the drill hole down to the monzodiorite contact (78 meters) contained alternating patchy OCP overprinted by weak IPZ alteration defined by actinolite + chlorite + calcite fractures and veins (Plate 45) with albite alteration selvages. Both are overprinted by weak to moderate SCA alteration defined by quartz + epidote + chlorite veinlets within a medium to coarse grained diorite. Patchy SA defined as pervasive albitization and complete destruction of both primary and secondary magnetite to hematite. Minor quartz + epidote ± chalcopyrite veinlets with K-spar alteration selvages are also noted and appear to post date earlier mentioned veins. Calcite appears late, infilling all sets of fractures. The abundance of albite throughout the upper section correlates to the area of low resistivity. Local areas of silicification and rare tourmaline vein brecciation (Plate 46) occur proximal and within overprinting PAZ and CRB alteration within east-southeast trending (60-80°) south dipping and south-southwest trending (50-60°) west-northwest dipping chloritic shears combined with the presence of an epidote + carbonate (calcite) altered latite porphyry appears to correlate to the pod of resistivity.

OPZ alteration occurs proximal to the upper contact within both a latite porphyry and a medium to coarse grained monzonite (Plate 47). An increase in OCP alteration defined by the presence of localized semi-massive magnetite veins and fractures with pervasive K-feldspar alteration selvages increase with depth and seemingly radiate from the lower intersection of latite porphyry. Both are overprinted by SCA to SC alteration defined by hematite alteration of magnetite and PAZ alteration the latter proximal to localized east-southeast trending (60-80°) south dipping shears. Minor quartz+epidote±calcite veinlets with K-feldspar alteration selvages occur throughout.

A moderately silica and carbonate altered south-southwest trending (50-60°) west-northwest dipping chloritic shear occurs on the chilled monzodiorite lower contact with a lower section of medium to coarse grained diorite containing predominately OPZ and patchy IPZ alteration. The structure also marks the transition from the interpreted high to low resistivity. Localized

areas of increased SIL alteration occur proximal to CRB and PAZ alteration within small (<1m) east-southeast trending (60-80°) south dipping chloritic shears was observed throughout the diorite.

A significant structural zone occurs on the upper contact with fine to medium grained (quartz) monzonite. This zone is interpreted to be south-southwest trending (50-60°) west-northwest dipping and an east-southeast trending (60-80°) south dipping chloritic shear structures. Pervasive to intense PAZ and late CRB alteration occurs throughout the zone as a result of the increased abundance of interstitial, hairline fractures and veins of calcite.

The abundance of SCA to SA alteration overprinting and altering secondary magnetite related to OPC and IPZ alteration reflects the airborne magnetic low observed within the area of the drill hole. The interpreted low charginability correlates to sporadic pyrite ± chalcopyrite mineralization occurring predominately in trace amounts. This mineralization can increase up to 3% (≤ 1m) as fine-grained disseminated blebs associated with areas of increased silicification, which occurs within or proximal to chloritic shears (Plate 48 and 49). Mafic replacement disseminations on K-feldspar altered vein selvages to quartz + epidote ± sulphides + calcite veins and fractures were observed. Where these fractures and veins intersect younger sheeted to stockwork actinolite and or magnetite veins and breccias, sulphide mineralization is generally pyrite dominate occurring as fine to medium grained disseminated blebs within or on the margins of (Plate 50). Two localized low-grade zones of mineralization were intersected proximal to areas of silica, carbonate ± magnetite healed chloritic shears. One of these low-grade copper mineralized zones returned 0.05% Cu, 0.03 g/t Au, 0.2g/t Ag and 7.20 ppm Mo over 17.30 metres (108.20 to 125.50m). This intersection occurs within an area of increased SIL alteration proximal to and within the south-southwest trending (50-60°) west-northwest dipping chloritic shear on the lower monzodiorite contact.



**Plate 45:** Sheeted and vein brecciated actinolite cut by epidote±quartz and late dilational calcite veins within pervasive, texturally destructive SCA within medium to coarse grained diorite @35.20 meters. Trace sulphides noted within the actinolite likely associated with epidote and quartz.

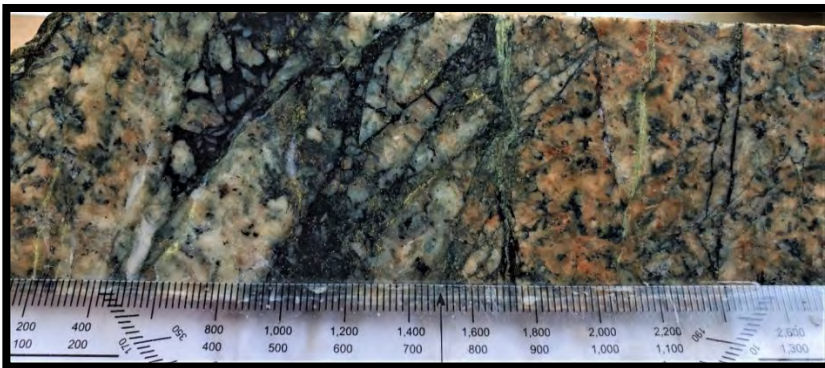


**Plate 46:** Tourmaline+quartz brittle (cataclastic) vein breccia contains disseminated and fractures of pyrite±chalcopyrite potentially related to quartz+epidote fractures @70.31m.

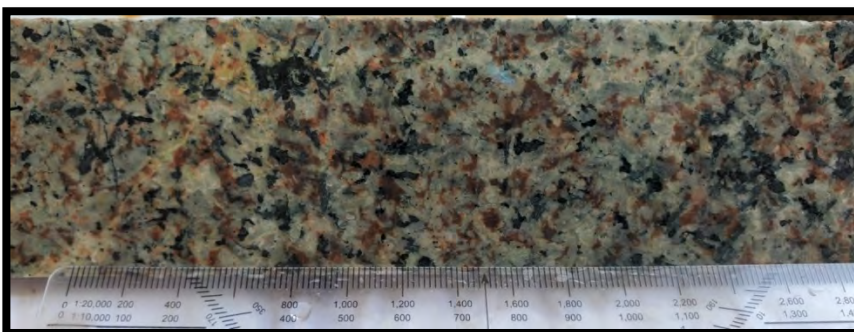


**Plate 47:** Barren, weak SCA altered medium to coarse grained monzodiorite @82.43 meters.

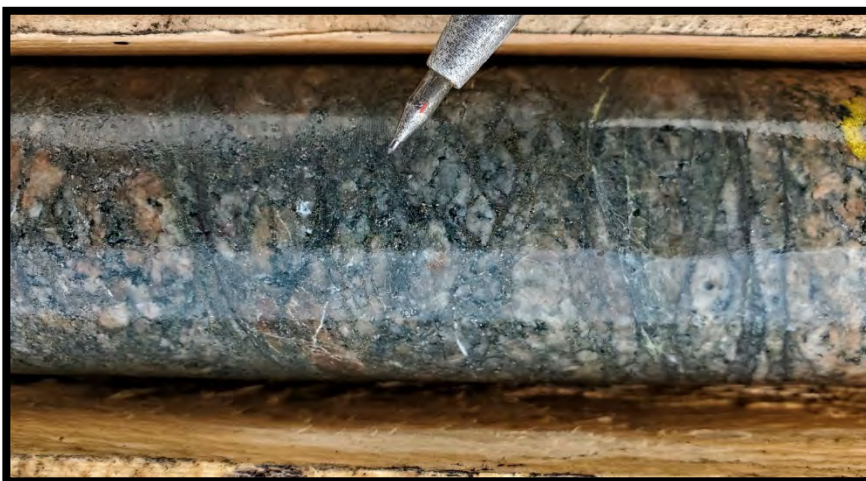


**Plate 48:** Pervasive SIL alteration overprints patchy K-feldspar alteration and localized chloritic micro-shears within monzodiorite. Pyrite±chalcopyrite occur as hairline fractures and very fine-grained disseminations @91.80m. Sample# 42360 containing 0.05% Cu, 0.02g/t Au, 0.43g/t Ag and 15.00ppm Mo over 0.50m.



**Plate 49:** Localized 20cm. weakly SIL altered chlorite-hematite shear containing deformed early quartz and calcite veining. Brittle reactivation of shear contains late calcite fractures. Interstitial to blebby pyrite±chalcopyrite @96.77m. Sample # 42365 containing 0.1% Cu, 0.07g/t Au, 2.93g/t Ag and 3.27ppm Mo over 0.50m.



**Plate 50:** Coarse grained blebs of chalcopyrite within 10cm magnetite+chlorite vein breccia proximal to chloritic shear @240.90m. Sample # 42476 containing pyrite±chalcopyrite - 96.77m. Sample # 42365 containing 0.13% Cu, 0.03g/t Au, 0.12g/t Ag and 108.00ppm Mo over 0.60m.

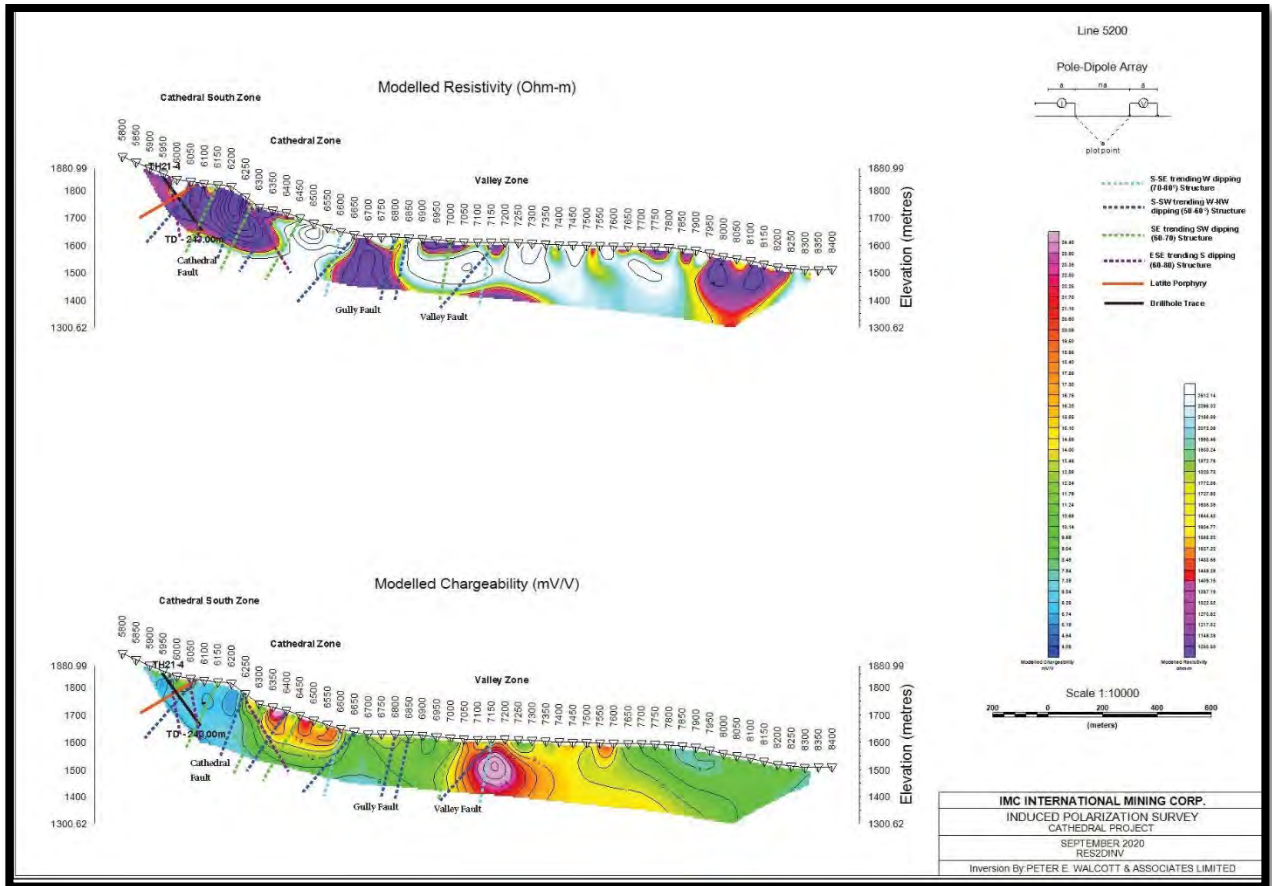


Figure 19: Drill hole trace with IP, TH21-4 (schematic)

### 6.5.5 Pinnacle

Two drill holes were collared within the Pinnacle Area at Station 3000N on line 5000E.

#### TH21-9 and TH21-10

##### *Objective*

The drill holes targeted the down dip potential of the Pinnacle Showing. Historical sampling of this Showing has returned up to 13.0 g/t Au from narrow upper-level auriferous late-stage hydrothermal high-grade quartz-arsenopyrite-chalcopyrite-pyrite veins (Naas 2013). A series of these southeast moderately southwest to sub-vertical dipping veins, and associated fracture-controlled mineralization, occur over a width of 60 metres (Naas, 2014). Due to topographic relief, the drill holes were oriented sub-perpendicular to the strike direction of the Pinnacle Showing vein system. The drill holes were collared within interpreted moderately high resistivity and moderately low chargeability decreasing to broadly moderate resistivity and increasing to moderate chargeability with depth (Figure 20).

## **Results**

The drill holes consisted of predominately moderate, pervasive OPZ alteration within medium to coarse grained diorite (Plate 51) and localized fine to medium grained sub-vertical cross-cutting (quartz) monzonite to (quartz) syenite (Plate 52) dykes. Patchy to rarely pervasive, weak to moderate K-feldspar alteration occurs as contact alteration and weak OCP alteration related to localized magnetite fractures and veins occurs proximal to frequently sheared contacts. Away from contacts, K-feldspar alteration often occurs as vein selvage alteration to late quartz+epidote fractures and veins.

Several south-southwest trending (60-70°) west-northwest dipping variably SIL, PAZ and CRB altered, healed and brecciated chloritic shear structures were intersected throughout both drill holes. In areas where these structures are intersected by south-southeast trending (70-80°) westerly dipping structures, increased gold, silver, copper and arsenic grades occur in quartz-calcite-arsenopyrite-chalcopyrite-pyrite veins, fractures and disseminations. Brittle reactivation of these structures (Plate 53) is dominated by localized brecciation and associated PAZ alteration infilled and locally healed by carbonate fractures, veins and associated CRB alteration related to east-southeast trending (60-80°) southerly dipping structures. These structures are interpreted to post date earlier intersecting structures and mineralization.

Two separate zones of mineralization occur with the intersected shear zones described above within TH21-9. The first zone returned 0.12% Cu, 0.97g/t Au, 1.19g/t Ag and 3.77 ppm Mo over 1.22 metres (42.78.70 to 44.00m). The second zone returned 0.08% Cu, 0.18g/t Au, 1.13g/t Ag and 19.10ppm Mo over 2.77 metres (115.49 to 118.26m).

Drill hole TH21-10 intersected a single significant mineralize zone, which returned 0.07% Cu, 0.21g/t Au, 0.58g/t Ag and 9.45 ppm Mo over 2.78 metres (115.25 to 118.03m).

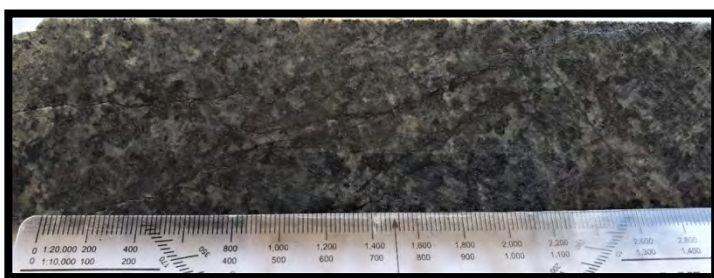


**Plate 51** Typical moderate OPZ and weak SIL alteration with shear related chlorite fractures within medium to coarse grained diorite. Plate here is from TH21-9 @138.50m.

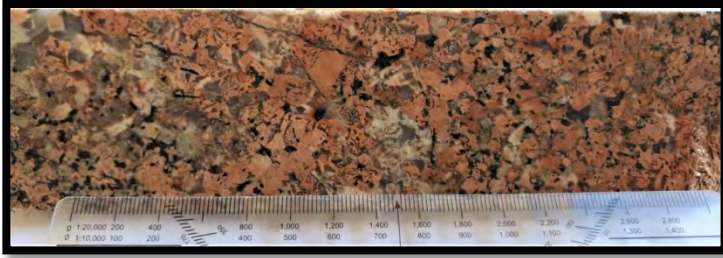


**Plate 52:** Coarse grained to pegmatitic (quartz) syenite @105.05m within TH21-9. These are frequently noted on the margins of most (quartz) monzonite dykes throughout the Cathedral, Gully Valley and Pinnacle areas.

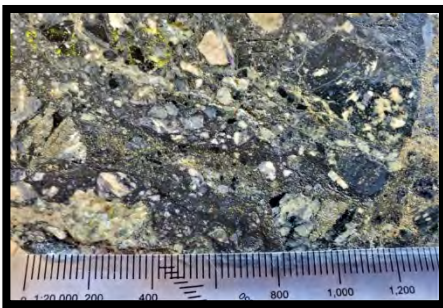


**Plate 53:** Polythitic breccia @117.41m within TH21-9 containing a chlorite-clay matrix infilled with arsenopyrite-pyrite±chalcopyrite±molybdenite and minor quartz. Late brittle faulting and fracture-controlled Fe-carbonate post date silicification and mineralization. Sample # 41695 containing 0.16% Cu, 0.39g/t Au, 3.7g/t Ag, and 84.80ppm Mo over 0.37meters.

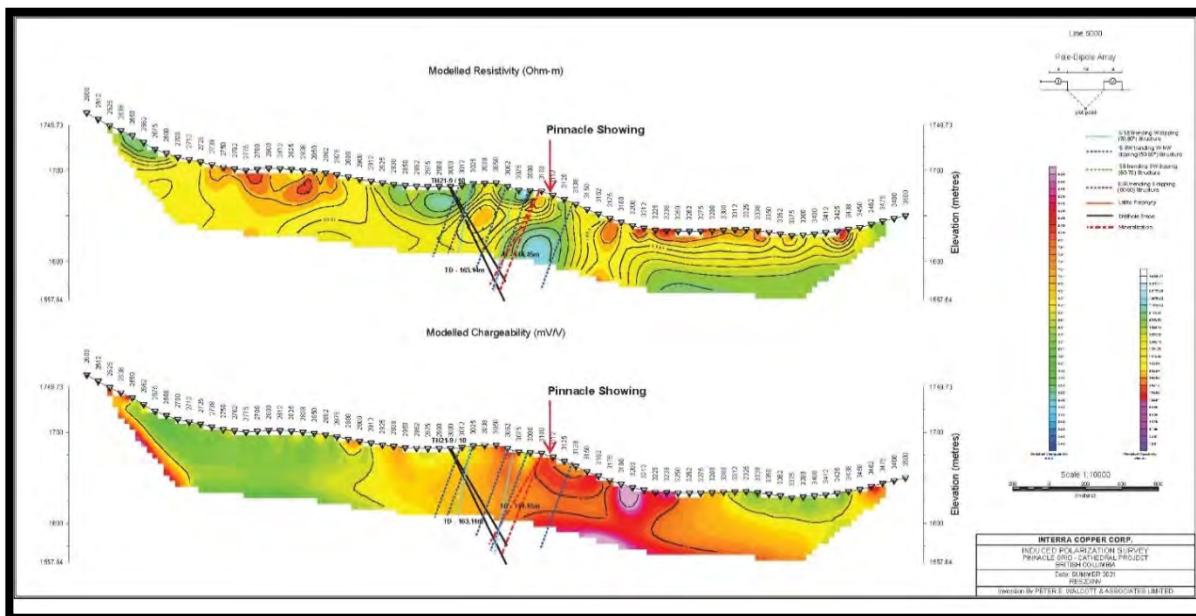


Figure 20: Drill hole trace with IP, TH21-9 and TH21-10 (schematic)

## 6.5.6 Analytical Results

Significant results from the drill program are presented in Table 14.

Table 14: Selected core sample results

Drill Hole ID	From	To	Length (m)	Results			
				Cu (%)	Au (g/t)	Ag (g/t)	Mo (ppm)
TH21-3	20.10	40.75	20.65	0.08	0.03	0.2	2.5
incl.	31.75	40.75	9.00	0.13	0.06	0.2	2.1
TH21-4	108.20	125.50	17.30	0.05	0.03	0.2	7.2
incl.	115.95	120.00	4.05	0.13	0.07	0.5	8.7
TH21-4	187.00	193.50	6.50	0.04	0.02	0.2	2.1
TH21-4	240.90	243.00	2.10	0.06	0.01	0.1	33.5
TH21-6	75.77	77.00	1.23	0.68	0.06	2.6	65.7
TH21-6	120.00	156.71	36.71	0.08	0.02	0.5	5.0
incl.	120.64	132.98	12.34	0.11	0.03	0.7	7.0
TH21-7	20.50	39.50	19.00	0.05	0.01	0.2	7.2
TH21-7	70.00	94.50	24.50	0.13	0.03	0.3	4.1
incl.	70.00	72.50	2.50	0.84	0.20	2.0	2.1
TH21-8	47.30	66.70	19.40	0.04	0.01	0.1	2.8
incl.	47.30	50.30	3.00	0.47	0.13	1.6	36.8
TH21-8	108.00	142.50	34.50	0.03	0.01	0.2	3.4
TH21-9	115.49	118.26	2.77	0.08	0.18	1.1	19.1
TH21-9	128.00	129.53	1.53	0.07	0.05	0.7	27.9
TH21-9	138.00	139.20	1.20	0.06	0.19	0.5	3.3
TH21-10	115.25	118.03	2.78	0.07	0.21	0.6	9.4
TH21-11	26.00	31.67	5.67	0.13	0.05	0.4	1.5
TH21-11	82.50	93.00	10.50	0.14	0.07	0.7	5.5
TH21-11	116.75	117.12	0.37	1.12	0.38	2.9	3.7
TH21-11	151.50	155.70	4.20	0.20	0.02	0.7	5.7
TH21-11	218.10	220.13	2.03	0.46	0.12	0.8	12.7
incl.	219.10	220.13	1.03	0.83	0.22	1.5	22.0
TH21-12	60.21	61.85	1.64	0.08	0.05	0.5	5.0
TH21-12	113.35	118.35	5.00	0.21	0.07	0.6	23.6

## 6.6 PETROGRAPHIC STUDIES

Upon completion of the drilling program, 18 drill samples (17 core, 1 surface rock) were collected and submitted to Vancouver Petrographics of Langley, BC for polished thin section study (Appendix VIa). Sample descriptions, included questions, accompanied each sample and are presented in Appendix VIb.

Samples were chosen in order to identify and confirm host lithology, alteration minerals and styles, vein composition and mineralization relationships to alteration. Additionally, the results of this work would be compared to historical petrographic studies of surface samples.



## **7.0 SAMPLE PREPARATION, ANALYSIS AND SECURITY**

### **7.1 SAMPLE PREPARATION**

All samples were transported by CME personnel from the field to CME's field office in Vavenby, BC. Rock samples were cut by rock saw with one half delivered to ALS Minerals of Kamloops, BC for sample preparation and analysis while the other half of the sample was retained for reference.

Sample numbers used to identify silt, soil and rock samples included a barcode, which allowed for each sample to be scanned and documented prior to shipping to the ALS laboratory.

Methodology of the sample preparation is presented in Appendix VIIa and is summarized below.

#### **Soil Sample Preparation (ALS Method Code: PREP-41)**

An entire sample is dried and then dry-sieved using a 180 micron (Tyler 80 mesh) screen. The plus fraction is retained unless disposal is requested. This method is appropriate for soil or sediment samples up to 1 kg in weight.

#### **Rock and Core Sample Preparation (ALS Method Code: PREP-31)**

The sample was logged in the tracking system, weighed, dried and finely crushed to better than 70 % passing a 2 mm (Tyler 9 mesh, US Std. No.10) screen. A split of up to 250 g is taken and pulverized to better than 85 % passing a 75 micron (Tyler 200 mesh, US Std. No. 200) screen.

Work involved crushing the rock sample through a jaw crusher and cone or roll crusher to -10 mesh. The sample was then split through a Jones riffle until a -250 gram sub sample was achieved. The sub sample was pulverized in a ring and puck pulverizer to 95% -140 mesh.

Rock sample pulps (certified reference materials) were homogenized. The pulp sample is poured into a small plastic container. The vials are placed into holders and then into a mechanical rolling machine. The samples are blended until they are completely homogenized.

### **7.2 SAMPLE ANALYSIS**

Multi-element and gold analysis was performed on all samples. Sample returning over limits in precious and base metals were subject assays. To complement the petrographic study, selected samples were subject to whole rock analysis.

Methodology of the sample analysis is presented in Appendix VIIa and is summarized below.

### **Soil and Rock Analysis - Multi-element ICP Analyses (ALS Method Code: ME-MS41)**

A prepared sample (0.50 g) is digested with aqua regia in a graphite heating block. After cooling, the resulting solution is diluted with deionized water, mixed and analyzed by inductively coupled plasma-atomic emission spectrometry. Following this analysis, the results are reviewed for high concentrations of bismuth, mercury, molybdenum, silver and tungsten 25 and diluted accordingly. Samples are then analysed by ICP-MS for the remaining suite of elements. The analytical results are corrected for inter element spectral interferences.

### **Rock Analysis - Copper, Lead and Silver Assays (ALS Method Code: ME-OG46)**

A prepared sample (0.4 g) is digested with concentrated nitric acid for 90 minutes in a graphite heating block. The resulting solution is diluted with concentrated hydrochloric acid before cooling to room temperature. The samples are diluted in a volumetric flask (100 or 250) mL with demineralized water and analyzed using atomic absorption spectrometry.

ICP-AES is the default finish technique for ME-OG46. However, under some conditions and at the discretion of the laboratory an AA finish may be substituted.

### **Core Analysis - Multi-element ICP Analyses (ALS Method Code: ME-MS61)**

The ME-MS61 Ultra Trace method combines a four-acid digestion with ICP-MS instrumentation. A four acid digestion quantitatively dissolves nearly all minerals in the majority of geological materials. A prepared sample (0.25 g) is digested with perchloric, nitric and hydrofluoric acids. The residue is leached with dilute hydrochloric acid and diluted to volume.

The final solution is then analyzed by inductively coupled plasma-atomic emission spectrometry and inductively coupled plasma-mass spectrometry. Results are corrected for spectral inter-element interferences.

### **Core Analysis - Copper and Zinc Assays (ALS Method Code: ME-OG62)**

Assays for the evaluation of ores and high-grade materials are optimized for accuracy and precision at high concentrations. Ultra high concentration samples (> 15 -20%) may require the use of methods such as titrimetric and gravimetric analysis, in order to achieve maximum accuracy.

A prepared sample is digested with nitric, perchloric, hydrofluoric, and hydrochloric acids, and then evaporated to incipient dryness. Hydrochloric acid and de-ionized water is added for further digestion, and the sample is heated for an additional allotted time. The sample is cooled to room temperature and transferred to a volumetric flask (100 mL). The resulting solution is diluted to volume with deionized water, homogenized and the solution is analyzed by inductively coupled plasma - atomic emission spectroscopy or by atomic absorption spectrometry. Results are corrected for spectral interelement interferences.

### **Soil, Rock and Core Gold Analyses (ALS Method Code: Au-ICP21)**

A prepared sample is fused with a mixture of lead oxide, sodium carbonate, borax, silica and other reagents as required, inquarted with 6 mg of gold-free silver and then cupelled to yield a precious metal bead.

The bead is digested in 0.5 mL dilute nitric acid in the microwave oven. 0.5 mL concentrated hydrochloric acid is then added and the bead is further digested in the microwave at a lower power setting. The digested solution is cooled, diluted to a total volume of 4 mL with demineralized water, and analyzed by inductively coupled plasma atomic emission spectrometry against matrix-matched standards.

### **Age Dating (ALS Method Code: Re-ISTP01)**

Areas of the sample with visible molybdenite underwent metal-free crushing followed by gravity and magnetic concentration methods to obtain a molybdenite mineral separate. Methods used for molybdenite analysis are described in detail by Selby & Creaser (2004) and Markey et al. (2007). The  $^{187}\text{Re}$  and  $^{187}\text{Os}$  concentrations in molybdenite were determined by isotope dilution mass spectrometry using Carius-tube, solvent extraction, anion chromatography and negative thermal ionization mass spectrometry techniques. A mixed double spike containing known amounts of isotopically enriched  $^{185}\text{Re}$ ,  $^{190}\text{Os}$ , and  $^{188}\text{Os}$  analysis is used. Isotopic analysis used a ThermoScientific Triton mass spectrometer by Faraday collector.

## 7.3 QUALITY CONTROL

Quality control protocol was implemented for soil and rock samples.

### 7.3.1 Control Samples

#### Rock Samples

During analyses of the rock samples, a single certified reference material (CRM) was inserted into the sample sequence one with each sample dispatch. The CRM was obtained from CDN Resource Labs of Delta, BC and came prepackaged in a 60 gram sample size. Certified values are presented in Table 15 and specifications for these CRM's are presented in Appendix VIIb.

Table 15: Certified reference material, rock samples

Standard	Recommended Values		
	Gold (Au)	Copper (Cu)	Molybdenum (Mo)
OREAS 152a	116 ± 5 ppb	0.385± 0.009 %	80± 5 ppm
CDN-CM-25	0.228 ± 0.030 g/t	0.194± 0.008 %	0.019± 0.002 %

All three certified reference materials returned acceptable results for all three elements. No blank standards were inserted into the sample sequence.

Sample numbers with results for all control samples submitted with rock samples are listed in Appendix VIIc.

#### Core Samples

During analyses of the rock samples, a single certified reference material (CRM) was inserted into the sample sequence approximately once every 35 samples. The CRM was obtained from CDN Resource Labs of Delta, BC and came prepackaged in a 60 gram sample size. Certified values are presented in Table 16 and specifications for these CRM's are presented in Appendix VIIb. The blank material consisted of decorative limestone rock obtained from Home Depot of Kamloops, BC. The recommended values for the blank material (referenced as CME-LMST) was determined by statistical analysis from historical analysis of similar material, which returned upper limits of 0.006 ppm for gold and 44.9 ppm for copper.

Table 16: Certified reference material, core samples

Standard	Recommended Values		
	Gold (Au)	Copper (Cu)	Molybdenum (Mo)
OREAS 152a	116 ± 5 ppb	0.385± 0.009 %	80± 5 ppm
CDN-CM-25	0.228 ± 0.030 g/t	0.194± 0.008 %	0.019± 0.002 %

The 148 control samples consisted of 75 blanks and 73 certified reference materials. All but two samples returned acceptable results. Samples 41341 and 42581 both failed on the blank material. Sample 41241 returned 0.007 ppm Au and 124.0 ppm Cu. Sample 42581 returned 0.001 ppm Au and 82.3 ppm Cu. Both samples were inserted into the sample sequence to

follow samples with significant visible copper mineralization. The sample preceding 41341 returned 1.835% Cu and the sample preceding 42581 returned 3.42% Cu. The result from ALS's investigation into these two samples was that the percentage of increase relative to the sample size was acceptable and therefore the analytical results for both sample batches were acceptable.

Sample numbers with results for all control samples submitted with drill core are listed in Appendix VIIc.

## 8.0 DISCUSSION

### 8.1 GAIL AREA

The current hypothesis for the resistivity low anomalies along line 2200N based on surface mapping integration with IP surveys is explained by an east-west trending fault towards the northeastern end of the line and a north-south trending fault further southwest on the line. Both faults have been crosscut by a large medium grained granodiorite intrusion which has displaced and segmented the fault zones. Evidence for granodiorite intrusions crosscutting faulted coarse grained diorite. Additionally, the low chargeability plot supports the presence of a more felsic intrusive lithology as compared to L2400N and L2500N, which have been mapped to contain predominately patchy silicified diorite.

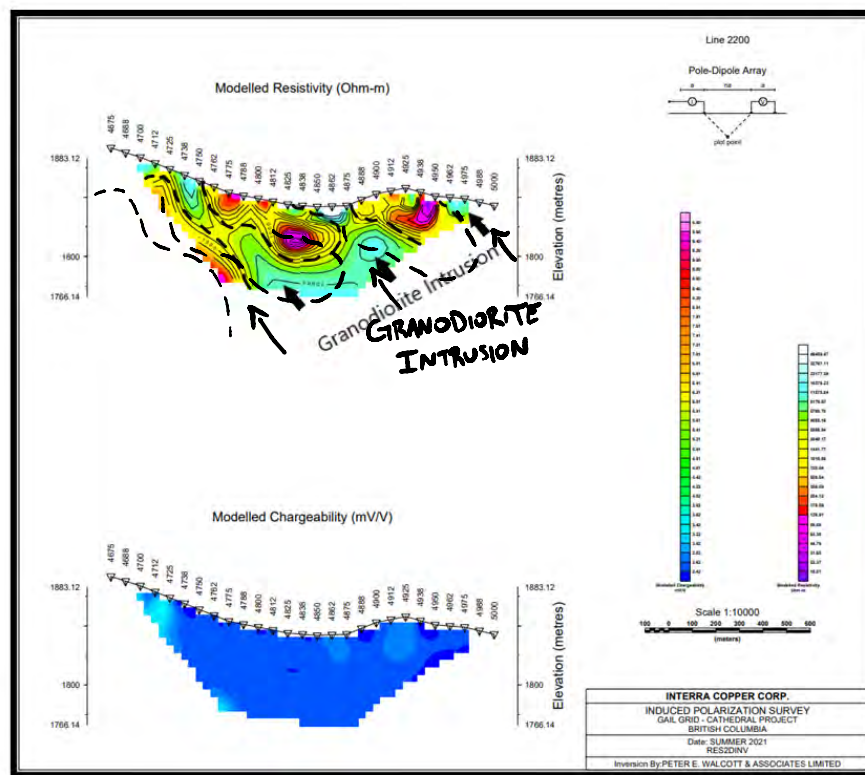


Figure 21: L2200N, Gail Grid, geological interpretation (schematic)

### **L2200N – Chargeability:**

Multiple surface mapped contacts occur between the diorite and granodiorite along and proximal to the northeast-southwest trending IP line. A large body of unmineralized granodiorite is located within the area and likely represents the contact margin between both intrusive bodies. The broad, surface and sub-surface area of low chargeability observed within the modelled chargeability represents a lack of appreciable mineralization within the area and is comparable to the lack of mineralization noted during surface mapping. This differs from mapping completed to the northwest and southwest along and proximal to L2400N and L2500N where surface and sub-surface chargeability correlates to localized quartz - pyrite  $\pm$  chalcopyrite  $\pm$  molybdenite vein mineralization within moderate to strongly silicified diorite.

### **L2200N – Resistivity:**

To the south along L2200N, proximal to station 4775E-4800E there is a resistivity low surface anomaly. A north-south trending, moderate west dipping (198/62), barren brittle structure with abundant secondary carbonate and minor K-spar alteration is mapped along the contact margin of the diorite and granodiorite where it intersects line L2200N at the location of the surface anomaly. The discontinuous nature of the low resistivity zones could be explained by the crosscutting granodiorite intrusions, which seemingly follow areas of increased resistivity observed on the modelled resistivity plot (see black dashed lines on figure 21 resistivity plot).

Two explanations for the decrease in resistivity observed between stations 4938E-4950E are provided:

1. E-W trending (112/82) barren brittle structure with abundant secondary carbonate infill intersects L2200N between stations 4900-4925E. It is likely the abundance of ankerite within and proximal to the structure relative to the surrounding rock that accounts for the decrease in resistivity.
2. Latite porphyry dyke mapped 70 m to the north of L2200N. The structure of this dyke is currently unknown in the area of L2200N, however a latite further southwest was mapped trending southeast and dipping moderately southwest (150/66). If this dyke follows on trend, it would intersect L2200N within the area of decreased resistivity. Additionally, most of the latite porphyries mapped contain increased carbonate (calcite) alteration and trace disseminated pyrite.
  - As seen to the south on L2200N, the discontinuous nature of decreased resistivity could be explained by crosscutting granodiorite intrusions.
  - Since the granodiorite is older than the latite porphyry, the crosscutting model would only support the E-W trending fault causation for the northeastern anomaly.
  - The sharp 90° bend at depth on the northeastern anomaly may provide insight on the flow path of the granodiorite intrusion and suggest the bullseye anomaly

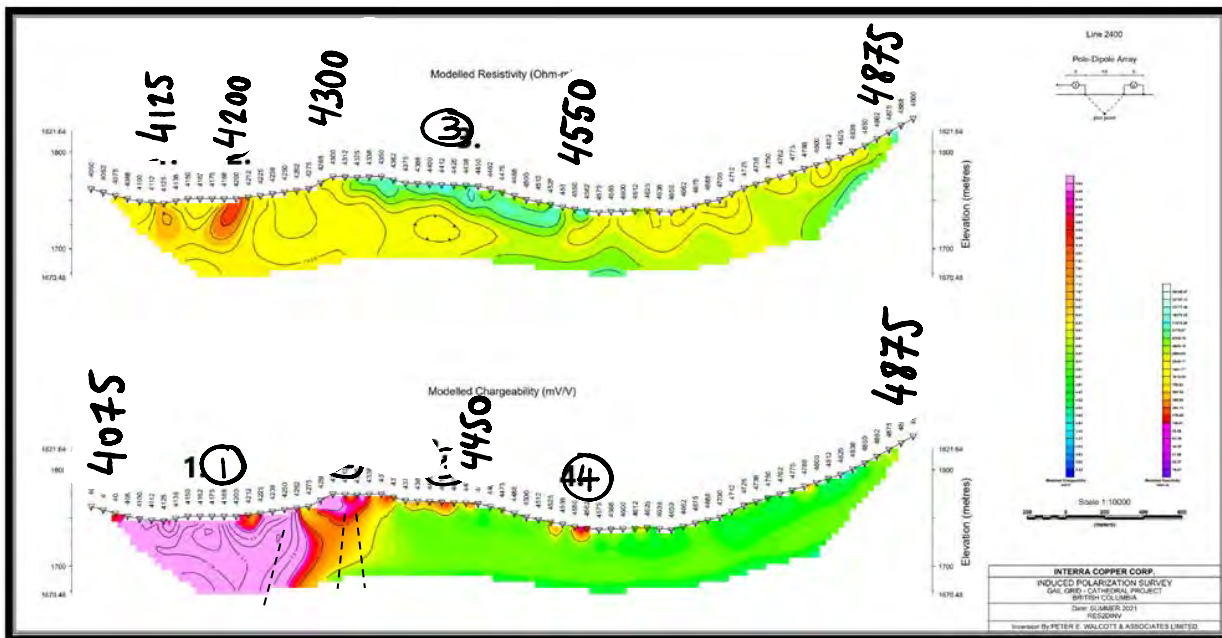


Figure 22: L2400N, Gail Grid, interpretation (schematic)

Surface resistivity interpretations (Figure 22) based on geological surface mapping (from SW to NE):

#### **Station 4125E**

Slight decrease in resistivity due to second order stream intersection that may be rich in metal ions from nearby Gail showing located within the stream catchment. The stream is likely located within a north-south trending structure, however further geological mapping to the south will be required to confirm its existence.

#### **Station 4200E**

Significant decrease in resistivity potentially as a result of a southeasterly trending, moderately west dipping (150/66), weak to moderate carbonate (calcite) altered and fractured latite porphyry dyke bearing trace disseminated pyrite mapped ~150m to the south that intersects L2400N at this station.

#### **Station 4312E to 4562E**

Increase in resistivity within moderate to strong silicified CG diorite as a result of localized quartz ± sulphide veining.

Surface chargeability interpretations based on geological surface mapping (from SW to NE):

#### **Station 4075E to 4262E**

Significant increase in broad surface and sub-surface chargeability as a result of several southeasterly trending subvertical to steeply west and easterly dipping quartz + pyrite ± molybdenite ± chalcopryrite veins mapped ~200m to the south and sulphide filled fractures frequently noted within moderate to strongly silicified CG diorite. Majority of the area

containing chargeability high from station 4100E-4200E contains very little to no outcrop due to extensive talus coverage.

**Station 4300E to 4350E**

Significant increase in surface and sub-surface chargeability as a result of several N-S to southeasterly trending subvertical to steeply west and easterly dipping quartz + pyrite ± chalcopyrite ± molybdenite veins mapped on L2400N within strongly silicified diorite.

**Station 4375E to 4450E**

Slight increase in surface chargeability, unknown as mapping has no indication of increased sulphides in the area. K-feldspar alteration is noted to increase slightly after station 4450E possibly as a result of increased quartz + epidote ± chalcopyrite veining, which is supported by increased Cu presence in soil samples within the same area. Trace disseminated chalcopyrite within k-feldspar altered diorite is possible as well.

**Station 4525E to 4562E**

Slight increase in surface chargeability, however the area is covered by talus and was not mappable. Soil data indicates increased Cu within the area, likely attributed to quartz + epidote ± chalcopyrite veining or disseminated chalcopyrite within k-feldspar altered diorite (similar to the previous interval).

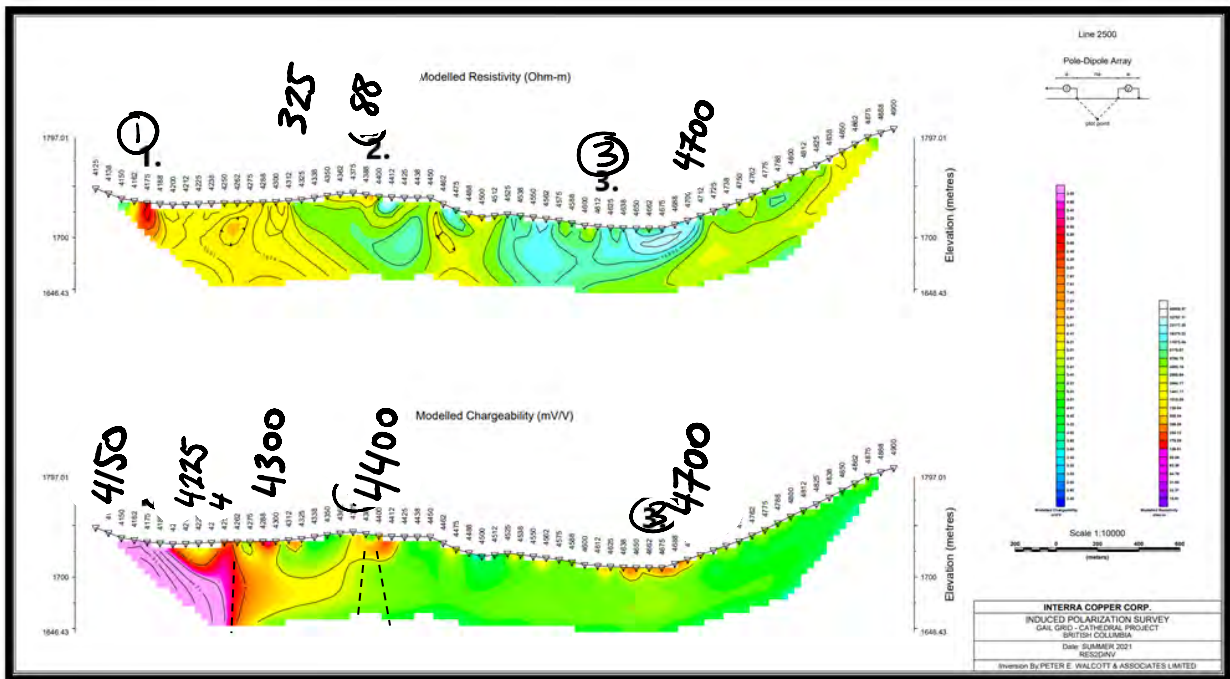


Figure 23: L2500N, Gail Grid, interpretation (schematic)



Surface resistivity interpretations (Figure 23) based on geological surface mapping (from SW to NE):

**Station 4175E**

Localized decrease in resistivity due to second order stream intersection that would be rich in metal ions from nearby Gail showing located within the stream catchment. The stream catchment may be located within a N-S trending structure based on geomorphology, however further geological mapping to the south is required to confirm and measure the structure in outcrop.

**Station 4325E to 4488E**

Increase in resistivity within moderate to strong silicified CG diorite as a result of localized quartz ± sulphide veining.

**Station 4525E to 4700E**

Unmappable area due to talus and vegetation coverage. Potential increased silicification within diorite. Anomalous Mo soil values within the area.

Surface chargeability interpretations based on geological surface mapping (from SW to NE):

**Station 4150E to 4250E**

Similar to L2400N, significant increase in broad surface and sub-surface chargeability due to abundance of localized N-S trending subvertical to steeply dipping polymetallic quartz veins and fractures mapped ~250m south and through L2400N on station 4200E. Hosted within moderate to strongly silicified CG diorite.

**Station 4300E to 4400E**

Significant spikes in surface and sub-surface chargeability as a result of several N-S trending subvertical to steeply west and easterly dipping quartz + pyrite + chalcopyrite ± molybdenite veins on strike to those mapped on L2400N on stations 4300E-4338E within strongly silicified diorite.

**Station 4625E to 4700E**

Unmappable area due to vegetation and talus coverage. Mo soil anomalies on trend with stream across multiple lines which could represent the E-W structure mapped at station 4800E on L2300N.

Compiling the results from geological mapping, IP surveying and rock and soil sampling, the Gail Area can be divided into four prospect zones. The four zones are illustrated in plan map within Figure 24 and described in detail below.

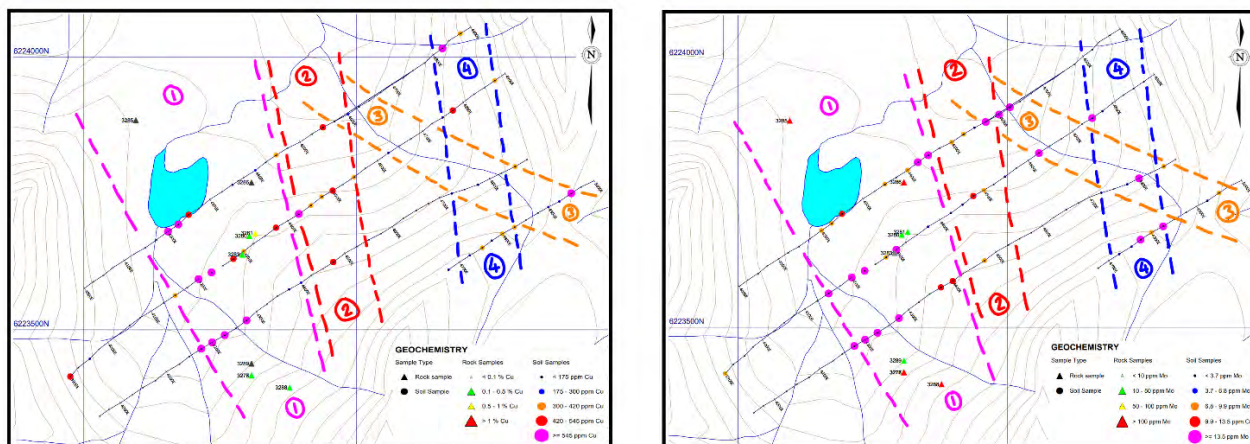


Figure 24: Gail Area interpretation (schematic)

### 1-Purple Zone

- Up to 300 m wide zone of high Cu-Mo concentration in soils.
  - Bound to the southwest by: 4150E (L2500N and L2400N) and 4175E (L2300N); bound to the northeast by: 4450E (L2500N) and 4400E (L2400N and L2300N).
  - Zone may extend significantly further to the southwest, to at minimum station 4075E on L2400N based on IP chargeability.
    - IP surveys on L2400N and L2500N end within the chargeability anomaly (southwestern boundary has not been established).
    - No samples (soils) were recorded southwest of station 4150E (all lines) due to extensive talus coverage (with two exceptions).
- Sulphide enrichment within the zone is attributed to quartz-molybdenite-chalcopyrite-pyrite bearing veins and disseminated sulphides within adjacent patchy silicified CG diorite.
  - Eight quartz sulphide bearing veins were mapped to intersect the zone:
    - Occur as northwest-southeast to north-south trending and steeply dipping.
    - Refer to sample #'s: 3277, 3278, 3280, 3281, 3283 and 3285, 3286, and 3288.

### 2-Red Zone

- Up to 125 m wide northwest-southeast to north-south trending Cu-Mo anomalous zone
  - Bound to the southwest by stations: 4425E (L2300N - L2400N), 4475E (L2500N); bound to the northeast by stations: 4550E (L2300N - L2400N), 4600E (L2500N).
  - Decrease in Cu-Mo grade relative to southwestern anomaly, potentially indicative of a transition away from ore.
  - Cu is slightly more abundant than Mo, interpreted to be a transition from large bull quartz-molybdenite-chalcopyrite-pyrite veins to smaller quartz-epidote-pyrite ± chalcopyrite ± molybdenite veins and fractures commonly with k-feldspar alteration selvages.

- Surface mainly covered by talus and unmappable, however a small outcrop between station 4475E-4500E on L2400N was mapped containing an increase in K-feldspar alteration.
- Quartz vein size during geological mapping noted to decrease from 15-20cm (purple zone 1) to 2-5cm width (red zone 2).
- Line 2400N has the strongest Cu values (no samples limit results on L2500N and L2300N)
  - Increase in resistivity at surface to 25m depth along this interval on L2400N appears to indicate an increase in silicification.
  - Chargeability “blips” at surface along the line are interpreted as localized thin areas of increased quartz-sulphide veining.

### **3-Orange Zone**

- 100m wide zone of anomalous Mo attributed to east-west trending fault (112/82) or a latite porphyry dyke.
  - Fault hosted within carbonate-epidote-chlorite altered CG diorite, mapped at station 4800E on L2300N.
  - Latite porphyry dyke mapped ~ 70 m NW from multiple Mo anomalies (dyke orientation unidentifiable due to random fractures/offsets).
    - Another latite porphyry dyke was mapped within the Gail showing (located in Purple Zone 1), quartz-molybdenite-chalcopyrite-pyrite bearing veins were located meters from the dyke following the same strike with similar dips – these veins may be utilizing the dyke contacts.
  - Zone bounded to the south by stations: 4850E (L2200N), 4725E (L2300N), 4625E (L2400N), and 4575E (L2500N); bound to the north by stations: 4975E (L2200N), 4850E(L2300N), 4725E (L2400N), and 4650E (L2500N).
- Increased resistivity on L2500N coincides with increased Mo concentration in soils – indicative of quartz and/or carbonate alteration causing mineralization.
- Resistivity low anomaly at station 4950E on L2200N is on trend with east-west fault
  - The low resistivity zone initially follows the 82° southern dip expected from the east-west fault until ~25 m depth, then the dip changes to sub-horizontal for another 25 m and the anomaly terminates.
    - Discontinuity attributed to crosscutting granodiorite intrusions.

### **4-Blue Zone**

- Up to 125 m wide north-south to northwest-southeast trending Cu-Mo anomalous zone
  - Zone bounded to the west by stations: 4700E (L2200N), 4725E (L2300N), 4750E (L2400N), and 4800E (L2500N); bounded to the east by stations: 4825E (L2200N), 4850E (L2300N), 4875E (L2400N), and 4900E (L2500N).
  - Soil no samples make zone boundaries difficult to establish.
- Sulphide enrichment attributed to north-south trending fault (198/62).
  - Fault mapped ~ 200 m north along trend from interpreted intersection point on L2200N proximal to station 4800E.

- Fault zone supported by moderate to strong silica and carbonate alteration within highly fractured CG diorite.
- Patchy silica and K-feldspar altered diorite mapped < 50 m to the northeast (above L2500N and L2400N).
- Latite porphyry dyke mapped 30 m southeast from station 4850E on L2300N.
  - Orientation of the dyke is unknown, and mineralization was not noted within the dyke. However, quartz-molybdenite-chalcopyrite-pyrite bearing veins were located meters from a latite porphyry dyke at the Gail showing in Purple Zone 1. Near the showing, veins follow the same strike with similar dips as the dyke, indicating these veins may be utilizing the dyke contacts.
- IP resistivity low anomalies corresponds to the same interval on L2200N.
  - Segmented nature of resistivity lows and mapping observations suggests mineralization is hosted within faulted and silicified diorite crosscut by later barren granodiorite intrusions.

## 8.2 CATHEDRAL AREA

Alkaline porphyry Cu-Au deposits of Quesnellia and Stikinia formed during a relatively short time interval that lasted from about 212 to 183 Ma and peaked at about  $205\pm 5$  Ma (Mortensen and others, 1995). They have alteration assemblages and patterns of alteration typically more complex and mineralogically diverse than those within calc-alkalic porphyry deposits. A comparison between alkaline and calc-alkalic porphyry deposits is presented in Table 17.

Understanding the timing relationships between these zoned mineral assemblages is being used to try and reconstruct the original geometry of the Cathedral Area and provide valuable vectorization information about the temporal and spatial evolution of fluids considered to be responsible for mineralisation. Areas containing a significant structural component frequently contain overprinting alteration assemblages or phases that typically creates mineralogical complexities within the zoned patterns of alteration used to identify assemblages related to the alkalic porphyry alteration model. Additionally, overprinting complexities are also recognized to occur as a result of deuteric alteration whereby alteration occurs as reactions involving changes in primary mineral phases during the process of late magmatic crystallization of the host.

Initial mapping studies carried out on the Thane property, particularly within the Cathedral and Gully areas observed alteration signatures and mineralogic characteristics comparable to an alkalic rather than a calc-alkalic porphyry deposit. All previously mapped and drill targeted zones within the property lack significant ore related phyllic and peripheral argillic alteration phases typically observed within a Calc-Alkaline porphyry system. Rather, the area contains ore related sodic-calcic and peripheral sodic and alkalic lithocap (sericite-quartz-carbonate and tourmaline) alteration assemblages. Alteration assemblages were interpreted to occur proximal to and extend outwards from the north-south trending (quartz) monzonite to (quartz) syenite intrusive phases of the Duckling Creek suite. K-feldspar is the dominate alteration mineral within the potassic phase and is frequently associated with magnetite veins and

breccias within all Thane Creek and Duckling Creek intrusive phases mapped and intersected. In rare instances, biotite has been observed altering primary mafics and as localized hairline fractures with K-feldspar-quartz and lesser magnetite. Both anhydrite and garnet are absent within all areas of potassic alteration mapped and within all thin sections studies. Additionally, secondary quartz appears ubiquitous throughout most of the area. As a result, virtually all potassic alteration observed within the Cathedral Main, South, Valley and Gully areas, likely occur as a combination of contact alteration related to Duckling Creek intrusive phases, deuteric alteration of K-feldspar on primary plagioclase within late phases of the Thane and Duckling Creek intrusives and weak outer calc-potassic K-feldspar dominate alteration related to magnetite veins and breccias. At this stage, calc-potassic alteration appears associated with either a Cu-Au Alkalic porphyry or potentially with a high-K calc alkaline Cu-Au-Mo system that straddles the alkaline sub-alkaline magma series and deposit type.

Table 17: Alkalic and calc alkalic porphyry deposit comparisons

Feature	Alkalic	Calc-Alkalic
Metal Zonation	Au-Cu; Cu-Au rare Mo	Cu-Au-Mo (high- K) Cu-Mo (-Au), Cu-Au-Mo (med-K)
Ore Related Alteration	Potassic: bt-or-mgt-ab-chl±anh Calc-potassic: act-bt-mgt-ep; grt-or-bt±ap±anh Sodic-calcic: ab-di-ep-chl-cal	Potassic: bt-or-ab±mgt±anh Phyllic: qtz-ms-py
Peripheral Alteration	Sodic: ab-chl-py Propylitic: chl-ab-ep-cal	Argillic: mnt-ill-py Propylitic: chl-ep-cal±act Advanced argillic: qtz-alu-dic-pyr
Quartz Veining	Rare in BC deposits; abundant in other regions	Ubiquitous
Related mineral deposit styles	Cu-Au skarn Au-Ag-Te alkalic epithermal	Cu-Au and Pb-Zn skarn Sediment-hosted Au
Type examples in British Columbia, Canada	Ajax, Mt Polly, Galore Creek, Mt. Milligan and Lorraine	Kemess, Brenda, Huckleberry, Highland Valley and Gibraltar

For the 2021 drill campaign at the Cathedral Main, South, Valley, Gully and Pinnacle areas, alteration mineralogy intersected within drill core was captured independently and assigned an alteration intensity as defined predominately by the destruction of primary minerals within the host rock (Table 17). The alteration guideline used was from table 2.5 within the Altered Volcanic Rocks textbook (Gifkins et. al., 2005). In order to accommodate data within a database system the alteration intensity was given a numerical value that corresponds to the descriptive term during core logging.

In order to assign an alteration assemblage to define spatial distribution within an Alkalic Cu-Au porphyry system, the higher intensity of alteration identified within the dominate main three alteration minerals were used. Other associated minerals in addition to the presence of sulphides as well as the presence of, and or destruction of, secondary magnetite (recorded magnetic susceptibility) were also included. They were then assigned into the alteration assemblage related to the Alkalic porphyry Cu-Au model. The alteration minerals and associated sulphide mineralization were also compared to areas of modeled surface and sub-surface increased resistivity and chargeability within the IP surveys conducted on soil and IP lines over the drill targeted areas of the property.

Table 18: Alteration assemblages of an Alkalic Cu-Au porphyry system.

Alteration Assemblage	Associated Minerals	Magnetic Signature	Chargeability Signature
Inner Calc-Potassic (ICP)	bt-act-mgt-or(K-spar)-qtz-bn	High	High
Outer Calc-Potassic (OCP)	or(K-spar)-chl-bt-ab-act-qtz- ±mgt-cp	High	High
Innermost Propylitic Zone (IPZ) (actinolite-epidote-hematite Subzone)	ab-chl-act-ep-hem-qtz-py ±mgt±cp	Moderate - High	Moderate
Outermost Propylitic Zone (OPZ) (Albite-Actinolite subzone)	ab-act-qtz-cal-py	Low- Moderate	Moderate
Sodic-calcic alteration (SCA)	ab-ep-chl±act	Low	Low
Sodic alteration (SA)	ab-qtz-hem	Low	Low
Alkalic Lithocap (AKL)	ab-or(K-spar)-ser-qtz-cal- py±tour	Low	High

## 9.0 INTERPRETATIONS AND CONCLUSIONS

### 9.1 INTERPRETATIONS

The Thane Property is wholly located within the Hogem batholith that intruded into the Nicola Group augite bearing volcanics of the Quesnel Terraine. Recent bedrock mapping and geochemical studies conducted by the British Columbia Geological Survey (BCGS) within the northern areas of the batholith, indicate punctuated emplacement of four distinct intrusive suites during a protracted (ca. 80 Ma) interval, from 207 to 128 Ma (Jones et. al., 2021) The four plutonic suites identified within the study include (from oldest to youngest): Thane Creek suite (207 and 194Ma), Duckling Creek suite (182 and 175 Ma), Osilinka suite (maximim

emplacement 160Ma) and the Mesilinka suite (135 to 128Ma). The Thane Creek suite of rocks contain diorite to quartz monzodiorite with lesser hornblende whereas the Duckling Creek suite contains alkaline rich rocks of biotite pyroxenite, syenite and monzonite that intrude into the Thane Creek suite. The Osilinka and Mesilinka suites consist of granitic rocks, intermediate to felsic porphyritic dikes and tonalite to granodiorite respectively. The Hogem batholith is known to host the Lorrain and Mt. Milligan deposits to the south and potentially the Kemess deposit to the north of the Thane property. Findings within the BCGS study on the batholith are conducive to those observed within the Thane Property.

Previous mapping and sampling campaigns conducted within the Cathedral Main, Cathedral South, Gully and Pinnacle areas generated an interpretation of a moderate, post-emplacement west-tilted alkalic porphyry system related to deeper emplacement of north-south trending small monzonite to syenite intrusions within the Duckling Creek suite (Gordon *et al*, 2018). The system was subsequently faulted (potentially as localized ramped thrusts) containing a local expression of province-scale, dextral strike-slip faulting and reactivation in the Eocene related to and within a step-over domain from the north-northwest striking Ingenika and Pinchi faults. As a result, it was interpreted the system had been thrust in slices to expose an approximate 2 km vertical extent of the hydrothermal alteration and mineralization system whereby the deeper porphyry related alteration assemblages and mineralization within the Cathedral Area were positioned onto shallower high-grade vein systems interpreted to occur within the Gully and Pinnacle areas to the south and north respectively.

Drilling targeted areas of increased resistivity and chargeability associated with the porphyry related extent of the hydrothermal alteration and mineralization system in addition to the structural relationship, and potential displacement of mineralization within the system. Additionally, they targeted both magnetic high and low anomalies observed within the airborne magnetic survey.

### **9.1.1 Cathedral Area**

#### **Geology**

Variable hydrothermally altered and sheared medium to coarse grained diorite to localized pods of (quartz) monzodiorite occur throughout the Cathedral Main, South and Gully areas. Within the area of drilling, they are rarely observed unaltered. Typically, low resistivity is observed within intersections containing increased OCP and IPZ alteration dominated by increased K-feldspar and albite respectively. High resistivity occurs typically in areas of increased SIL, PAZ and CRB alteration related to late quartz+epidote+calcite±sulphides and silica±magnetite±calcite healed and brittle reactivated chloritic shears. North-south trending alteration assemblages appear to transition from narrow, contact related, potentially biotite hornfels to OCP through to OPZ alteration. These assemblages appear to extend both vertically and westward about the north-south trending (quartz) monzonite to (quartz) syenite intrusives. Chloritic shear structures occur throughout and on contact margins with later intrusive phases. The structures appear to pre-date and post date porphyry related alteration assemblages. Increased sulphides consisting of pyrite-chalcopyrite±molybdenite±arsenopyrite are noted locally within and proximal to structures that correlate with low grade Cu, Au, Ag and moderate Mo as well as increased chargeability. Relative to the (quartz) monzonite, geochemically the diorite contains elevated Ca, Co, Mg, Ni, Sr, and V.

The occurrence of four north-south trending sub-vertical to easterly dipping fine-medium grained (quartz) monzonite bodies contain variable hydrothermal alteration assemblages. They range from OCP to OPZ, implying that hydrothermal alteration and subsequent mineralization postdates their emplacement. The most westerly of the four was previously mapped as a small, southwesterly trending body surrounded by talus that outcropped within the Cathedral South area. It was intersected within a significant fault zone at the base of TH21-4. A second sub-vertical smaller dyke occurs approximately one kilometer to the east (on surface) within the Cathedral Main area. Surface exposure of this dyke is 16 meters in width and it is intersected predominately at the base of TH21-1 as narrow dykes that branch out throughout TH21-3 and TH21-12. The third and larger of the four dykes occurs approximately 60 meters to the east (on surface) from the second dyke. At surface, it encompasses the entire cliff face down to the valley floor (~100m) and narrows in surface exposure to approximately 10 meters in the south along the west side of the gully within the Gully area. The dyke is intersected within TH21-2 and TH21-5 and splits into two separate dykes at depth within the Cathedral Main area. Its southern extent occurs as narrow branching sub-vertical dykes at the base of TH21-7 and TH21-11 within the Gully area. The fourth (quartz) monzonite body occurs within the Gully area. On surface it is an 80m wide north-south trending dyke located on the east side of the Gully topographical feature. It is intersected within the upper sections of TH21-7, TH21-8 and mid-way through TH21-11. Coarse grained to pegmatitic (quartz) syenite are frequently observed on contact margins. Typically, low resistivity is observed within intersections containing increased OCP and IPZ alteration that frequently radiates from contact margins dominated by increased K-feldspar and albite+actinolite respectively. Areas of high resistivity occur in areas of OPZ alteration at depth and in areas of increased AKL, SIL, PAZ and CRB alteration related to late tourmaline+quartz+pyrite and quartz+epidote+calcite±sulphides veins in addition to silica±magnetite±calcite healed and brittle reactivated chloritic shears. Due to the frequent presence of magnetite on contacts, increased sulphides consisting predominately of coarse granular and often blebby pyrite with lesser chalcopyrite±molybdenite±arsenopyrite are noted as magnetite replacement. Coarse grained granular pyrite commonly with elevated gold appear related to an earlier phase of deformed quartz+calcite veins within shears. Contact zones containing increased magnetite and sulphides correlate with low grade Cu, Au, Ag and moderate Mo as well as increased chargeability. Relative to diorite, geochemically (quartz) monzonite contains elevated Ce, Cr, K, U and Mo.

Small (<5m) dyklets of K-feldspar rich, frequently pegmatitic (quartz) syenite occur sporadically at the Cathedral Area. Due to their sporadic occurrence, typically noted proximal to areas of increase K-feldspar alteration, previous mapping campaigns were unable to accurately isolate this unit in the field. Originally, these dykes were thought to represent a possible recrystallization phase of the diorite proximal to rarely preserved contact margins with the (quartz) monzonite. They seemingly appear to blend into the (quartz) monzonite host with a decrease in grain size in conjunction with an increase in K-feldspar±silica alteration. They were also considered to potentially represent late K-feldspar rich, pegmatitic granites related to the Mesilinka suite. In drill intersections, their presence within the diorite away from contact margins has the appearance of discontinuous pegmatitic pencil dykes with sharp contacts and moderate K-feldspar+silica alteration halos and were thought to imply close



proximity to a (quartz) monzonite contact. Thin section analysis completed on a sample from TH21-1 at 29.62m does confirm they are a coarse grained to pegmatitic (quartz) syenite containing trace low grade chalcopyrite+bornite mineralization associated with late quartz+epidote+calcite fractures. Analysis of the geochemistry from samples collected from drilling indicate the unit typically contains a significant increase in Ce and Li relative to diorite and only a slight increase in the same elements relative to (quartz) monzonite. As such, they have been interpreted to be inclusive within the Duckling Creek suite and represent post (quartz) monzonite emplacement that frequently but not exclusively intrude along diorite-(quartz) monzonite sub-vertical contact margins.

Three 4 to 7 metre wide, north-south trending, shallow (~30°) west dipping latite porphyry dykes have been identified intersecting all above-described intrusive suites. They appear analogous to felsic porphyry sheets observed within the Osilinka suite as described by Ootes et al., 2019. Two separate dykes are intersected within the Cathedral Main and Gully areas as an upper and lower dyke. The upper latite porphyry is intersected in the Gully area at the top of TH21-11 and at depth within TH21-1, TH21-2 and TH21-5 within the Cathedral Main area. The lower latite is intersected within in TH21-2 and narrows to (<1m width) within TH21-3 within the Cathedral Main area. The third is intersected in the Cathedral South area within TH21-4 on the upper contact and cutting the monzodiorite. Contacts with earlier intrusive phases are typically sharp, and chilled locally containing a trachytic texture defined by primary plagioclase alignment parallel to contact margins. They typically contain OPZ alteration consisting of chlorite, epidote and carbonate (calcite) overprinted by PAZ alteration within or proximal to chlorite sheared and brittle faulted contacts. Locally, porphyry related OCP and overprinting IPZ hydrothermal alteration and associated low-grade indicator mineralization are noted and imply hydrothermal alteration and subsequent mineralization postdates their emplacement. They typically occur within areas of increased resistivity within OPZ alteration, proximal to SIL and PAZ alteration related to increased quartz ± epidote ± calcite veining and silica + carbonate (calcite) healed chloritic shearing. Relative to diorite, geochemically the latite porphyry contains elevated K and a decrease in Na. Relative to the (quartz) monzonite, geochemically the latite contains elevated Na, Sr and V and a decrease in U. Geochemically the monzodiorite and latite appear similar.

### **Alteration**

Surface exposures and drill hole intersections at the Cathedral Main, Cathedral South and Gully areas include vertical and lateral alteration assemblages extending outboard of the north-south trending (quartz) monzonite that closely resemble ore related and peripheral alteration observed within a Cu-Au alkalic porphyry system. Mineral associations are often difficult to define due to the presence of hydrothermal alteration overlap related to contact alteration. Both early and late phase hydrothermal fluid pulses are often displaced structurally within the area. Typically, areas containing high resistivity appear associated with structurally related silicification and veining within and proximal to chloritic shear structures that accompany areas of increased chargeability. Low resistivity values tend to be more associated with alteration assemblages containing increased albite, actinolite carbonate (calcite) and locally K-feldspar in addition to reduced silicification.

The most important alteration types include:

***Potassic (early/contact related)***

The earliest phase of potassic alteration occurs proximal to the north-south trending, sub-vertical (quartz) monzonite intrusive phase. It appears only locally preserved as biotite alteration (subsequently altered to actinolite+chlorite±epidote±calcite) of primary pyroxene and hornblende within the diorite and (quartz) monzodiorite hosts, possibly representing biotite hornfels immediately proximal to the contact margins. In rare instances, pyrrhotite is noted within these areas. As a result of pervasive ore related and peripheral porphyry overprinting alteration, combined with structure related alteration and mineralization this phase of alteration is rarely preserved both vertically and laterally within the system.

A second phase of K-feldspar dominate potassic alteration associated with minor silicification is interpreted to be intrusion-related, contact-type alteration proximal to coarse grained to pegmatitic (quartz) syenite intrusive phases. The dykes frequently, although not exclusively, utilize sub-vertical diorite-(quartz) monzonite contact margins. Where present, they result in patchy to pervasive contact K-feldspar alteration halos within both the diorite and (quartz) monzonite. As contact margin dykes contain gradational contacts within the (quartz) monzonite, the increased K-spar alteration relative to the diorite may have occurred prior to complete cooling of the (quartz) monzonite. This alteration phase appears to be barren, however in areas where late hydrothermal veins and fractures are present, low grade copper mineralization occurs.

***Outer Calc-Potassic (OCP)***

OCP alteration is defined by the increase in magnetic susceptibility associated with the presence of hairline fractures, veins and localized breccias of magnetite with pervasive K-feldspar alteration halos. Minerals typically associated with an Alkalic OCP alteration assemblage such as biotite, anhydrite, garnet and typical abundance of disseminated to stockwork like chalcopyrite mineralization are noted to be absent. Magnetite outside of localized veins and breccias occurs as weak primary mafic replacement with both K-feldspar and albite alteration respectively. Earlier interpretations indicate pervasive OCP alteration to be associated proximal to the north-south trending (quartz) monzonite within the Cathedral Main and Gully areas. Although magnetite veins and breccias are often noted proximal to (quartz) monzonite contacts, drill intersections demonstrate they cross-cut and post date both the (quartz) monzonite and the latite porphyry frequently infilling chloritic shears on contact margins. As a result, OCP alteration occurs as a structurally controlled alteration assemblage that appears to extend from south-southwest trending structures. It is often overprinted by other alteration assemblages potentially utilizing the same structural plane that is further reactivated by late shears and brittle structures.

***Inner Propylitic Zone (IPZ)***

IPZ alteration is the inner high temperature actinolite subzone to the system and is defined as the presence and increase of actinolite and associated albite with lesser epidote and chlorite alteration. IPZ alteration is the most dominate and extensive hydrothermal alteration assemblage observed and extends laterally to the west-southwest within the Cathedral South

and frequently at depth within the Cathedral Main and Gully areas. It commonly occurs with chlorite as mafic replacement of primary mafics, hairline fractures and localized sheeted to stockwork veins. Patchy albite alteration is common within areas of replacement and is a pervasive alteration selvage to fractures and veins containing actinolite. IPZ alteration also appears to be a structurally controlled alteration assemblage that commonly overprints OCP and extends outboard of the same south-southwest trending structures. Previously mapped stockwork veins within the Cathedral South area confirm this trend. Epidote within IPZ alteration occurs as localized zones of patchy to pervasive texturally destructive alteration related to epidote±quartz veins that are commonly overserved within the Cathedral South area. Where areas of epidote alteration increase an intermediate temperature epidote subzone style and type of alteration should be considered.

### ***Outer Propylitic Zone (OPZ)***

OPZ alteration is the outer low temperature chlorite subzone to the system and is defined as the presence and increase of chlorite, quartz, calcite, pyrite and lesser epidote and sericite. OPZ alteration predominately occurs at depth within diorite and (quartz) monzonite as well as frequently in late porphyry within the Cathedral Main and Gully areas. Previous mapping indicates OPZ alteration occurs to the west-northwest as a northerly trending assemblage both horizontally and laterally above IPZ alteration within diorite. At depth within the Cathedral South drill hole, OPZ is structurally juxtaposed to IPZ alteration.

### ***Sodic-Calcic (SCA)***

SCA alteration occurs peripheral to ore related alteration and is defined by the presence and increase of albite, epidote, calcite, chlorite. Diopside has never been identified within the Cathedral or Gully areas. SCA alteration is difficult to isolate due to overlapping alteration assemblages. In areas where it has been recorded, it frequently occurs separating IPZ from OPZ alteration at depth proximal to structures. SCA alteration was predominately intersected overprinting both OPC and IPZ alteration within monzodiorite within TH21-4 at Cathedral South.

### ***Sodic Alteration (SA)***

SA alteration consists of pervasive, texturally and magnetite destructive alteration consisting of albite with lesser quartz, hematite and pyrite. It is easily identified due to the pervasive and texturally destructive increase in albite. Quartz occurs interstitially and as veins and fractures. Hematite typically is noted as both mafic and magnetite replacement and within localized areas of increased shears. SA alteration was previously mapped as an east-west trending pod within the Cathedral South area. A single intersection occurs within TH21-1 at depth at the Cathedral Main area drill, overprinting IPZ alteration.

### ***Alkalic Lithocap (AKL)***

AKL alteration typically occurs in the upper sections of the Alkalic system as the equivalent to phyllic and argillic alteration assemblages within a Calc-Alkaline porphyry system. Within the Alkalic system they typically contain less acidic alteration assemblages of albite, sericite

and K-feldspar as opposed to an increase in clays and associated quartz-sericite and abundant pyrite within the Calc-Alkaline system. Initial mapping within localized areas of the Cathedral South and Cathedral Main combined with several thin section analysis noted tourmaline with K-feldspar, sericite, quartz and pyrite. Initial interpretations considered the potential for lithocap roots extending through both the OCP and ICP alteration assemblages. Although AKL has been included as an assemblage within drill holes, intersections at this stage are capturing massive to brecciated tourmaline+quartz+pyrite±calcite±sericite veins and localized blobs frequently proximal to structures. They may potentially be related to a late hydrothermal fluid pulse within the system as they appear to cut all porphyry related alteration. They are typically noted within the upper drill hole sections within both the Cathedral South and Gully areas.

### ***Silicification (SIL)***

SIL alteration occurs as a strong, pervasive increase in interstitial, hairline fractures and veins of secondary quartz often proximal to and within healed chloritic shears.

### ***Phyllic Alteration (PAZ)***

PAZ alteration is completely related to late brittle structures containing clay gouge with quartz, sericite, chlorite, calcite or pyrite.

### ***Carbonate Alteration (CRB)***

CRB alteration occurs as a strong, pervasive increase in interstitial, hairline fractures and veins of secondary carbonate predominately as calcite, frequently associated with PAZ alteration.

### ***Hornfels (HFLS)***

HFLS occurs as a contact alteration assemblage that is rarely preserved within diorite and (quartz) monzodiorite proximal to the (quartz) monzonite due to overprinting hydrothermal alteration and significant faulting. Where noted, it typically contains rarely preserved fine grained biotite±magnetite replacing mafics within an increase of pervasive interstitial silica.

### **Structure**

The Cathedral Main, South, and Gully areas contain a strong element of structural control. Previous mapping campaigns within the Cathedral and surrounding areas identified potential thrust related south-southwest moderately west dipping structures, south-southeast moderately west dipping dextral reverse structures, and southeast moderate to sub-vertical south dipping potential dextral strike-slip structures. Southeast trending typically brittle structures are also noted within the areas and post date the above noted structures.

Drilling within the Cathedral Main, South and Gully areas confirmed the following:

#### ***Potential Thrust/Reverse Faults***

Two regionally significant faults were interpreted previously to represent thrusts within the Cathedral Main area. Both thrusts termed “The Cathedral Thrust” and “The Gully Thrust” respectively strike south-southwest containing a calculated structural contour dip of 45° to the west. The Cathedral structure is located to the west and separates the Cathedral Main and Cathedral South areas. The Gully structure trends southerly within the base of the gully on the western edge of the Gully area seemingly parallel to the eastern edge of the north-south trending (quartz) monzonite. Its northern extent is extrapolated proximal to the cliff face on the eastern side of the Cathedral Main area, separates the Cathedral Main and Valley Area to the east and continues northward to the western margin of the Pinnacle area. Both structures indicate a dextral oblique component and were noted to truncate mineralization. They were not targeted or intersected within the drilling campaign. A significant parallel structure to the Cathedral and Gully structures has been mapped in the area between them and was intersected at 267.00 meters within TH21-2 and at 229.50 meters within TH21-5. This structure is interpreted to dip moderately (50°) to the west and is observed as a 15 to 37 meter wide fault zone containing abundant carbonate (calcite) veining within pervasive clay-sericite-hematite-carbonate±silica alteration of the host diorite and (quartz) monzonite intrusives. Most hematite alteration is proximal to isolated and altered chloritic shears and areas of magnetite veining and brecciation. Silica healed chloritic shears and related dilational brecciation frequently associated with these structures appears to have been overprinted by late cross-cutting brittle deformation and carbonate (calcite) veining potentially related to both southeasterly and east-southeasterly trending structures. It’s interpreted location within the drill holes occur within a highly resistive and chargeable area observed within the modelled chargeability and resistivity. Similar to the Cathedral and Gully structures, this structure also appears to truncate mineralization, however this may be due to the late cross-cutting structures noted above reactivated in the Eocene. From the northwest to southeast, these structures are generally separated at approximately 200-meter intervals. At this stage, there is no accurate information regarding the direction or distance associated with displacement of these structures and seemingly they do not appear to be a focal point for increased mineralization potential.

#### ***Reverse Faults***

Several reverse faults appear to outcrop within the Cathedral Main, South and Gully areas. On surface, the reverse faults are characterized by <2 to 50 cm of silica±carbonate(calcite) chloritic healed cataclastic zones of deformation with reverse dip-slip kinematics and dextral strike-slip. There appear to be two different sets of structures and both cut all porphyry related alteration, contain chloritic dilational brecciation, contribute to and frequently contain mineralization trends and low-grade copper-gold intersections. Due to the increased silica and sulphides within them, they are frequently noted to occur within, or proximal to, areas of increased modelled chargeability and resistivity. These structures are also considered to have been reactivated during the Eocene and there is no accurate information regarding the direction or distance associated with displacement of these structures.

South-southeasterly trending sub-vertical ( $80^\circ$ ) westerly dipping chloritic shear structures cut both the diorite and (quartz) monzonite and typically have core axis angles ranging from  $20-30^\circ$  in drill core. They are interpreted to be a focal point for increased low-grade copper mineralization as well as increased chargeability observed within all prospect areas. Frequently, where these structures intersect south-southwest trending thrust/reverse faults, increased mineralization appears to bleed into the structure. Magnetite veining and brecciation and associated K-feldspar and albite alteration related to OCP and IPZ as well as quartz-epidote±sulphide veins and fractures mapped on surface and intersected within drill holes appear sub-parallel to this structural trend. These structures are interpreted to post-date the south-southwest trending thrust/reverse faults and appear to contain and post-date porphyry related episodes of fluid pulses that are subsequently overprinted due to reactivation. They are commonly infilled and healed with silica, magnetite, pyrite and carbonate (calcite) that all contain various degrees of multiple ductile shearing. Often, these structures contain an increase in early fine-coarse grained, locally semi-massive granular and shear strained pyrite replacing magnetite. Au/Cu ratios are noted to increase substantially with this stage of pyrite mineralization. Locally they are healed and brecciated by late carbonate (calcite) related to southeast trending structures that frequently contain arsenopyrite.

Southeast trending moderately ( $60-70^\circ$ ) southwest dipping structures appear more common throughout the area. Within drill intersections, these structures contain core axis angles ranging from  $70-80^\circ$  on easterly and westerly drilled holes. They are interpreted to post-date and frequently infill both above noted structures. Similarly to the south-southeasterly trending structures above, these structures frequently contain an increase in mineralization associated with quartz-carbonate (calcite)-sulphide veins and fractures that typically contain an increase in arsenopyrite. Locally, weakly mineralized discontinuous hairline fractures of actinolite with albite alteration selvages also appear to utilize this structural plane.

Surface mapping has identified southeast trending reverse and strike slip (dextral and sinistral) faults that are sub-vertical to moderately ( $70-80^\circ$ ) southerly dipping. As with the structures mentioned above, they are typically observed as silica±carbonate (calcite) healed and locally brecciated chloritic shear structures. These structures are also frequently intersected within drill core, however interpreting extents is difficult due to their southerly dips and frequent intersections within previous noted structures. They are more commonly observed within the southern prospect areas of the Cathedral South and south of the Gully areas and post-date porphyry related alteration and appear to postdate all above noted structures.

Virtually all structures mapped within the prospect areas appear to correlate with areas of significant linear to broad increased resistivity and localized breaks in chargeability highs observed in the 2-D IP interpretation.

### **Mineralization**

Previous mapping campaigns within the Cathedral Main and Gully areas identified south to southeasterly striking, shallow to moderate ( $30-70^\circ$ ) westerly dipping quartz-sulphide bearing hydrothermal veins associated with increased pervasive to patchy K-feldspar dominate OCP and actinolite+albite dominate IPZ alteration. An increase in sulphide mineralization and vein

abundance as well as copper and gold grades within surface samples was coincident with increased chargeability within the 600 and 200 square meter anomalies at the Cathedral Main and Gully areas respectively. Drill intersections within the sub-surface chargeability high on all IP lines confirm the presence of increased low-grade copper-gold mineralization within and proximal to areas of increased chargeability related to south-southeast trending moderate southwest dipping and southeast trending steeply south dipping structures. Copper and gold mineralization at depth corresponds primarily to quartz-epidote-sulphide bearing hydrothermal veins associated with K-feldspar alteration selvages and less so with increased actinolite veining and associated albite alteration. Additionally, quartz-sulphide bearing veins and fractures predominately appear to post date porphyry related alteration and all intrusive phases intersected. Reduced grades within drill hole intersections compared to surface sampling is interpreted to be a result of secondary supergene enrichment at surface.

At the Cathedral South area, mineralization is associated with sheeted to stockwork like actinolite±magnetite±epidote-sulphide veining related to outboard IPZ with patchy to pervasive albite alteration related to SCA and SA and broad resistivity. Magnetite, associated with OCP alteration is noted within the Cathedral South area, however it is commonly strongly overprinted throughout by IPZ, SCA and SA alteration. Interestingly, significant elevated Au/Cu and Cu/Mo ratio's are noted in comparison to the Cathedral Main and Gully drilled areas. Both occur proximal to the top of the drill hole within increased IPZ alteration dominated by albite+actinolite overprinting OCP alteration. The increased Au/Cu ratio appears to be associated with pyrite±chalcopyrite disseminated within late carbonate (calcite) veins. Increased Cu/Mo ratio is associated with quartz±epidote veins and fractures with K-feldspar alteration selvages.

At the Cathedral Main area, the chargeability high was interpreted as a 600 square meter bulbous to bullseye, sub-vertical to slightly east dipping sub-surface feature that extended to approximately 300 meter depth. At the Gully area the chargeability high was interpreted as a 200 square meter bulbous, slightly east dipping sub-surface feature that extended to approximately 250 meter depth and considered open to the west. All eight drill holes targeting the chargeability high areas at Cathedral Main and the Gully area intersected localized, indicator low-grade Cu-Au and Mo mineralization associated with chalcopyrite, pyrite, molybdenite and lessor arsenopyrite and bornite. Mineralization was not continuous through the modelled chargeability high zones. A significant decrease in sulphide mineralization and associated Cu-Au-Mo grades did occur in areas identified as low chargeability.

Sulphides were noted to occur within or proximal to late quartz-epidote hydrothermal hairline fractures and veins that were sub-parallel to and utilized south-southeast and southeast trending westerly dipping chloritic shears structures. In areas where these veins cross-cut or infilled earlier magnetite veining and breccias, typically proximal to (quartz) monzonite intrusive contact margins, magnetite replacement was observed.

Significant intersections of copper-gold mineralization at the Cathedral Area occur in the following styles:

- Isolated, frequently discontinuous quartz±epidote±prehnite±calcite hairline fractures and veins with K-feldspar alteration selvages containing fine-coarse grained chalcopyrite+pyrite±molybdenite±bornite within all intrusive phases;
- fine grained disseminations of chalcopyrite+pyrite±bornite within or on margins replacing chlorite-actinolite and biotite altered primary mafics and variable sphene±hematite altered primary magnetite;
- sheeted to semi-stockwork, discontinuous actinolite±chlorite±magnetite hairline fractures with albite alteration selvages containing fine grained disseminated chalcopyrite+pyrite;
- semi-massive, magnetite replaced mineralization, typically observed as fine to coarse grained disseminations and blebs of chalcopyrite+pyrite±bornite±molybdenite where mineralized quartz veins intersect secondary magnetite veins and breccias;
- semi-massive and blebby pyrite±chalcopyrite mineralization proximal to or within silica±magnetite±carbonate (calcite) healed brittle/ductile chloritic shears, dilational breccias and shear related chloritic fractures; and
- hairline fractures, veins and blebby pyrite±chalcopyrite within tourmaline veins.

Thin section studies of both surface and drill core samples, combined with drill core analysis, indicates mineralization and alteration discovered to date at the Cathedral Area is related to a weakly mineralized plutonic porphyry copper system. This system is mainly controlled along veinlets and micro-fractures rather than major veins and significant disseminations. Sulphides within veinlets and micro-fractures are mainly comprised of chalcopyrite with lesser pyrite and rare bornite, which is suggestive of a chalcopyrite-rich, low total sulphide system. This system is closely associated with quartz, epidote and rare biotite with a lesser association with K-feldspar, albite, actinolite and chlorite. Structurally, alteration and mineralization appear closely associated with south-southeast trending and westerly dipping chloritic shear structures that post-date Duckling Creek (quartz) monzonite to (quartz) syenite and Osilinka latite porphyry intrusive phases. Gold is not always associated with copper, but is associated more closely with granular, fine to coarse grained, often sheared, pyrite replacing magnetite within the shear structures. As a result, copper-gold mineralization, as part of a potassic alteration assemblage, is interpreted to be below the depths reached during the current drilling program and is located to the west-southwest of the Cathedral and Gully areas immediately south of the Cathedral South area, proximal to the ARC Showing.

### **9.1.2 Cathedral Valley**

The Valley area contained a blind, bulbous to several bullseye shaped sub-vertical to north-easterly dipping chargeability highs within a broad resistivity high and magnetic low. A



single drill hole (TH21-6) intersected fine to medium grained, equigranular (quartz) monzonite. Like the Cathedral Main and Gully areas, indicator low-grade copper mineralization occurs proximal to, and associated with, south-southeast trending (70-80°) westerly dipping chloritic shears. Alteration includes weak to moderate pervasive interstitial silica, sericite ± epidote replacement of plagioclase, and chlorite ± actinolite ± epidote replacement of primary biotite and amphibole, which represents OPZ alteration. Porphyry related OCP alteration is evidenced by localized magnetite ± specularite veins with K-feldspar alteration selvages, which only occur proximal to south-southwest trending (50-60°) west-northwest dipping shear structures. The intersection of these two structures corresponds to the targeted bullseye chargeability high. Outside of the south-southeast trending structure, K-feldspar occurs as vein selvage alteration about late quartz + epidote + calcite ± sulphide veins and fractures that overprints OPZ alteration. A slight increase in widespread K-feldspar is also attributed to late magmatic (deuteric) replacement of primary plagioclase (Sample 42999). The broad modelled resistivity high is interpreted to be the result of weak to moderate interstitial secondary silicification throughout the (quartz) monzonite and within silica + carbonate (calcite) healed and brecciated shear structures.

The Valley represents a broad area of distal OPZ altered (quartz) monzonite containing localized zones of increased ore related alteration and low-grade indicator copper mineralization. These zones are associated with south-southwest and south-southeast trending structures with a moderate to steep westerly dip.

### **9.1.3 Pinnacle**

The Pinnacle area is dominated by medium-coarse grained diorite cross-cut by localized intrusive bodies of north-south trending, sub-vertical, fine to medium grained (quartz) monzonite and southeast trending, moderate south-southwesterly dipping dykes of megacrystic K-feldspar porphyry and latite porphyry. All phases are dominated by weak to moderate OPZ porphyry related alteration that contains moderate to strong chlorite replacement of primary mafics, weak to moderate sericite replacement of primary feldspar and weak to moderate interstitial silica and calcite. OCP alteration related to magnetite veining and brecciation is significantly reduced within the Pinnacle area and is restricted to the western side of the valley along the diorite-(quartz) monzonite contact margin that trends southerly into the Cathedral Main and Gully areas. Silicification, carbonate (calcite) alteration and sulphide mineralization mapped on surface is predominately restricted and proximal to silica and carbonate healed chloritic shears that utilize intrusive contact margins.

Mineralization occurs within multi-phase hydrothermal veins and fractures with the following styles;

- vuggy and or crustiform quartz-carbonate + arsenopyrite + pyrite + chalcopyrite ± molybdenite veins frequently infilling south-southeast trending moderate to steeply southwest dipping and south-southwest trending moderate west-northwest dipping chloritic shear zones;

- silica + pyrite ± chalcopyrite healed vein breccia's containing late secondary carbonate (calcite ± Fe-carbonate) infill and fractures. These veins commonly appear to utilize and heal brittle southeast trending (60-70°) southwest dipping structures and may be related to east-southeast trending southerly dipping structures mapped in the area; and
- milky quartz ± epidote ± pyrite veins and fractures with K-spar alteration selvages observed within and on contact margins of diorite-(quartz) monzonite and latite porphyry intrusive phases as well as within south-southwest trending chloritic shear planes. Outside of shear structures, most appear to be predominately north-south trending sub-vertical to steeply west dipping.

Two drill holes (TH21-9 and TH21-10) targeted the down dip potential of the Pinnacle Showing. The Showing consists of a series of auriferous, hydrothermal quartz-arsenopyrite-chalcopyrite-pyrite veins along the contact margins between diorite and (quartz) monzonite. On surface, mineralization occurs within zones of moderately high chargeability and moderately low resistivity.

Drill holes intersected predominately moderate pervasive OPZ alteration within medium to coarse grained diorite and localized fine to medium grained sub-vertical cross-cutting (quartz) monzonite to (quartz) syenite dykes. OPZ alteration is dominated by moderate to strong chlorite and weak to moderate silica and calcite. Weak OCP alteration related to localized magnetite fractures and veins with K-feldspar alteration selvages occur proximal to frequently sheared contacts. All contacts were southwest to southeast trending (60-80°) westerly dipping silica and carbonate healed chloritic shears. Most appear to have been reactivated and healed by carbonate (calcite±Fe-carbonate) that post-dates both silica and magnetite veining and brecciation.

Mineralization in drill core consisted of, in order from oldest to youngest:

- OCP related magnetite ± quartz veining within and proximal to diorite-(quartz) monzonite contact margins likely associated with south-southwest trending west-northwest dipping frequently reactivated and subsequently silica and carbonate healed and brecciated chloritic shears;
- Quartz + calcite + pyrite + chalcopyrite ± molybdenite veins frequently infilling south-southwest trending west-northwest dipping structures replacing magnetite and appear to be associated with south-southeast trending moderate to steeply southwest dipping structures (Projected to Pinnacle Showing);
- Quartz + carbonate(± Fe-carbonate) + arsenopyrite + pyrite + chalcopyrite veins frequently infilling both south-southwest trending moderate west northwest dipping and south-southeast trending moderate to steeply southwest dipping chloritic shear zones, which can be brecciated (observed at Pinnacle Showing); and

- milky quartz ± epidote ± pyrite veins and fractures with K-spar alteration selvages that also appear to be associated by south-southeast trending structures.

## 9.2 CONCLUSIONS

### 9.2.1 Gail Area

The highest priority target at Gail occurs along the southwestern end of lines L2300N, L2400N, and L2500N, which has been referred to in this report as the Purple Zone. Mineralization within this zone consists of pyrite, chalcopyrite, and molybdenite with rare secondary native copper hosted in quartz veins. Disseminated sulphides along micro-fractures proximal to these veins, hosted in diorite, is also present. The increase in chargeability on L2400N and L2500N correlates to the increase in mineralization associated with these veins. The anomaly is open to the southwest.

### 9.2.2 Cathedral Area

The Cathedral Area continues to demonstrate strong potential to host a structurally controlled westward tilted copper – gold ± (molybdenum) alkalic porphyry style mineralization system hosted within the Late Triassic to Middle Jurassic Thane Creek to Duckling Creek intrusive suites within the Hogem batholith. Post emplacement tilting and porphyry related alteration is structurally controlled by southwest trending west dipping chloritic shear structures that are cross-cut and infilled by low-grade quartz + epidote + carbonate copper and molybdenum mineralized veins and fractures associated with southeast trending west dipping structures. Increased Au/Cu and Cu/Mo ratios within the Cathedral South drill hole, combined with favorable geochemical and alteration signatures including a nearby magnetite breccia hosting high grade copper and gold grades (ARC Showing) indicates further drilling should focus to the west, southwest and potentially northwest within the Cathedral South area.

The drill campaign supported further evidence of north-south trending zones of copper-gold mineralization with calc-potassic to peripheral outer propylitic hydrothermal alteration assemblages relate to a structurally controlled moderately westward tilted Alkalic porphyry system.

Distal peripheral outer propylitic to patches of sodic alteration extend about ore related calc-potassic to sodic-calcic alteration at depth within the Cathedral Main and Gully areas. This alteration extends to the Pinnacle, Valley and Cathedral South areas. At the Cathedral South area, peripheral outer propylitic alteration extends horizontally into the mountainous terrain overlying and intermingled with pervasive sodic alteration. Ore related calc-potassic to sodic-calcic alteration assemblages occur within the Cathedral Main, Gully and at depth within the Cathedral South areas as overprinting assemblages that are structurally controlled by potential thrust related south-southwest trending moderately west-northwest dipping typically magnetite and silica healed chloritic shear structures. These structures are frequently infilled by multiple hydrothermal fluid pulses and sequences of both ductile and brittle reactivation and are considered the earliest structural set within the area. They typically, although not

exclusively, contain an increase in Au/Cu ratios associated with granular pyrite replacement of magnetite.

Low-grade copper indicator mineralization is frequently associated with increased chargeability and resistivity, which occurs as hydrothermal quartz-epidote fractures and veins with K-feldspar alteration selvages containing sulphides of chalcopyrite - pyrite ± molybdenite ± chalcocite ± bornite. They are structurally controlled and associated with south-southeast trending moderate to steeply west dipping dextral reverse, typically silicified chloritic shear structures, which post-date, infill and replace porphyry related alteration (magnetite) and structures. A significant increase in epidote and quartz-epidote veins and fracture intensity containing low-grade copper mineralization overprints calc-potassic and inner propylitic alteration within the Cathedral South area. This increase corresponds to a broad increase in both Au/Cu and Cu/Mo ratios not seen in other areas of the property and could be a potential vector to an outer stockwork around the central quartz-rich stockwork at depth in the western area of the Cathedral South area. Sampling of a massive magnetite breccia (ARC Showing) located approximately 350 meters to the southwest of the Cathedral South drill hole returned 11.1% Cu, 2.77g/t Au and 29.20 g/t Ag (Gordon *et al*, 2018).

A late hydrothermal alteration and mineralization event within the area occurs as structurally controlled carbonate (typically calcite) + quartz + arsenopyrite + pyrite+ chalcopyrite ± molybdenite veins and breccias associated with southeast trending moderate to steep southerly dipping dextral strike-slip structures.

Both hydrothermal alteration and mineralization events post-date the latite porphyry intrusive phase, which is interpreted to be related to the Osilinka suite (maximum emplacement 160Ma). As a result, both the hydrothermal alteration and quartz-epidote vein mineralization may be related to the Mesilinka suite of quartz monzonite to granodiorite (135 to 128Ma) intrusive phases. This interpretation is significantly different to the Re-Os date for molybdenite mineralization at Gail (202.8 +/-0.8Ma) and to other porphyry deposits within the Hogen batholith (Mt. Milligan, Lorraine and Kemess), all of which formed between 210 to 180 Ma. The latite porphyry may have been mis-identified, as a result of the significant alteration observed throughout the area, and the mineralization instead be related to localized monzonite (megacrystic) porphyry dykes. Additional work pertaining to differentiating these units within areas of increased alteration and mineralization is required.

Although the Cathedral Area hosts diorite-syenite intrusive phases and sodic, to calc-potassic assemblages associated with silica-undersaturated alkaline systems, similarities to a silica-saturated alkalic system include the increase and presence of secondary silicification and molybdenum that may indicate a late change similar to findings at the Lorraine deposit related to pegmatitic dykes (Devine *et. al.*, 2014).

## 10 RECOMMENDATIONS

### 10.1 NON DRILLING

All historical data is recommended to be entered into the SQL database that was developed during the current work program. Once entered, queries should be developed to compare surface and sub-surface data:

- Geochemical, magnetic, alteration and mineralization analysis of intrusive phases, alteration assemblages, base and precious metal associations and structural related groupings; and
- Geochemical queries of lithological units and alteration of these units as they compare to other lithologies, this can also be completed using IoGAS software;

To assist with the understanding of the Cathedral Area, a digital 3-dimension model of the geology and structure is recommended. In addition to utilizing both surface and sub-surface geological and structural data, LiDAR, geophysical surveys and geochemistry should be incorporated into the modelling process.

The creation of stacked profiles showing geophysics, surface geology, soil geochemistry and drill hole data, where available, is recommended for each grid line that was surveyed by IP.

Collect a molybdenum sample within the Cathedral area for a Re-Os age date and correlate with Re-Os date of (202.8 +/-0.8Ma) of mineralization from molybdenite within a north-south trending quartz-sulphide vein at Gail.

Geological mapping and prospecting are recommended to include:

- At the Cathedral Area, conduct an in depth vein study in order to accurately classify A,B,C,D and M type vein fluid phases associated with an alkalic porphyry system;
- At the Cathedral Area, to the west, southwest and northwest (within the Cathedral North area) and proximal to contact areas of the Hogem with Takla Volcanics to the southeast of the Gully area;
- Conduct further and more detailed mapping at the Cirque (Ootes Showing) prospect as well as the Gail prospect to further identify lithological and structural constraints to the vein mineralizing system and incorporate the findings into the mineralizing potential of the property. Rock sampling of the Ootes Showing returned 77.8 g/t Au (Naas, et al, 2020) and from the CJL area, rock sampling returned up to 9.51% Cu, 28.9 g/t Ag and 680 ppm Mo (Naas, 2016b);
- Expand mapping within the Gail Showing to the east towards the Ten prospect proximal to the Takla volcanic and Hogem batholith intrusive contact margin; and
- Conduct further and more detailed mapping at the CJL prospect to further identify lithological and structural constraints to the high-grade copper mineralization hosted

within the monzonite to syenite and localized pyroxenite interpreted Duckling Creek intrusive suite proximal to the Takla volcanic contact margin.

Geophysical studies are recommended and include:

- Conduct several 100 meter spaced east-west oriented pole-dipole IP surveys within the area of the Ootes Showing, located to southwest of the Gail area. Designed spacing for the surveys should be in excess of 400 meters depth in order to provide optimal depths of penetration for the potential of blind targets related to a porphyry settings.
- Conduct ground magnetic surveys over all previous IP lines as well as any new lines in order to further isolate and identify both residual and secondary magnetics within all prospect areas.
- Soil sample at 25 metre intervals along all new grid lines established for geophysical surveying.

Investigate the availability to conduct a major, minor and trace element analysis using electron microprobe and laser ablation inductively-coupled plasma mass spectrometry of chlorite as an evaluation tool for further mineral exploration. This can be compared with the strip logs as an exploration vector within the broad outer to inner propylitic environment

Investigate the availability to conduct a Sulphur Isotope Zonation study broadly throughout the Thane property, particularly within the Gail and CJL and locally within the Cathedral Main, South, Gully and Pinnacle areas. Make comparisons with values collected in order to potentially provide a regional and localized zonal reference for exploration and a means to vector toward sulphides vector for further drilling focused activities.

## **10.2 DRILLING**

Drill targets from previous years need to be adjusted to account for updated interpretation and to deal with the steep topography in the western area of the Cathedral South area.

A total of 2,000m of drilling as a minimum to properly test structurally the controls on mineralization and the westerly tilt porphyry potential in the west, southwest and north western areas of the Cathedral South area (Table 19).

Due to topography, drill hole orientation will be westerly, south-westerly and potentially sub-vertical and likely in excess of 400m if down dip structurally controlled mineralization is encountered.

Virtually all core is competent enough to use a downhole structural orientation tool to provide further confirmation of structural orientations of major silica healed chloritic shear structures, lithologic contacts, both mineralized and barren veins, magnetite breccia's and broad alteration assemblages.

Drilling is recommended at the Gail Area, once the previously recommended ground studies have been completed. An estimated 1,000 metres is anticipated to be the minimum meterage, but the actual amount will be determined once the collected data has been compiled and synthesised.

Table 19: Recommended drill holes, Cathedral Area

ID	UTM		Az.	Dip	Depth (m)	Objective
	Easting	Northing				
PDH-1	346580	6218325	235	-60	400	Down dip of west-southwest tilt and ore related alteration and mineralization. Within magnetic low transitions to moderate magnetics. Collars within low chargeability unknown at depth. Down dip of south-southwest trending moderate west-northwest and southeast trending moderate to steeply southwest dipping structures. Within magnetic and low chargeability.
PDH-2	346580	6218325	045	-60	400	Up-dip of south-southwest trending moderate west-northwest and southeast trending moderate to steeply southwest dipping structures, drills underneath sodic to sodic-calcic and potentially into IPZ to OCP alteration at depth. Potential to intersect south-southeast trending steeply west dipping mineralization and related structures. Within magnetic and low chargeability but limited sub-surface data due to end of the lines (5300-5400N).
PDH-3	346600	6218650	045	-60	300	300m step-out to the north of TH21-4 collar. Up-dip of south-southwest trending moderate west-northwest and southeast trending moderate to steeply southwest dipping structures, drills underneath sodic to sodic-calcic and potentially into IPZ to OCP alteration at depth. Potential to intersect south-southeast trending steeply west dipping mineralization and related structures. Within magnetic and low chargeability but limited sub-surface data due to end of the lines (5300-5400N). Collar may need adjusting due to talus slope cover.
PDH-4	346653	6218691	235	-60	400	Down dip of west-southwest tilt and ore related alteration and mineralization. Within magnetic low transitions to moderate magnetics. Collars within low chargeability unknown at depth. Down dip of south-southwest trending moderate west-northwest and southeast trending moderate to steeply southwest dipping structures. Within magnetic and low chargeability.
PDH-5	346540	6218025	80	-55	200	Test depth and lateral extent of SW trending shallow to moderate west dipping high-grade magnetite-chalcopryrite-pyrite mineralized ARC horizon and potential for SSE trending steeply dipping mineralization and structures possible ESE trending structures also noted. Located on the margin of low to moderate magnetics within diorite to monzodiorite.
PDH-6	346540	6218025	280	-55	300	Test down-dip of magnetite vein and potential for west-southwest tilt and ore related alteration and mineralization. Drilling into increasing magnetics within diorite to monzodiorite. Unknown beyond that.

### 10.3 BUDGET

The estimated cost of the recommended work program is \$2,280,000 and is itemized in Table 20. Support Costs are included within each work item. In addition to camp and helicopter access, support costs include pad building and core analysis for drilling and sample analysis for prospecting and soil sampling. Cost estimates for each work activity may be reduced by the sharing of support costs.

The budget does not include an estimate on the cost for the major, minor and trace element analysis study or the sulphur isotope zonation study. Further investigation into the availability and costs is recommended.

Table 20: Proposed exploration budget

Item	Cost (\$CDN)
Data Compilation, 3-D modelling & Age dating	40,000
Geological mapping and prospecting – Gail & CJL	250,000
Geological mapping and vein studies - Cathedral	200,000
Geophysical surveys	200,000
Soil surveys	50,000
Diamond drilling – Cathedral (2,000m)	1,000,000
Diamond drilling – Gail (1,000m)	500,000
Reporting	40,000
<b>Total</b>	<b>\$2,280,000</b>



## 11.0 REFERENCES

- Andrews, P., Berthelson, D., Lipiec, I.,  
2017. Mount Milligan Mine Technical Report on the Mount Milligan Mine, North Central-Central British Columbia., Centerra Gold Inc. – NI 43-101 March 22, 2017, pg.8.1.
- Bath, A.B., Cooke, D.R., Friedman, R.M, Faure, K., Kamenetsky, V.S., Tosdal, R.M., and Berry, R.F.,  
2014. Mineralization, U-Pb geochronology, and stable isotope geochemistry of the Lower Main Zon of the Lorraine Deposit, North-central British Columbia: a replacement-style alkalic Cu-Au porphyry. In: *Economic Geology*, v. 100, pp. 979-1004.
- Baxter, P. and Devine, F.  
2007 Summary Report on the 2006 Exploration Program on the Jajay/Lorraine and Jam/Tam/Misty Properties, Omineca Mining Division, B.C.; for Teck Cominco Limited.
- Bissig, T., and Cooke, D.R.,  
2014 Introduction to the Special Issue devoted to alkalic porphyry Cu-Au and epithermal Au deposits. In: *Economic Geology, Special Issue on Alkalic Porphyry Deposits*, v. 109, pp. 819-825.
- Cooke D.R., Hollings P., Wilkinson J.J. and Tosdal R.M.  
2014 *Geochemistry of Porphyry Deposits*. In: Holland H.D. and Turekian K.K. (eds.) *Treatise on Geochemistry, Second Edition*, vol. 13, pp. 357-381. Oxford: Elsevier.
- Devine, A.M., F., Chamberlain, M., C., Davies, G.S., A., Friedman, R., Baxter, P.,  
2014. *Geology and District-Scale Setting of Tilted Alkalic Porphyry Cu-Au Mineralization at the Lorraine Deposit, British Columbia*. In; *Economic Geology*, June 01, 2014, Vol.109, 939-977.
- Deyell C.L. and Tosdal R.M.  
2005 *Alkalic Cu-Au Deposits of British Columbia: Sulfur Isotope Zonation as a Guide to Mineral Exploration*, Geological Fieldwork 2004, Paper 2005-1 191
- Duuring, P., Rowins, S., McKinley, B., Dickinson, J., Diakow, L., Kim, Y. and Creaser, R.  
2009 *Magmatic and structural controls on porphyry-style Cu–Au–Mo mineralization at Kemess South, Toodoggone District of British Columbia, Canada*. *Mineralium Deposita*. 44. 435-462.
- Ferri, F., Dudka, S., Rees, C., Meldrum, D., and Willson, M.  
1992. *Geochemistry and Mineral Occurrences of the Uslika Lake Area, British Columbia*. BC Open File 1992-11, Geological Survey Branch, British Columbia Geological Survey.
- Giroux, G. and Lindinger, L.J.

2012. Summary Report on the Lorraine-Jajay Property for Lorraine Copper Corp., May 17 2012.

Garnett, J. A.,

1978. Geology and mineral occurrences of the southern Hogen Batholith; B. C. Ministry of Mines and Petroleum Resources, Bulletin 70, 75 pages.

Gifkins C, Herrmann W, Large R

2005 Altered volcanic rocks: A guide to description and interpretation. Centre of Ore Dep Research Uni of Tasmania, Aus:15pp and 73pp.

Gordon, P., Febo, G., Hay, W.,

2018 Report on the Structural Geology, Alteration Assemblages and Mineralization Styles of the Cathedral Area at the Cathedral Property, Omineca Mining Division, British Columbia, Canada. Unpublished report for CME Consultants Inc. January 10, 2018

Jago, C.P.,

2008 Metal- and alteration-zoning, and hydrothermal flow paths at the moderately-tilted, silica-saturated Mt. Milligan Cu-Au alkalic porphyry deposit. Unpublished MSc thesis, University of British Columbia, 2008, 227 pages.

Jones, G., Ootes, L., Milidragovic, D., Friedman, R., Camacho, A., Luo, Y., Vezinet, A., Pearson, D.G., and Schiarizza, P.,

2021 Geochronology of northern Hogen batholith, Quesnel terrane, north-central British Columbia In: Geological Fieldwork 2020, British Columbia Ministry of Energy, Mines and Low Carbon Innovation, British Columbia Geological Survey Paper 2021-01, pp. 37-56.

Kahlert, B.H.

2006a. Assessment Report on the ATEN Property, Prospecting and Sampling August 2005, unpublished report for Commander Resources, Assessment Report 28205.

2006b. Assessment Report on the MATE Property, Prospecting and Sampling August 2005, unpublished report for Commander Resources, Assessment Report 28233.

Kulla, G.

2001. Geological and Geochemical Report on the Tenakihi Property; unpublished report for Phelps Dodge Corporation of Canada, Limited. Assessment Report 26530.

Logan, J.M., and Mihalynuk, M.G.,

2014 Tectonic controls on early Mesozoic paired alkaline porphyry deposit belts (Cu-Au+Ag-Pt-Pd-Mo) within the Canadian Cordillera. In: Economic Geology, Special Issue on Alkalic Porphyry Deposits, v. 109, pp. 827-858.

Le Maitre, R.W., Le Bas, M.J., Streckeisen, A., and Zanettin, B.,

1986 A chemical classification of volcanic rocks based on the total alkali-silica diagram. Journal of Petrology, Vol. 27 Part3, pp745-750.

Middlemost, Eric A.K.,  
1994 Naming materials in the magma/igneous rock system. In: Earth Science Reviews, December 1994, Volume 37, Issues 3-4, pp 215-224.

Leitch, C.H.B.

2020a Petrographic Report on 17 Samples from Cathedral Project, October 29, 2020.

2020b Petrographic Report on 24 Samples from Thane (Cathedral) Project, June 26, 2020.

Leriche, P.D., and Luckman, N.

1991. Geological and Geochemical Report on the MATE Property, unpublished report for Swannell Minerals Corporation by Reliance Geological Services, November 20, 1991; Assessment Report 22122.

Leriche, P.D.

1993. Geological and Geochemical Report on the MATE Property, unpublished report for Swannell Minerals Corporation by Reliance Geological Services, February 24, 1993; Assessment Report 22659.

Markey, R, Stein, HJ, Hannah, JL, Selby, D, and Creaser RA

2007 “Standardizing Re-Os geochronology: A new molybdenite Reference Material (Henderson, USA) and the stoichiometry of Os salts”. References. Chemical Geology, 244, 74-87.

Naas, C.O.

2020. Report on Ground Geophysics and Geochemistry at the Cathedral Property. unpublished report.

2019. Geochemistry, Geology and Prospecting at the Cathedral Area of the Cathedral Property, unpublished report, Assessment Report 38499.

2018. Geochemistry in the Southern Area of the Cathedral Property, unpublished report, Assessment Report 37736.

2016b. Report on the 2016 Exploration Program on the Cathedral Property, unpublished report for Thane Minerals Inc. by CME Consultants Inc., November 29, 2016.

2016a. Report on the 2015 Airborne Geophysics, Aerial Photography and Prospecting of the Cathedral Property, unpublished report for Thane Minerals Inc. by CME Consultants Inc., March 10, 2016.

2013b. Report on the 2013 Rock and Soil Sampling at the Pinnacle Showing and Lake Area of the Cathedral Property, unpublished report for Thane Minerals Inc. by CME Consultants Inc., November 27, 2013.

2013a. Report on the 2012 Exploration Program of the Cathedral Property, unpublished report for Thane Minerals Inc. by CME Consultants Inc., July 18, 2013.

2011. Data Compilation, Geological and Prospecting on the Thane Creek Mineral Claims, unpublished report, Assessment Report 32106.

Naas, C.O, and Gordon, P

2020. Report on the 2020 Exploration Program of the Thane Property, unpublished report for IMC International Mining Corp. by CME Consultants Inc., December 18, 2020.

- Nelson, J.L. and Bellefontaine, K.A.,  
1996 The geology and mineral deposits of north-central Quesnellia; Tezzeron lake to Discovery creek, Central British Columbia. BC Ministry of Employment and Investment Geological Survey Branch, Bulletin 99.
- Ootes, L., Bergen, A., Milidragovic, D., Graham, B., Simmonds, R.,  
2019 Preliminary geology of northern Hogem batholith, Quesnel terrane, north-central British Columbia. In: Geological Fieldwork 2018, British Columbia Ministry of Energy, Mines and Petroleum Resources, British Columbia Geological Survey Paper 2019-01, pp. 31-53.
- Ootes, L., Bergen, A., Milidragovic, D., Graham, B., Simmonds, R.,  
2020 An update on the geology of northern Hogem batholith and its surroundings, north-central British Columbia. In: Geological Fieldwork 2019, British Columbia Ministry of Energy, Mines and Petroleum Resources, British Columbia Geological Survey Paper 2020-01, pp. 25-47.
- Royal Oak Mines Inc.  
1997. Annual Report 1997, for the Securities and Exchange Commission of Washington, DC, Form 10-K, by Royal Oak Mines Inc. (SEDAR)
- Selby, D and Creaser, RA  
2004 “Macroscale NTIMS and microscale LA-MC-ICP-MS Re-Os isotopic analysis of molybdenite: Testing spatial restrictions for reliable Re-Os age determinations, and implications for the decoupling of Re and Os within molybdenite”. *Geochimica et Cosmochimica Acta*, 68, 3897-3908
- Walcott, A  
2020. 2019 Cathedral Property Induced Polarization Survey, unpublished report for Thane Minerals Inc. by Peter E. Walcott & Associates Limited, April 2020.

## 12.0 SIGNATURE PAGE AND CERTIFICATE

The date of this report, entitled “*Report on the 2021 Exploration Program of the Thane Property*” is March 28, 2022. Signed by:

*Original document signed by  
Christopher O. Naas, P. Geo*

*March 28, 2022*

---

Christopher O. Naas, *P. Geo.*  
President  
CME Consultants Inc.

---

Date

## CERTIFICATE

I, Christopher O. Naas, *P.Geo.*, do hereby certify that:

1. I am President of CME Consultants Inc. with a business address of 16188 Morgan Creek Crescent, Surrey, BC V3Z 0J2;
2. This certificate applies to the report entitled “*Report on the 2021 Exploration Program of the Thane Property*”, dated of March 28, 2022 (the “Report”);
3. I am a graduate in geology of Dalhousie University (*B.Sc.*, 1984); and have practiced in my profession continuously since 1987;
4. Since 1987, I have been involved in mineral exploration for precious and/or base metals in Canada, United States of America, Chile, Venezuela, Ghana, Mali, Nigeria, and Democratic Republic of the Congo (Zaire); for diamonds in Venezuela; and for rare metals in Nigeria. I have also been involved in the determination of base metal and gold resources for properties in Canada and Ghana, respectively, and the valuation of properties in Canada and Equatorial Guinea;
5. I am a member in good standing of the Association of Professional Engineers and Geoscientists of British Columbia (Registration Number 20082);
6. I have visited the Thane property during the course of exploration and the subject work program of the Report was under my management control;
7. I have read the definition of “qualified person” set out in National Instrument 43-101 and certify that by reason of my education, affiliation with a professional association and past work experience, I fulfill the requirements to be a “qualified person” for the purposes of National Instrument 43-101;
8. I am an Officer and Director of Interra Copper Corp. and I own shares of Interra Copper Corp. I am not independent of Interra Copper Corp.;
9. As of the effective date of the Report, to the best of my knowledge, information and belief, the sections of the Technical Report for which I am responsible for preparing contain all scientific and technical information that is required to be disclosed to make the Technical Report not misleading.

Signed and dated at Surrey, British Columbia, this 28<sup>th</sup> day of March, 2022.

*Original document signed by  
Christopher O. Naas, P. Geo.*